Technical and Design Optimizations of the Polymer Extrusion 3D Printing Process towards Circular Economy

by

Tanay Kuclourya

A thesis submitted in partial fulfillment of the requirements for the degree of

Master of Science

Department of Mechanical Engineering
University of Alberta

ABSTRACT

Plastics have emerged as one of the essential materials present on the planet. However, its accumulation can negatively impact the environment if not disposed of properly. To counter this issue, the 'Circular Economy' is one such economic growth model with one of the objectives of using plastic resources efficiently. Several plastic recycling methodologies have been derived, out of which Distributed Recycling via Additive Manufacturing (DRAM) is one of them. It is a closed-loop material reprocessing solution that promotes a circular economy. In this thesis, three main research objectives are targeted. The first objective is to form an optimal link between two different areas of knowledge domains: plastic recycling and additive manufacturing. With an aim to validate the theoretical models related to these two fields, a Scientometric analysis followed by a critical review has been conducted to measure the former knowledge domains of plastic recycling and additive manufacturing. The second research objective is yet another attempt to promote the concept of Circular economy as it tends to fill the literature gaps related to material properties and effect of recycling at different stages of the DRAM process through some experimentations. This thesis contributes to these research gaps by comparing the effect of reprocessing cycles (recycling) with the effect of FDM printing parameters such as Raster angle orientation, Infill density and Extrusion Temperature on the mechanical properties of the 3D printed material. By setting up Design of Experiments, these four parameters are ranked based on their impact on the tensile properties of PLA dog bone specimens. Additionally, a novel analysis on time and the number of specimens to be 3D printed at each reprocessing stage has also been conducted for assisting the future researchers in managing their printing schedule especially in the recycling domain. Lastly, with a vision of utilizing Plastic Solid

Wastes (PSW) in 3D printing and contributing to Circular Economy, the third and the final objective of this thesis is to design a novel 3D printing system which targets high throughput and expands the range of feedstock material. A successful attempt has been made in this direction by designing a hybrid high-throughput 3D printer which works on the FDM and Direct FDM technologies. The focus and scope of this thesis was to utilize this hybrid system to print both virgin as well as recycled PLA separately, with a future goal to use both the technologies simultaneously for printing multi-material structures and also to use non-conventional printing materials. In this work, after several trials of printing and setting up some printing parameters, the proposed system was able to print with virgin as well as recycled PLA.

PREFACE

Original work has been presented in this thesis by Tanay Kuclourya. One journal paper related to this thesis has been published, while two more papers are under review in other journals. The three papers are listed below. This thesis has been organized in paper format after following the paper-based thesis guidelines.

1. **Tanay Kuclourya**, Roberto Monroy, Enrique Cuan-Urquizo, Armando Roman-Flores, Rafiq Ahmad, "Scientometric Analysis and Critical Review of Fused Deposition Modeling in the Plastic Recycling context" *Cleaner Waste Systems.* Available at SSRN: https://doi.org/10.1016/j.clwas.2022.100008

   Tanay Kuclourya performed the literature review, while Roberto Monroy provided guidance for the review methodology. Enrique Cuan-Urquizo and Armando Roman-Flores reviewed the paper. Rafiq Ahmad supervised the Project.
2. **Tanay Kuclourya**, Roberto Monroy, Rafiq Ahmad, "Design of Experiments to Compare the Reprocessing effect with FDM printing parameters on Mechanical Properties of PLA specimens towards Circular Economy", *Progress in Rubber, Plastics and Recycling Technology*. (Under review)

   Tanay Kuclourya did the literature survey, conducted all the experiments, and did the result analysis. Roberto Monroy and Rafiq Ahmad supervised the Project.
3. **Tanay Kuclourya**, Roberto Monroy, Miguel Castillo, David Baca, Rafiq Ahmad, "Design of a hybrid high-throughput Fused Deposition Modeling System for Circular Economy Applications", *Clean Technologies and Recycling.* (Under review)

Tanay Kuclourya designed the Hybrid system and did the mechanical assembly, while Miguel Castillo did the electronics assembly. David Baca guided in the multi-component printing. Roberto Monroy and Rafiq Ahmad supervised the Project.

ACKNOWLEDGEMENTS

Firstly, I would like to thank god for providing me with this opportunity to work on such a wonderful project where I gained a lot of knowledge and executed it to finish this thesis.

A special thanks to my supervisor Dr. Rafiq Ahmad, Associate Professor - Department of Mechanical Engineering -University of Alberta, for his constant support and guidance. This thesis would not be possible without his belief in me. Thanks to Dr. Roberto Monroy, Postdoctoral Fellow at the University of Alberta, for being my mentor and friend. I cannot imagine this work being successful without his valuable feedback and help at each and every step of this research. I would also like to thank my colleagues Mr. David Baca and Mr. Miguel Castillo from the LIMDA team for providing valuable advice throughout this thesis.

Furthermore, this project would not be possible without the help of the Natural Sciences and Engineering Research Council of Canada, Alberta Innovates, Laboratory of Intelligent Manufacturing, Design and Automation (LIMDA), and the Department of Mechanical Engineering at the University of Alberta.

Finally, I am forever indebted to my beloved parents, Mr. Mukesh Kuclourya and Mrs. Kavita Kuclourya, for their unconditional love, support, and encouragement which have been crucial in this journey and succeeding of the program. I am also grateful to my sister, Mrs. Tanvi Mankodi, and brother-in-law, Dr. Ronak Mankodi, for keeping me focused and on track. Apart from my own efforts, this thesis is a result of the constant guidance and motivation from all my family members.

Thank You

Table of Contents

List of Tables

List of Figures

LIST OF ABBREVIATIONS

AM	Additive Manufacturing
DRAM	Distributed Recycling via Additive Manufacturing
EAM	Extrusion Additive Manufacturing
FDM	Fused Deposition Modeling
DFDM	Direct Fused Deposition Modeling
PLA	Polylactic Acid
RA	Raster Angle
ID	Infill Density
ET	Extrusion Temperature
RP	Reprocessing Cycles

Chapter 1 Introduction

The first chapter talks about the background of plastics and the recycling process. It also gives information on how additive manufacturing is used for plastic recycling which is basically the motivation of this research. Based on this literature, three research objectives are defined. Suitable actions taken to encounter these research objectives are also mentioned. Lastly, the thesis is mapped and shown in an organized way in the form of a flowchart.

1.1 Background and Motivation

In recent years, plastic materials have had significant contributions to several technological developments [1], [2], [3] and applications due to their main properties and critical advantages compared to other materials such as metals, ceramics, wood, etc. [4]. For instance, characteristics such as the high ratio between mechanical and flexural strength [5], low density [6], [7], lower energy required to process them [8], [9], higher chemical resistance [3], [10], and versatility in many fields such as automotive [11], [12], packaging, construction, medicine, and other industries make them the optimal material selection for many products [4]. Nevertheless, as the market consumption per person and world population has increased, the production of plastics has similarly gradually increased, leading to a consumption/accumulation ratio that produces severe problems in terms of environmental impacts and contamination [13].

According to the European Union reports in 2012, it is considered that plastics production has increased by 500% in the last 30 years, and it is estimated to further increase up to 850 million metric tons annually by 2050 [14]. Additionally, only 15% of the produced plastic is recycled, and excess Plastic Solid Wastes (PSW) end up in the oceans and landfilling areas [15]. At the same time, the lack of manageability of PSW has led to an exponential accumulation in their volume across the world [16], where it is reported that only 26% of the PSW is mechanically recycled, 0.3% is used for feedstock recycling, and 35.6% is used for incineration, letting a 38% being disposed of [15]. Therefore, the management [17], processing [18], and disposal of plastic waste [19] have become significant issues in the scientific community, where strategies for a plastic-free waste economic cycle are being developed.

Notably, as shown in Figure 1-1, several methods of handling PSW are available. Mechanical recycling is an essential step involving reusing reprocessed plastic to form a new product with the same inherent characteristics [20]. When mechanical recycling seems impractical, a chemical method is used where PSW is converted into fuels and chemical feedstock through several chemical reaction processes, such as pyrolysis [21]. Suppose the PSW is in a condition that it cannot be converted into new products. In that case, it is used as a source of energy conservation through incineration. The harmful effects of this process, such as the emission of CO_2 and toxic chemicals [22] are often overlooked because of the high calorific value of PSW. Finally, landfilling is the ultimate option for PSW, which cannot be further processed nor can be used for energy [23], [24]. Although this process may have null impacts on the environment, it is not viable in the long term, as this has been noticed by the European Commission, which has set a goal for zero landfilling of plastic wastes by 2025 [15]. Figure 1-1 shows the different modes of recycling in consideration of different economic models discussed in detail in the upcoming section.

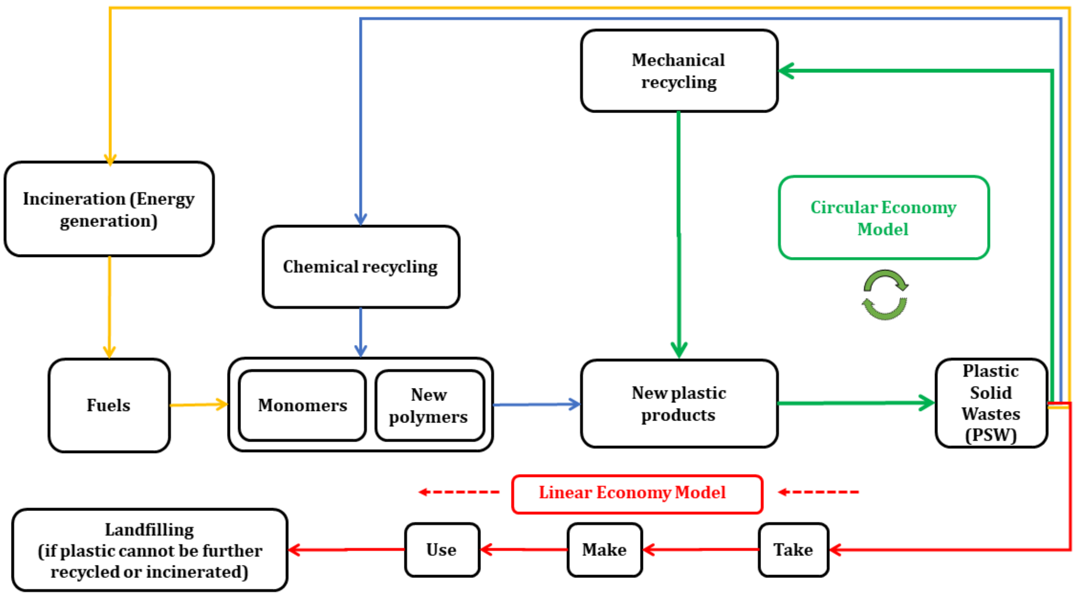

Figure 1-1 Different modes of plastic recycling (Adapted from [25])

Additionally to the drastic accumulation problem previously mentioned, plastic residues increase environmental pollution in land and water resources and bring long-term irreversible harmful effects on human life and ecosystem wealth [26]. With this in mind and due to the main problem, this issue represents, two significant concerns can be concluded. First, the current linear plastic economy is not sustainable [27]–[29]. Second, there is an essential need to reuse and recycle plastics optimally [30]–[32]. For this purpose, the most common alternatives for plastic recycling have been analyzed. Some of them can represent various disadvantages; either they can be unavailable, have higher carbon footprints [33], and are not economically worthwhile in many situations [34]. However, the case of mechanical recycling is a strategy that can be considered optimal and a major part of the waste management solution [35]–[38]. It promotes the idea of industrial ecology wherein PSW are processed so that there are only products and no wastes [34], and many industries can target cost reduction using recycled plastic [39].

Nonetheless, the low degree of plastic reprocessing can still be a significant concern regarding material properties [40]. In addition, recycling these materials over repeated cycles leads to the deterioration of their original performance properties [40]. Therefore, better control over their material's life and finding a way to maintain their key capabilities are needed [41], [42]. Once a solution is achieved, it will improve the recycling rate, increase recycled content, and minimize the plastic conveyed to landfill [43].

For the specific previous situation raised and getting into the point of plastics products material's life characterization, it is essential to mention that the seven different types of commodity plastics which are PET (resin code-1), HDPE (resin code-2), PVC (resin code-3), LDPE (resin code-4), PP (resin code-5), PS (resin code-6) and Others (resin code-7) [44], whose application does not require exceptional engineering properties but are mass-produced [44]. Each has a different chemical composition and a recycling rate based on the difficulty of separating mixed plastic after disposal [40]. Sorting methods such as cryogrinding [45], [46], hand sorting, mechanical/gravity sorting [47], [48] are the most common methodologies employed [40]. The separation's precision for each method is critical to displace virgin material without representing an up-scaled cost to the recycled plastic product chain [40]. For instance, Polyethylene Terephthalate or PET (commodity code 1) has the highest recycling rate [49] but accounts for only 14.39% of the total plastic waste [40]. Moreover, when formulating for performance, recycled material is often mixed into virgin material [40]. This reduces the material cost and minimizes the effects of degradation [40]. Depending on the mixing ratio, either the virgin material is diluted with recycled material [50], [51], or the latter is diluted with the former [40]. By using a constant mixing ratio during continuous processing, the regrind itself is diluted by the material that has been reprocessed once, twice, three times, and so on [40]. Therefore the composition of a material with a proportion of recyclate (q) after (n) cycles can be calculated as shown in the equation below [40]:

$$\sum_{i=1}^{n} q^{(n-i)}(1-q) = 1$$

For a small proportion of recyclate, the re-grinded material contains only minimal amounts of material that has passed through a large number of reprocessing cycles, but that has been reprocessed more than five times and is highly degraded [52]. On the contrary, for higher proportions of recycled materials, the number of reprocessing cycles is limited [52]. For this case, the dilution effect is very important to consider as it decreases the resulting mechanical properties of the final component [52], and it has to be minimized by controlling the number of reprocessing cycles that the material undergoes or by adjusting the amount of the virgin material employed. When using and reprocessing these materials, they undergo several degradation effects related to oxidation reactions, UV light exposure, and intermolecular thermal-mechanical stresses [52]. The former substantially affects the bonding between the polymerization chains and reduces the average molecular weight of the polymer, leading to a decrease in its stiffness [52]. In Figure 1-2, the relationship between average molecular weight, temperature, glass transition, and thermal degradation window for a typical and recycled plastic commodity is illustrated. It can be observed that the minimum processing temperature reaches the point of degradation at a certain average molecular weight. Hence, finding the optimal relationship for the finished polymer product is necessary while providing flow properties that make it straightforward to shape the material during the manufacturing process [52]. Figure 1-2 shows the relation between the average molecular weight, processing temperature (T_P), and thermal degradation temperature (T_R) for both virgin and 'n' times recycled polymer.

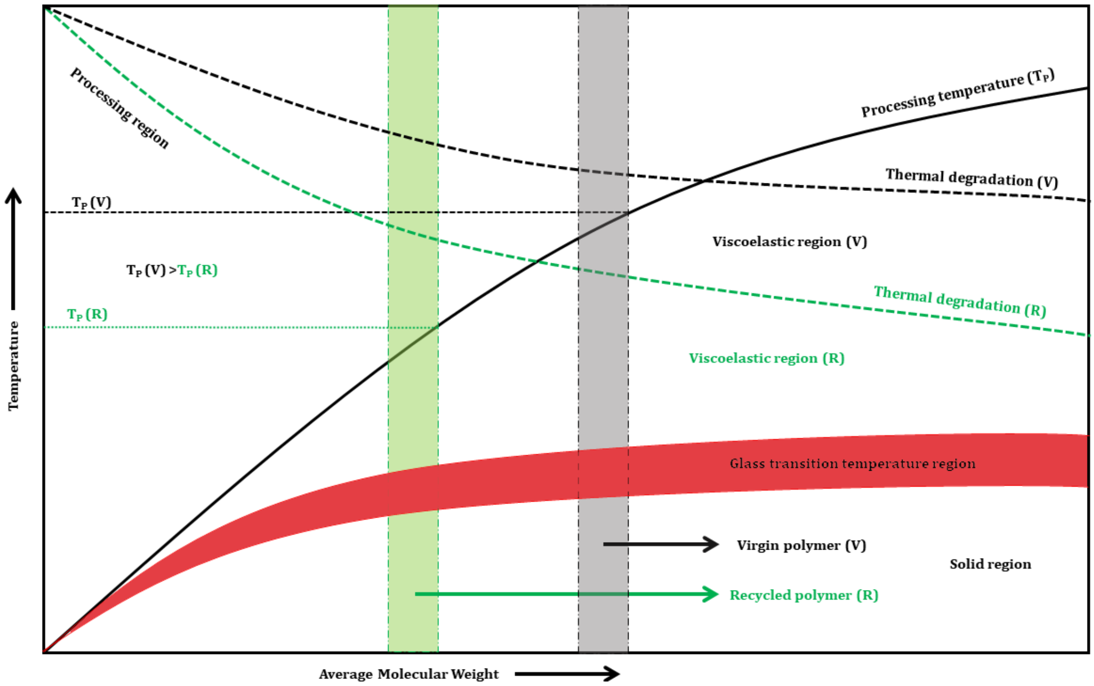

Figure 1-2 Relation Between Molecular Weight, Temperature and Thermal Degradation for virgin and recycled polymer [adapted from [13]]

In the same way, as from the mesoscale point of view, when a polymer is subjected to heat or deformation, there is an increase in its internal energy [53], [54] due to the rise in the rate of rotation of any freely moving group in the polymer [13]. This weakens the intermolecular forces [55], [56] and develops ruptures in the polymerization chain, increasing the distance between the molecules and maximizing the free volume in the material, leading to a reduction in its bonding stiffness and total material strength [57].

Figure 1-3 illustrates the typical correlation between molecular weight, processing conditions (viscosity), and stiffness/strength for recycled plastic. As it can be concluded, it is fundamentally important to consider this relation in terms of product and process development for mechanically recycled plastic. At the same time, it serves as the main ground base for the optimal application of several recycling methodologies that achieve maximizing performance and higher recycling rates [58], [59]. Moreover, the success of a recycled product in terms of reducing the environmental impact must be accompanied by optimal market and social strategies [60]. As it is observed in Figures 1-2, and 1-3, even though the main mechanical properties of the material have a decrement in their respective values with respect to their virgin counterpart due to mechanical degradation by virtue of recycling, the positive indication is that still the material can be of prime importance for various other product applications [61], [62] and consequently decrease the accumulation of total plastic content in the natural environment as well as the CO_2 emissions from the energy consumption required to synthesize a new virgin material [63]. In the next sections, the main plastic recycling strategies and various economic models are revised to achieve this objective, particularly the "Circular Economic Model" which is considered of prime importance [64].

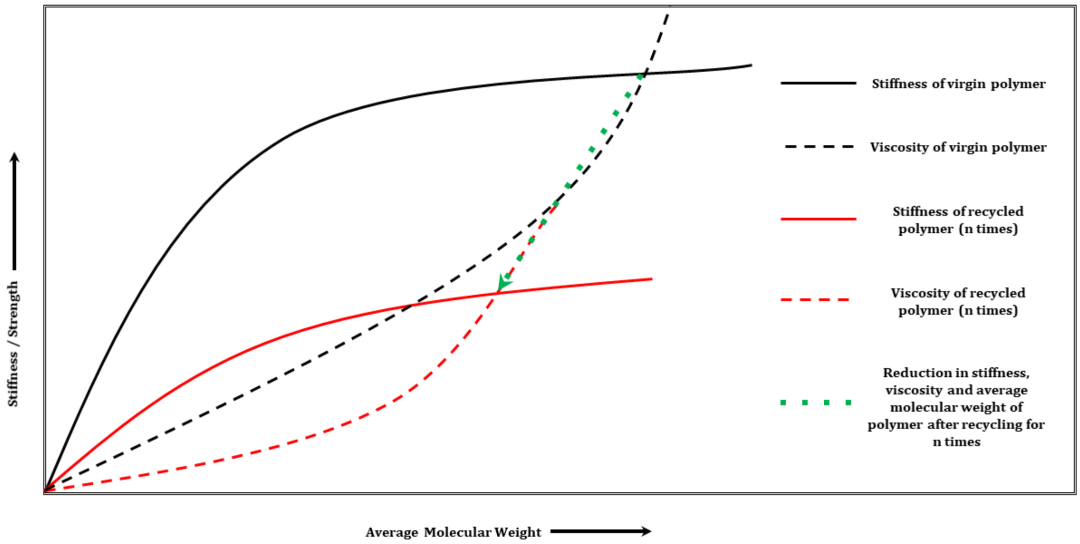

Figure 1-3 Relation between Average Molecular Weight, Stiffness and Viscosity for virgin and n-times recycled polymer [adapted from [52]]

1.2 Circular Economy Model based on Plastic Recycling

Just as important as the environmental strategies and primary material's characterization interdependencies; additionally, the social-economic standpoint plays a critical role in the various steps that have been taken to promote plastic recycling [64]. Particularly, several models have been developed that allow the flow of plastic material in a closed-loop system [65]–[67] and achieve optimizing production cost reduction [63]. As for the extent of this thesis, only the explanation of the Circular Economy model is included in the scope of this work; for instance, a particular emphasis is on the case of the "Circular Economy" model, which promotes plastic recycling by working on the principle of the 3R's (Reduce, Reuse and Recycle) [63]. Additionally, this model can be extended to 3 other R's phases: Recover, Redesign, and Remanufacture [63]. To show a description of this cycle, a diagram of its main stages is portrayed in Figure 1-4.

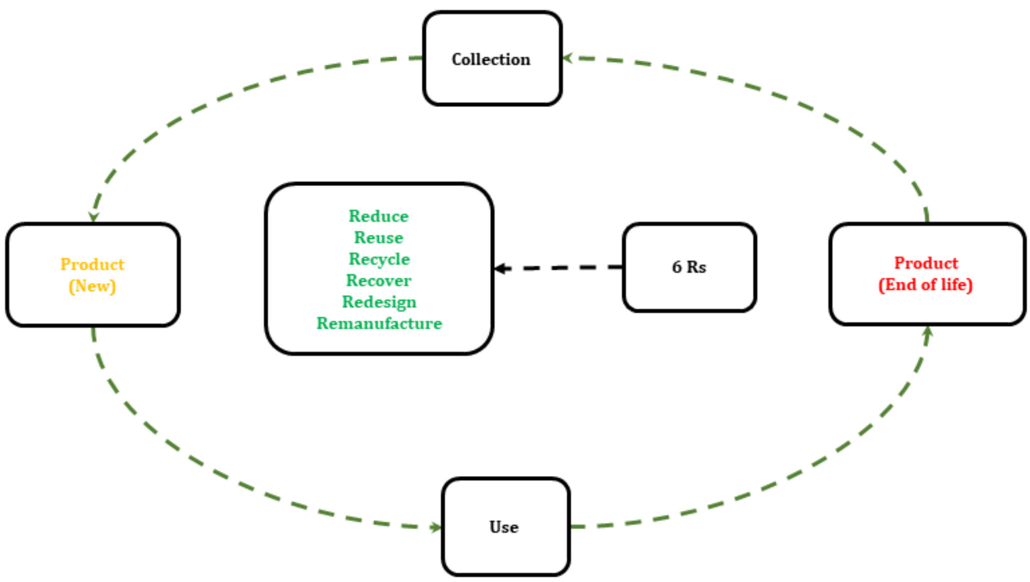

Figure 1-4 Circular Economy Model [adapted from [63]]

Furthermore, to support this model, it is fundamental to understand its main core objectives, which are based on the standards set by the European Economy Package [68] and demand for low plastic consumption, less CO_2 emission from fossil fuels and its derived components, and high efficiency of material use [64]. Particularly, special attention is put on plastic wastes coming from some major fields, which are: demolition and construction [69], food packaging waste [70], bioproducts [71], and critical raw materials [68]. The package also specifies some crucial goals, which include 65% efficiency in the recycling of municipal wastes, 75% efficiency in the recycling of packaging wastes, and a 10% reduction in landfilling by 2030 [63].

Recently, as it has been noticed, the implementation of this model in several commercial chains, led by the set goals established, has proved to be a better alternative for the earlier existing "take-make-dispose" one [72] and up to the date, the extension of this model to the most important manufacturing chains is a required key factor [72]. Therefore, for this thesis, the application of the "Circular Economy" model in terms of the additive manufacturing processes is essential to apply the methodology of "Distributed Recycling via Additive Manufacturing" (DRAM) [73] which is explained in the next section.

1.3 Distributed Recycling via Additive Manufacturing (DRAM)

As a compilation of the previous factors mentioned and object to the main focus of this thesis, the former recycling strategies are analyzed in terms of the additive manufacturing (AM, 3D printing) process. AM is a technology that involves part manufacturing through the layer-by-layer deposition of a material using 3D computer model data [74]–[79]. Various types of known AM methods such as Material Extrusion

Process (Fused Deposition Modelling (FDM)) [80]–[82], VAT Photopolymerization process (Stereolithography (SLA) [83]–[85] and Digital Light Processing (DLP)) [86], [87], Powder Bed Fusion Process (Selective Laser Sintering (SLS)) [88]–[90], Material Jetting Process (Polyjet printing) [91], [92] and Sheet Lamination Process (Laminated Object Manufacturing (LOM)) [93]–[95] are in the current market [96]. As for the scope of this thesis, special attention is put on the Fused Deposition Modeling (FDM) process, which has been noticed as the one which possesses the main advantages as it can bring an optimal transition from a linear economy to a circular economy due to its versatility for part design [97], low complexity [98], [99], relatively low-cost investment [100], multi-material plastic product capabilities [101], [102], and vast product customization possibilities [103]. To emphasize this point, a typical DRAM chain contains six stages – recovery, preparation, compounding, feedstock, printing, and quality [72], as shown in Figure 1-5. The recovery phase deals with the collection of plastics, whereas the preparation phase includes the processes such as identification, sorting, and size reduction [72].

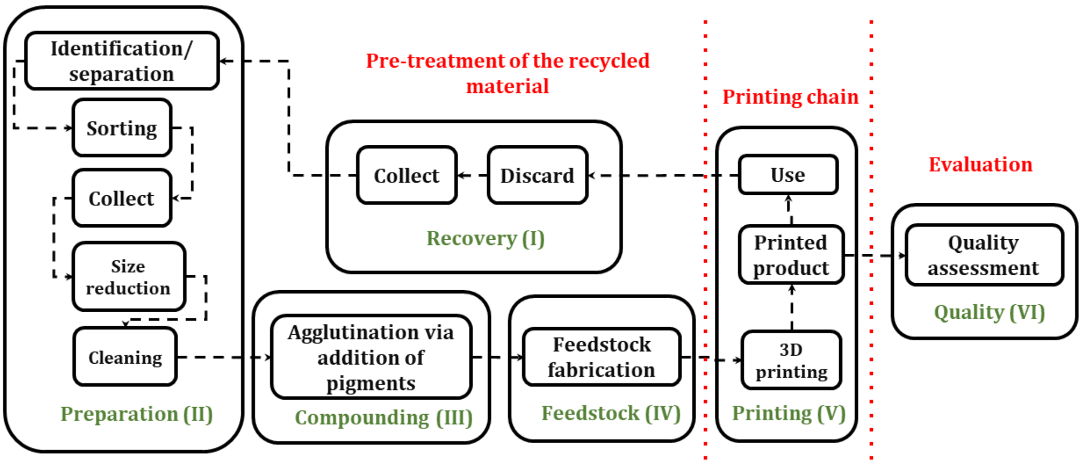

Figure 1-5 Closed-loop recycling framework of Distributed Recycling via Additive Manufacturing (DRAM) (adapted from [72])

The compounding phase aims toward creating a single or composite material to be used as a feed material. The ultimate aim of the feedstock phase is to come up with a recycled material that is adequate to be 3D printed [104], [105]. The printing phase deals with the 3D printing of the material obtained from the previous phase [72]. In the Quality phase, the material quality is evaluated at three different instances – raw material stage, feedstock, and after the part has been printed [72]. However, there is still a lack of literature on recovery and preparation stages. It also should be noted that different thermoplastics have different applications for DRAM purposes [72]. HDPE, when recycled, can be used in technical applications and for areas where high life of the product is required [106], [107]. PLA can be used for imparting high tensile and flexural strength [72]. One approach to waste management within the 3D printing domain was using the un-sintered polymer of Selective Laser Sintering (SLS) process in the Fused Filament Fabrication (FFF) process [108]. Some studies have shown that the filaments for the FFF process made from un-sintered powder in SLS exhibited good mechanical properties [109], and it expands an abroad research focus on different combinations of AM processes in the context of recycling [110], [111].

Additionally, another topic with null or insufficient information is the link between FDM printing parameters and part quality for materials reprocessed several cycles. Although there are some studies conducted that have shown the viability of polymers such as ABS, PA12, and others over multiple reprocessing cycles [112], [113]. There is still a research gap in determining the optimum FDM parameters for different recycling cycles to obtain an optimum print quality. Furthermore, exploration of novel systems that account for decreasing the up-scaled cost of the recycling chain has brought important attention to where directly PSW material can be integrated into the

FDM process via additional hardware configurations, such as the case of Direct Deposition Fused Modeling techniques. Nevertheless, similar to the previous research segments, a lack of information that needs to be encountered is still there.

1.4 Research objectives

Based on the discussions done at the end of the previous section, three major research objectives are presented in this thesis. Each objective has been addressed in separate chapters. The objectives, as well as the actions taken, are described in detail below.

O1. Develop a detailed review of additive manufacturing (particularly FDM, which is the most common AM method) in the plastic recycling context. The aim would be to gather literature to establish a link between the domains of additive manufacturing and plastic recycling for future research.

Action: A Scientometric analysis (explained in section 2.2.2) followed by a critical review has been executed on the Fused Deposition Modeling process in context to the plastic recycling process.

O2. Determine the optimum FDM parameters for different recycling cycles of the DRAM to obtain an optimum print quality.

Action: A series of experiments have been performed on plastics after conducting a Design of Experiments via Taguchi analysis (explained in section 3.3.3). Through these experiments, an attempt has been made to compare reprocessing with the effect of FDM printing parameters on the mechanical properties of PLA specimens. This comparative analysis makes several inferences that contribute to the DRAM process.

O3. Design, prototype, and test a novel a high throughput 3D printing head system to utilize Plastic Solid Wastes directly using the FDM process.

Action: A successful attempt has been made to design a high throughput hybrid system working on FDM and DFDM technologies. It can print plastics in their filament as well as shredded or pelletized forms.

1.5 Thesis Structure

This section provides a mapping of the entire thesis. This thesis starts with an Introduction chapter (Chapter 1) which provides the background and motivation for this research. It also provides literature for defining the three research objectives of this thesis. These three research objectives are addressed one by one in the next three chapters. Chapter 2 discusses the Scientometric analysis and critical review as a part of the mixed review methodology adopted to link plastic recycling and additive manufacturing domains. It provides an intense literature survey on plastics, the recycling effect on plastics, FDM process parameters, and their effect on the mechanical properties of 3D printed thermoplastics. Chapter 3 describes the experimentations done to fill the literature gaps at various stages of the DRAM process. It includes Stress-strain analysis of the specimens having varying properties such as different infill densities, extrusion temperature, raster angle orientations, and different reprocessing conditions. A novel analysis of the time and number of specimens to be 3D printed at the start of every reprocessing cycle is also included. Chapter 4 includes the design of a hybrid 3D printing system that aims to give a higher throughput and utilize plastic in pellets, flakes, grinded pieces, or filaments. It includes a literature survey based on screw geometry, EAM, and basic electronics related to stepper motors and sensors. It also discusses the limitations as well as future scopes of the design. Lastly, Chapter 5 concludes the thesis and discusses the research contributions, limitations, and future scopes of this work.

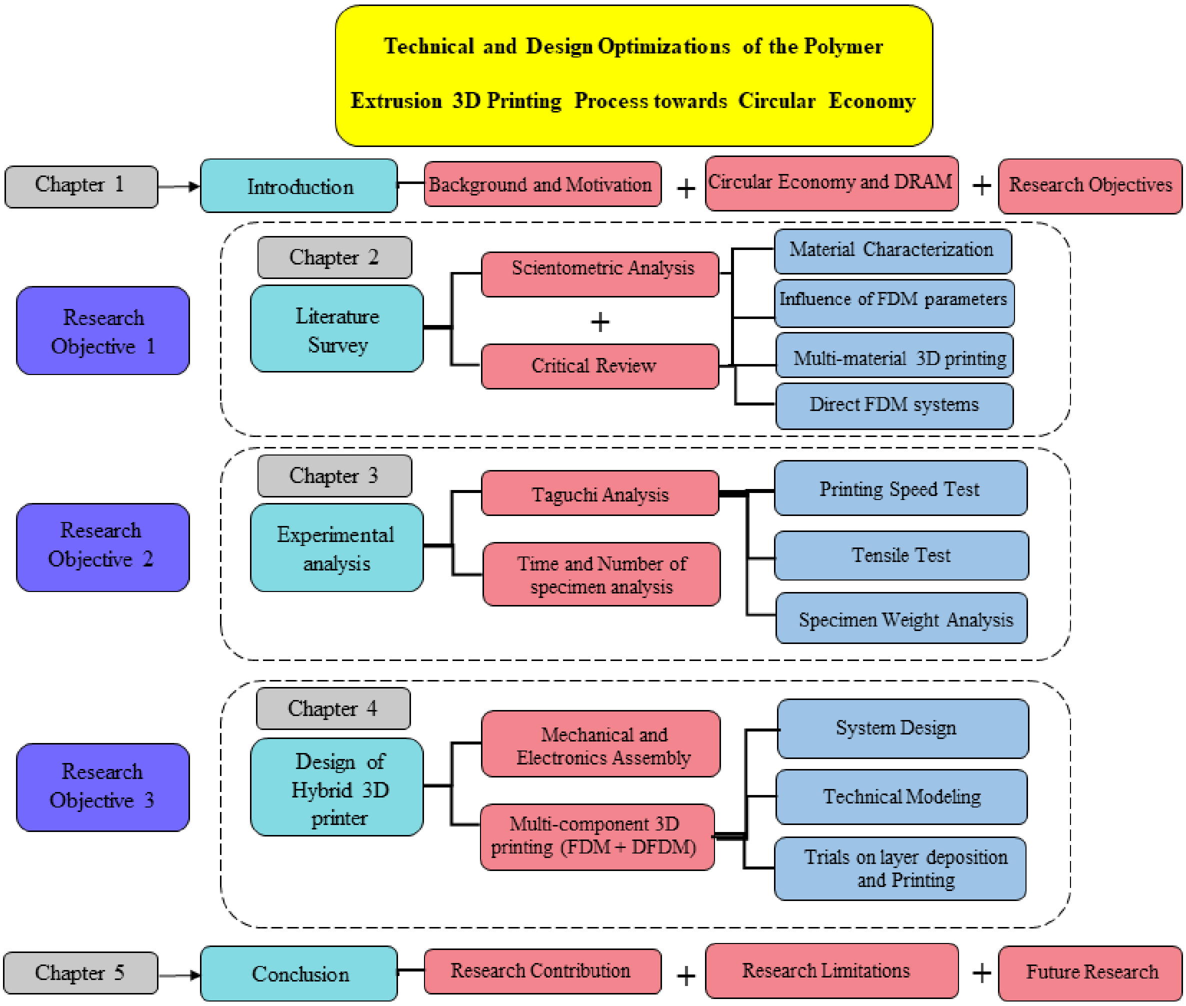

Figure 1-6 Pictorial representation of thesis layout

Chapter 2 Scientometric Analysis and Critical Review of Fused Deposition Modeling in the Plastic Recycling context

2.1. Introduction

Despite the high essentiality of plastics, their accumulation in the environment can be a big threat if they are not disposed of properly. Hence, there is a need to implement economic growth models which work towards using these resources efficiently and in the most environment-friendly way. The circular economy stands by this need, and DRAM is one of the perfect examples which promote this model. It is DRAM that brings the concept of AM in plastic recycling and hence is a base of this thesis. However, a lack of consolidated literature on these two domains brings many setbacks in the ongoing research works. Arising from this position and to portray a baseline for solving the issue mentioned, the current thesis starts with a formal methodology that attempts to consolidate the most critical research publication available in the FDM and recycling context. For this, a Scientometric analysis is conducted initially, and its results are presented. This is followed by a critical review in which special attention is put on the topics such as circular economy, material characterization of recyclable plastics in additive manufacturing, FDM parameters, multi-material mixing of plastics, and direct FDM systems.

2.2. Research Method

As mentioned in the previous chapter, the first objective of this thesis aims to provide an extensive review of multiple domains such as plastics, recycling, economic models supporting recycling, use of additive manufacturing technologies such as Fused deposition modeling (FDM) in the recycling context as well as multi-material mixing of plastics, and lastly concluding with some possible future directions in this field. It was necessary to initially develop the systematic survey to cover these multiple domains in a single review and form a bridge between all these topics. To ensure this, an approach of mixed-review methodology was adopted, including the steps of data acquisition, scientometric analysis, and critical review. This methodology is depicted in Figure 2-1. The Scopus literature database was used as a source for retrieving the relevant research results following the meta-analyses guidelines [114]**.** Based on these results, a scientometric analysis was done to form a connection between past studies and the ongoing trends in this area [115]–[119]. Parallelly, a critical review was conducted, discussing the above-mentioned topics in detail. The research method is elaborated in the following subsections.

2.2.1. Data Acquisition

For this work, the data acquisition is made as per the methodology provided by *Zhang* [120]. As already mentioned, the Scopus database was selected for the literature review because, compared with other databases such as Google Scholar, PubMed, and Web of Science, it had a more extensive collection of journal publications [121]**.** For this work, the search equation used in the database was - TITLE-ABS-KEY ("Plastic recycling") OR ("FDM") OR ("Circular economy"). This allowed the database to look for all the publications with these words in either their title, abstract, or keywords. The initial result fetched as many as 68,022 publications, which were then subjected to many filters. Firstly, only open access and peer-reviewed journal publications were considered. Secondly, only the publications from the year 2013-2021 were selected to increase the possibilities of including contemporary and latest technologies in the area. Thirdly, the results were screened based on several keywords related to the field. Lastly, English was selected as the language due to its universal reach. After these successive rigorous screenings, the final number of relevant publications was reduced to just 1452. This amount in the final number indicates that this field is specific, emerging and has many future scopes.

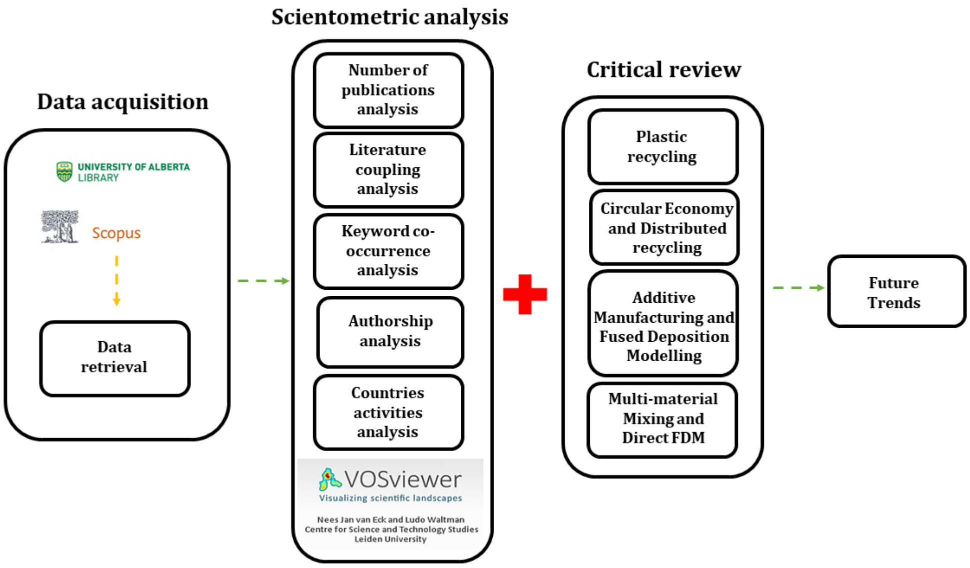

Figure 2 - 1 Research methodology

2.2.2. Scientometric Analysis

Scientomteric analysis is a type of review which analyses the evolution of a research over a definite period of time [122]. It measures scholarly literature by focusing on the quantitative aspect of any research and is derived from large-scale bibliographic data [123]. The concept of scientometrics has already been in existence since the 1950s [124], [125]. The term ‘Scientometrics’ which means ‘’measurement of science,” was first coined by Nalimova and Mulchenko in 1969 [126]. The main purpose of the scientometric analysis is to form a bridge between existing knowledge structures and current emerging trends in a given research field [127]. Since recycling of plastic and fused deposition modeling are extensive topics, it becomes difficult to analyze these areas only with the help of a critical review. Hence, a scientometric analysis has inculcated a multi-dimensional view of these fields. This involves- number of publications analysis, literature coupling analysis, keyword co-occurrence analysis, authorship analysis, and countries publication analysis. This is done with the help of network visualization and density visualization of data [128]–[130]. VOSviewer software was used for generating these visualizations[131], [132].

2.2.3. Critical Review

It should be noted that scientometric analysis is just a tool to analyze the trends of not-so-common parameters such as country-wise collaborations on projects, co-authorship analysis, etc. However, it cannot be used for in-depth research. Hence, a critical review was conducted. An attempt has been made to discuss several aspects, such as plastic recycling, distributed recycling by additive manufacturing, and fused deposition modeling. The critical review presented in this chapter aims to connect the dots between these topics. Lastly, it should be made clear that the results from the scientometric analysis have not been directly used for the critical review process. Instead, critical review and scientometric analysis were done parallelly. As mentioned earlier, the sole aim of the scientometric analysis was to gain insight into these topics, particularly the current trends in publications related to these topics.

2.3. Results and Analysis

2.3.1. Number of Publications Analysis

As already mentioned, the total number of relevant results was 1452 published between 2013 and 2021. Figure 2-2 shows the graph for the number of annual publications every year. It can be seen that there is an upward trend which indicates that additive manufacturing of plastics is continuously attracting researchers worldwide. An astonishing increase of 14500% can be seen in the annual percentage growth rate for the number of publications from 2013 to the ending year 2021. This increment in the number of publications can also be attributed to more advanced additive manufacturing technologies in recent years [133].

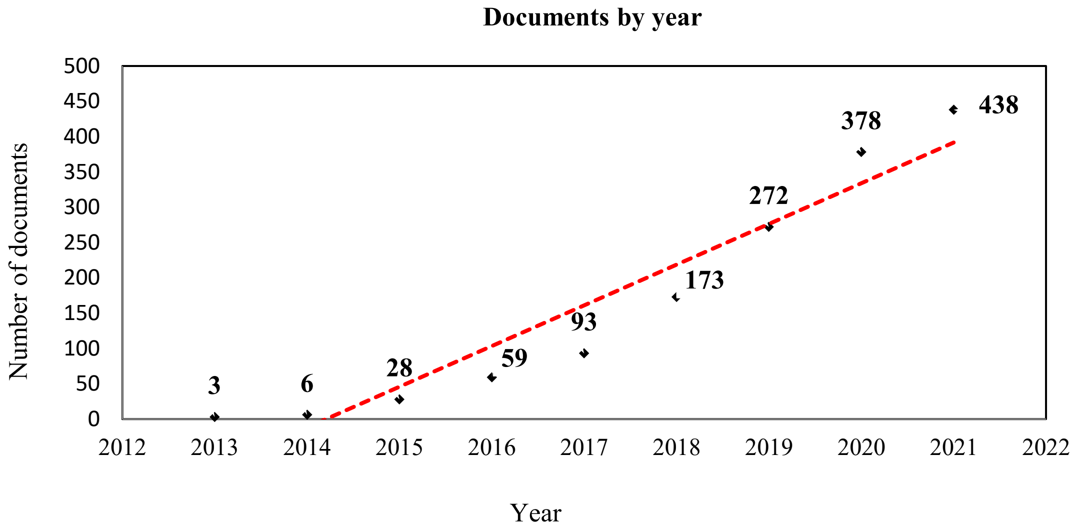

Figure 2 - 2 Number of annual publications per year targeting plastic recycling, FDM and circular economy

2.3.2. Literature Coupling Analysis

The literature coupling analysis showed how different journals worldwide have contributed to the field of plastic recycling and additive manufacturing technologies. Table 2-1 summarizes the number of publications for every journal (contributing at least 12 documents). Top journals like the Journal of Cleaner Production, Advanced Sciences, and Additive Manufacturing collectively contributed to nearly 25% of publications. The Journal of Cleaner Production had the maximum number of relevant publications (197) as well as the maximum number of citations (5604). In contrast, Materials and Design had the highest average number of citations per article (34.8).

Table 2 - 1 Number of publications for every journal (contributing at least 12 documents)

Journal	Number of relevant articles	Total percentage of publications (%)	Total citations from these articles	Average citations per article
Journal of cleaner production	197	13.6	5604	28.4
Applied sciences (Switzerland)	94	6.5	381	4.1
Energies	83	5.7	504	6.1
Additive manufacturing	69	4.8	1740	25.2
Materials and design	51	3.5	1777	34.8
Rapid prototyping journal	38	2.6	953	25.1
International journal of advanced manufacturing technology	32	2.2	1091	34.1
IEEE access	25	1.7	102	4.1
Micromachines	25	1.7	145	5.8

Sensors (Switzerland)	20	1.4	203	10.1
Journal of manufacturing and materials processing	19	1.3	87	4.6
Sustainable production and consumption	16	1.1	89	5.6
SN applied sciences	15	1.1	32	2.1
Materials plastice	14	0.9	50	3.6
MM science journal	13	0.9	13	1
Progress in additive manufacturing	12	0.8	176	14.7
International journal of production research	12	0.8	296	24.7
Journal of materials engineering and performance	12	0.8	35	2.9

2.3.3. Keyword Co-Occurrence Analysis

Keywords play an essential role in making any research publication searchable, and hence a detailed analysis of keyword networking provides a knowledge domain of the research topics. It also establishes an interrelationship between different topics in the same field. To conduct this network analysis, an open-source software-VOSviewer was used. It is a powerful tool for representing bibliometric mappings graphically. These mappings are distance-based and can include items such as authors, sources, organizations, and countries. The smaller the distance between the mappings, the stronger the relationship is. VOSviewer works on the clustering technique in which all the items to be analyzed are clustered together and labeled. In keyword analysis, the number of keywords in a cluster determines the size of the label [134].

For keyword co-occurrence analysis, author keywords, as well as index keywords, were taken into consideration. The minimum occurrence of the keywords was set to 65. Only 19 out of 11053 keywords passed this screening. Further, similar results such as '3d printing' and '3-d printing', 'fdm' and 'fused deposition modeling', etc. were grouped together. Some keywords which were not directly related to the scope of this work were eliminated from the results, such as 'fabrication', 'manufacture', etc. After all the filters, the total number fell to 12. The results are summarized in Table 2-2. For a better demonstration of the scientometric analysis, more relevant keywords were included for the network visualization. The minimum occurrence of the keywords was set to 15, which gave a total of 153 keywords out of 11053. The network visualization can be seen in Figure 2-3.

In the network analysis through VOSviewer, the occurrence of the keyword was set as the parameter to indicate the weight of the label. It can be seen from the analysis that keywords such as '3D printers', 'Additive manufacturing', 'Fused deposition modeling', and 'Circular economy' have bigger label sizes when compared to other labels, which denotes that these words have a higher frequency. The link strength for any keyword indicates its total linkages with other keywords. From Table 2-2, it can be seen that the keyword 'fused deposition modeling' has the maximum total link strength (1393). This implies that fused deposition modeling is a necessary process when it comes to the topic of plastic recycling.

Table 2 - 2 List of keywords related to plastic recycling, additive manufacturing, and their relevant network data

Keywords	Number of occurrences	Total link strength
circular economy	573	337
3D printers	477	1230
additive manufacturing	387	859
3D printing	487	1351
fused deposition modeling	464	1393
sustainable development	115	199
tensile strength	99	322
mechanical properties	96	306
recycling	80	127
layered manufacturing	66	307
sustainability	65	128
product design	63	138

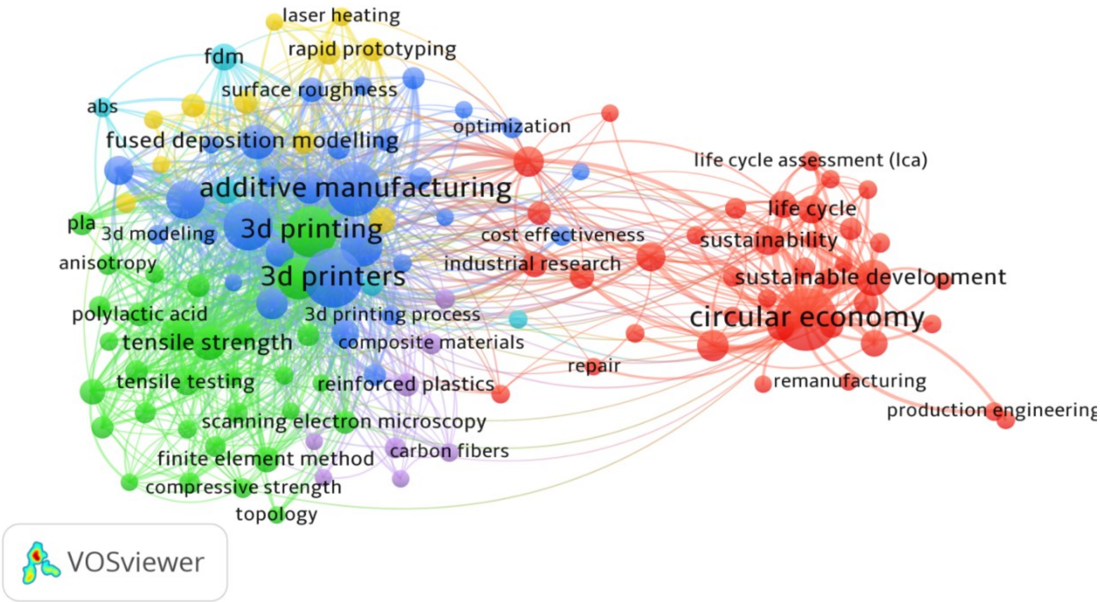

Figure 2 - 3 Network visualization for 153 keywords

2.3.4. Authorship Analysis

The list of authors having a minimum of 6 relevant publications (as derived from the Scopus database) is summarized in Table 2-3. The authorship analysis shows that out of 5205 authors, 19 authors have at least six publications related to plastic recycling and additive manufacturing technologies. Pearce J.M. is found to be the most productive scholar in this field, having the maximum number of citations (899) and the maximum number of publications (14). Bocken N. has managed to get the highest average number of citations (64.2) compared to all other authors.

Table 2 - 3 List of authors publishing the most publications related to plastic recycling and additive manufacturing

Author	Number of relevant publications	Citations	Average citations
Pearce J.M.	14	899	64.2
Liu Y.	10	131	13.1
Li Y.	10	200	20.0
Zhang J.	8	93	11.6
Zhang Y.	8	102	12.8
Wang I.	8	131	16.4
Lundstrom M.	8	119	14.9
Travieso-Rodriguez J.A.	7	166	23.7
Jerez-Mesa R.	7	166	23.7
Pei E.	7	147	21.0
Li Z.	7	49	7.0
Salmi M.	6	63	10.5
Li J.	6	113	18.8
Klemettinen L.	6	16	2.7
Wang C.C.L.	6	48	8.0
Percoco G.	6	31	5.2

Chen X.	6	172	28.7
Bocken N.	6	415	69.2
Balkenende R.	6	49	8.2

With the help of VOSviewer software, it was possible to analyze the relationship of co-authorship, as shown in Figure 2-4. The density visualization analysis shows the formation of several clusters in different colors. This analysis indicates that the authors present in the same cluster have had collaborations in the past and have co-authored at least one publication. For instance, Wang Q., Liu Y., and Yu Z. belong to the same cluster and have co-authored some publications. On the other hand, authors like Chen X. and Naghieh S. have no collaborations with other authors.

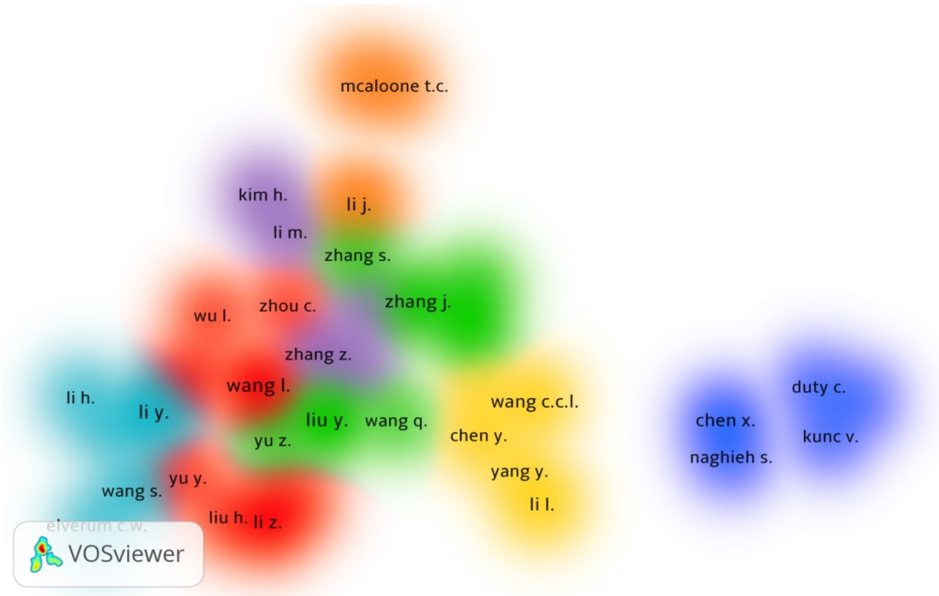

Figure 2 - 4 Density visualization for co-authorship

2.3.5. Countries Activities Analysis

Table 2-4 shows the analysis of the relevant results based on their place of publication. Out of the 94 countries obtained from the results, only those having at least 64 publications related to plastic recycling and additive manufacturing are considered in the table. It can be seen that the United Kingdom (UK) is the leading country in terms of both the number of publications (247) as well the number of citations (7365). It is followed by the United States (US), which has the second-highest number of citations (6272). Although the Netherlands has significantly fewer publications than the United Kingdom, it has the maximum average citations per publication compared to any other country.

Table 2 - 4 List of countries publishing the most publications related to plastic recycling and additive manufacturing

Country	Number of relevant publications	Citations	Average citations
United Kingdom (UK)	247	7365	29.8
United States (US)	198	6272	31.7
Spain	135	1686	12.5
China	100	1129	11.3
Finland	64	1363	21.3
Netherlands	82	3085	37.6
Italy	137	2840	20.7

Sweden	64	1421	22.2
Germany	75	1659	22.1
Poland	75	461	6.1

For analyzing the collaborations between the countries, Figure 2-5 shows network visualization between different countries having publications in additive manufacturing and plastic recycling. The connecting lines denote the co-authorships between different countries. It can be seen that the UK has research links with the rest of the countries. The US, Netherlands, and Italy have strong connections with the remaining countries.

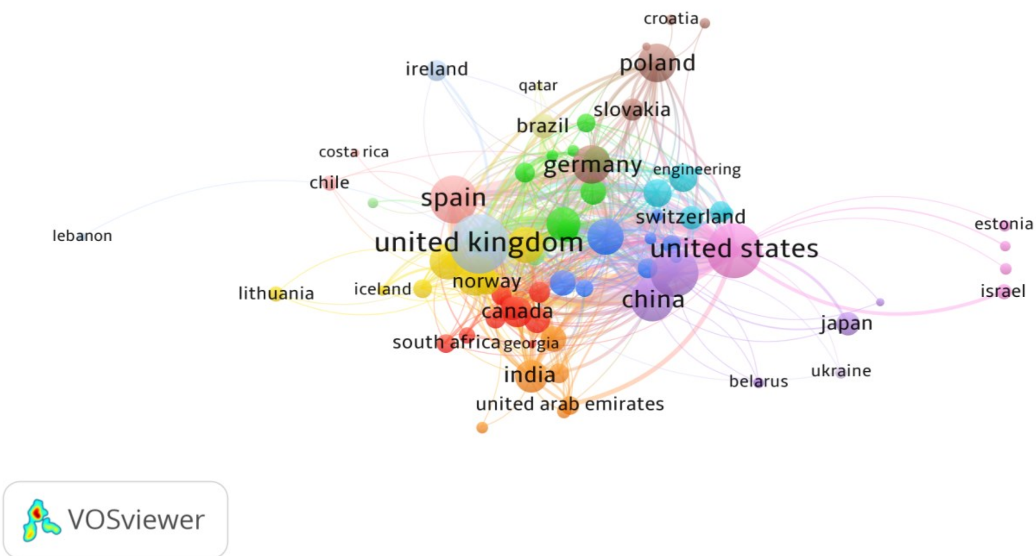

Figure 2 - 5 Visualization for collaboration between countries

2.4. Critical Review of Current Research of AM and Plastic Recycling

As was stated in the scientometric analysis results, the knowledge domains between the Fused Deposition Modeling process and the circular economy concept require special attention in specific topics where optimal connections in terms of material characteristics, processing parameter optimization, and novel recycling systems or technological approaches can be found. Hence, specific topics related to this matter are described in the upcoming sections.

2.4.1. Materials Characteristics of Recycled Polymers in Additive Manufacturing

Recycling polymer wastes into 3D printing filaments can save up to 100 million megajoules of energy per year compared to centralized recycling processes [14]. In addition, as a typical consumer-end FDM 3D printer can cost around 100 USD [135], an on-site recycling system employing polymer wastes would be able to reduce the cost of some consumer goods by up to 99% [14], leading to a highly competitive market advantage while creating new plastics products [136], [137]. In the same way, a positive environmental impact is generated as AM technologies have been estimated with the potential of saving up to 5% of CO_2 emissions in the manufacturing sector at a global scale [63]. Hence, the imperative necessity to find out efficient ways of recycling plastics and utilizing them to create useful products in this process chain is required [138], [139]. FDM seems to be a possible solution with a high degree of future implementation, but there are still some limitations [140]. With the boom of the 3D printing technique, worldwide plastic consumption already reached 18,500 tons in 2020 [141]. So there is always an added risk of waste generation if the end by-products are not correctly disposed of or recycled [142]. Although much of the waste is being recycled through various means depending on the material properties, the amount of waste generated from this process is still uncertain [143].

Lately, 130 different 3D printing materials have been classified among polymers, ceramics, metals, etc. [141]. Since the interest of this work is to narrow the analysis to plastic materials, characteristics of the most common thermoplastics for recycling purposes have been discussed. The most common materials for desktop FDM printing are ABS (Acrylonitrile Butadiene Styrene) and PLA (Polylactic Acid) [144]. Studies have shown that ABS has an amorphous nature and high fluidity at high glass transition temperatures [144]. However, at the same time, the hygroscopic nature of ABS (due to polar nitrile groups) results in high water absorption, which may affect the quality of the final 3D-printed products [145]. Polymer-based biomaterial such as PLA (Polylactic acid) has been used extensively in dentistry applications because of their mechanical and biological characteristics [141]. Nonetheless, the properties and limitations of 3D printing materials have an essential role in the quality of the printed product, but several precautions have to be taken when dealing with both of these materials [135]. For instance, 3D printing with ABS or PLA as feedstock materials often produces ultra-fine aerosol (UFA) fumes and can be harmful to humans [135]. Since ABS lacks UV resistance; it is modified into ASA (Acrylonitrile styrene acrylate) in order to ensure quality printing [146]. As a summary in Figure 2-6, a pyramid of 3D printable plastics, which are characterized based on service temperature and crystallinity is shown for stablished comparison.

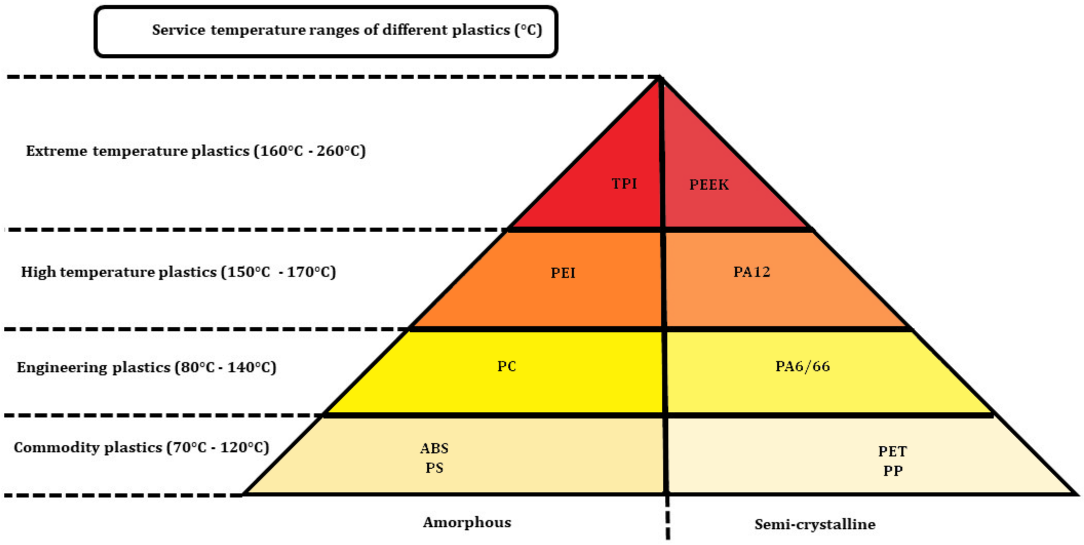

Figure 2 - 6 Pyramid of plastic performance (adapted from [147],[148])

As it can be noticed, other than ABS and PLA, PET (Polyethylene terephthalate) is another common thermoplastic used in the FDM process. PET is one of the most important engineered plastics in its virgin state and is used in broad areas such as food packaging materials, automotive products, and electronic equipment [149]. It has superior mechanical properties and good thermal stability [149]. Since it is a non-biodegradable plastic and one of the most suitable materials to recycle compared to aluminum [150], [151], DRAM is an economical way to reduce PET waste [149]. In the studies of *Kreiger* [152], it was shown that recycled PET could be a potential material for distributive manufacturing which focuses on the manufacturing of value-added parts and products but has a lower performance than the virgin counterpart as it undergoes various thermal and mechanical stresses during multiple processing cycles [152].

Other than these common thermoplastics, some not-so-common polymers can be used as potential alternatives for recycling [135]. Materials like HIPS (High Impact

Polystyrene) are still under-valued in terms of their ability to 3D print good quality products and are used mainly for printing support structures [40], but it shows minimal variation in the melt viscosity when subjected to reprocessing [135]. It undergoes chain scission by mechanical and thermal degradation due to the multiple reprocessing steps, increasing its MFI (melt flow index) and processability [135]. Further, over multiple recycling steps, HIPS experiences an increase of tensile stress at break and a decrease in elongation at break and presents a material behavior transition that takes place from ductile to brittle [40]. In the same way, Polycarbonate (PC), the main constituent of electronic waste categorized as commodity number 7, has proved to be another potential recyclable material [40] as it can be reprocessed up to five cycles, without any significant variation in its tensile strength and modulus [153]. Nevertheless, a 37% and 42% decrease have been found in the elongation at break and the toughness values, respectively [40]. Additionally, in terms of the environmental impact, it has been found that it has become essential to recycle PC to prevent the leaching of "Bisphenol A" which can bring harmful damage during landfilling [40]. In summary, there are still only a limited number of thermoplastics that are available for 3D printing that is well established in the DRAM context. Another approach is the use of compatibilizers [154]. In some studies, it has been shown that plastics such as PET, PS (Polystyrene), and PP (Polypropylene), when used individually, are not ideal feedstock materials for the FFF method due to several possible reasons such as water absorption tendency, lack of control of crystallinity which leads to poor printing [155]. Despite having almost similar toughness, PP does not have enough strength to be called engineering plastic like ABS [155]. However, its mechanical properties can be significantly improved with PS or PET [155]. This reinforcement generally demands the use of a compatibilizer as PP is immiscible and incompatible with both PS and PET [154].

Of the several 3D printing technologies which can be used for these plastics, FDM is the most common method [156]. It is a method in which the thermoplastics are deposited in their filament form in a specific pattern by the melt extrusion method [157]. Figure 2-7 shows what a typical FDM process looks like. The term FDM is often used interchangeably with FFF as both refer to the same 3D printing process. Although a similar ideology has been followed in this work, and the terms FDM and FFF are used with the same intent, it is still important to know the minute difference between terms. FDM technology was invented in the 1980s by Stratasys ltd. who also patented the term FDM in 1989. Thereon, all the companies working on the same technology have been using FFF [158]. The feedstock materials used in this method have a low melting point and low viscosity to be easily extruded from the nozzle [156]. This leads to efficient deposition and adhesion under low-pressure layers [156].

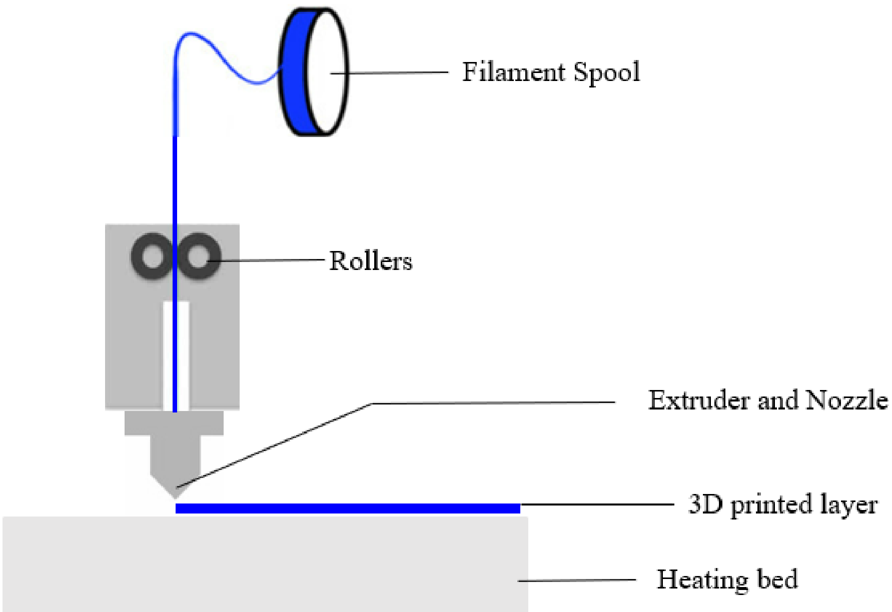

Figure 2 - 7 Fused Deposition Modeling (FDM) process

The use of recycled plastics in the FDM process has been acknowledged in recent times due to increased sustainability and many reduced costs and providing high-value output [156]. Several companies have acted on this idea and started making commercial filaments from recycled plastics [159]–[163]. For example, Kickfly® manufactures ABS filaments which comprise 95% of recycled materials. On the other hand, companies like Refil®, Maker Geeks®, and B-PET® sell filaments made from recycled PLA and PET. Some start-ups like ProtoCycler® have even made a single-unit plastic recycler that can grind as well as extrude [164]. The recycling of plastics using the FDM process is a systematic process and involves many different stages [165]. Initially, the thermoplastics are shredded and pelletized [165]. The pellets are then dried before processing, as this drying effect governs the flow behavior of plastics [166], [167]. If not appropriately dried before extrusion, it often leads to a non-uniform filament diameter, resulting in poor printing [165]. Inadequate drying may result in bubble formation in the printed part [168], [169], which leads to the formation of voids that ultimately deteriorates the mechanical properties of the 3D printed part [165]. After the filament has been extruded, the cooling process plays a major role in affecting the crystallinity of the filament [170], [171]. Rapid cooling may lead to improper inter-layer diffusion of polymer chains which can lead to failure at those interfaces [165]. The upcoming section describes various FDM parameters with an approach toward optimizing the quality of the FDM products.

2.4.2. Influence of process parameters of Fused Deposition Modelling (FDM) to assess Recycled Plastic Product

The FDM process consists of multiple processing parameters set either from the virtual model design or conditions to manipulate the plastic flow behavior and solidification or by printing machine specifications [172]. Therefore, the FDM parts have varying properties based on their combinations [173], [174]. Parameters such as layer thickness, raster angle, and orientation, road width, air gap, etc., have specific impacts on the end properties of the plastic component produced [172]. For example, layer thickness, raster angle, and air gap directly affect the elastic performance of the FDM printed product [140]. Changes in these parameters can lead to insufficient material flow, which generates voids or air gaps in the volume of the FDM product structure, ultimately reducing the effective cross-sectional area and affecting the part quality [140]. Since strength and dimensional accuracy are the two most important aspects to be considered while manufacturing FDM parts [175], it is essential to find the most optimum combinations of parameters that enhance mechanical properties. The given examples can very well explain the need for these optimal parameter-combinations: high printing speed improves the printing efficiency [176] but at the cost of less plasticizing effect of extrusion materials [177], whereas low printing speeds can lead to uneven filament diameter [178], which may complicate the fusion bonding process [179]. In this case, a better quality product can be achieved by implementing optimal parameter conditions for printing speed, filament diameter, and material plasticity [180]. Another example is the printing temperature which affects the crystallinity of the material and, ultimately, the mechanical properties of the printed product [181]. Very high extrusion temperatures often lead to material degradation [182], due to which the material is not able to regain its shape on deposition [183], which leads to filament deformation and dimensional inaccuracy [184]. However, low extrusion temperature does not fully melt the material, which can result in nozzle clogging [181]. Hence, poor mechanical performances are often attributed to extreme process parameters, which can either be excessive or insufficient [185]. This section provides a brief review of different studies conducted recently or in the past that have manipulated several machine process factors to observe the change in tensile properties of the FDM printed parts.

Since FDM is a material extrusion process, temperature plays a vital role in the quality of the end products [186]. FDM is known to cause thermal degradation as it involves high temperature [186]. This deterioration can be explained by the filaments losing viscosity to increased fluidity at high temperatures, leading to the generation of voids in the printed parts, which results in reduced strength [187]. Extrusion temperature and base temperature play a significant role in governing the strength of the PLA and ABS fabricated parts [188]. For PLA, the relation between the tensile strength and the extrusion temperature is linear until a temperature range of 200-220°C, after which the properties start deteriorating [189].

Parameters such as Raster angle (RA) directly influence the anisotropy of the FDM parts [190], [191]. The printed structure in which the raster is aligned in the longitudinal direction display high tensile strength, while the parts having raster along the transversal direction have low tensile strength [172]. FDM roads often lead to discontinuities at radiused corners, which lead to the generation of stress concentrations at such transitions [57]. Tensile strength and stiffness can be enhanced by using negative air gaps while creating the parts [57]. Along with the properties of the raster angle, the amount of material present inside the 3D printed component, called infill or infill density [192], [193], is also a critical parameter as it significantly affects the tensile strength and modulus of the printed parts [194]. To attain high strength and low weight, it is vital to choose an optimum infill percentage [194]. Reduction in the infill density reduces the load-bearing capacity of the parts, which affects the specific flexural strength and the mechanical properties significantly [195]. As the infill percentage increases, the stress increases as the resistance area increases, resulting in higher tensile strength [196]. Infill percentage affects the bond strength of the layers [197]. Apart from infill density, the infill pattern is also one significant parameter [198], [199], and it checks the interaction within the filaments when the load is applied [200]. Changing infill patterns affects building time, energy consumption, material strength, and surface quality [200]. Studies have shown that due to the crisscross layer arrangement, the grid pattern imparts the highest tensile strength when compared to other infill patterns [201]. Another study conducted by *Chadha A.* showed that the highest strength under both bending and tension was displayed by triangular patterns followed by grid and honeycomb structures [202].

The print-head component 'nozzle' is an integral part of the FDM system [203], [204] and is also responsible for causing significant variations in the print quality [205]. An increase in the nozzle diameter leads to wider raster deposition, which results in the overlapping of neighboring strands and better fusion on solidification [205]. A study by *Jatti V.S.* on PLA parts showed that at constant layer thickness (Lt), an increase in the nozzle diameter leads to enhanced flexural strength [206]. Also, as Lt decreased, the strength of the PLA parts increased [206]. So, it was concluded that as the ratio of nozzle diameter to layer thickness increases, it results in higher flexural strength of PLA [206]. These results, however, cannot be generalized as a specific parameter can lead to different effects in mechanical properties for different materials. For instance, in a study conducted on PA12 by *N. Vidakis*, it was observed that the strength of the parts decreased when layer height was increased from 0.15 mm to 0.20mm. The mechanical strength, however, increased for values of layer height between 0.20-0.25mm [207]. Although the tensile strength of both ABS and PLA filaments decreased with increasing

Lt, the impact and compressive strength had a direct relationship with Lt [208]. However, this relation might not be valid for low infill densities as the large voids can decrease the compressive strength [209]. This analysis of the relation between compressive strength and Lt for ABS provided by *Naimon* was contradicted by *Nomani* who showed that lower Lt leads to better compressive strength [210]. Low values of layer height results in a greater number of layers which leads to more deposition interfaces that promote better adhesion bonding strength which ultimately increases the mechanical strength of the ABS specimens [210]. A past study conducted by *Pritish* has stated that the impact strength of ABS decreases with increasing Lt [211], which contradicts the findings of *Naiomon*. High layer thickness leads to poor micro-bonding between the interface which results in low toughness and hence poor impact strength [211]. Hence, the effect of the interaction of multiple parameters is vital and needs to be considered in the printing conditions as this may lead to various discrepancies in the results and lead to poor surface finish [209]. The stair-stepping effect is one of the common reasons for the poor surface finish in layered manufacturing technologies [212]. The small thickness of layers usually prevents this effect to some extent. Less thickness also reduces manufacturing time and hence reduces manufacturing costs [213]. Besides layer thickness, optimal part orientation is another aspect that can help reduce material consumption and lead to faster production time [214]. Similarly, another significant influence on the quality of a 3D printed product related to the virtual modeling stage is the orientation of printing [175]. Build orientation (BO) is an important parameter that forms a bridge between the orientation of the print and its strength [172]. Various studies have been conducted in the past to observe the effect of different orientations on the tensile properties of the FDM printed material [172]. Some general conclusions [172], [175], [179] state that On-edge (O) and Flat (F) specimens have the highest tensile and flexural strength as well as stiffness, whereas Upright (U) specimens have the lowest ones. The reason can be attributed to the concept of failure modes- interlayer fusion bond failure and trans-layer bond failure [175]. For U specimens, the samples experience a pull force perpendicular to the loading direction, which results in inter-layer fusion bond failure. This way, the applied load is withstood by the bonds between the adjacent layers and not by the roads themselves [200]. The strength of these specimens comes out to be even less than the strength of the individual fibers [200]. On the other hand, for O and F specimens, the pull force is parallel to the loading direction. Hence, the force of the applied load was withstood by the individual fibers resulting in trans-layer failure, which led to greater strengths [215]. Figure 2-8 shows different process parameters of FDM such as infill pattern, infill density, raster angle, and build orientation.

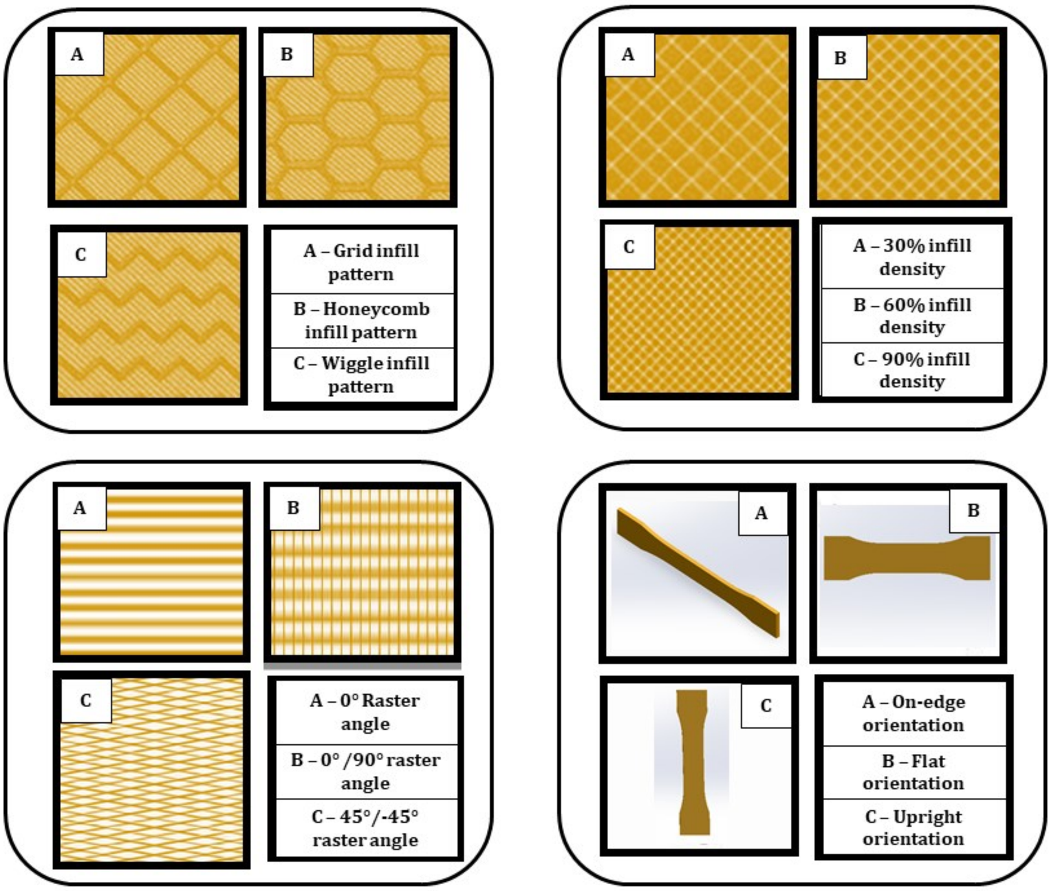

Figure 2 - 8 Process parameters for FDM- Infill pattern, Infill density, Raster angle, and Build orientation

A summarized compilation is shown to collect the counter effects between the most important FDM process parameters on the tensile strength of specific plastics materials in Table 2-5.

Table 2 - 5 Literature review on the effect of FDM process parameters on tensile strength of different thermoplastics

Material	Parameters examined	Remarks	Source
PLA-Wood (Ratio - 70%:30% by weight)	Layer thickness (Lt), Extrusion temperature (ET), Raster angle (RA), Printing speed (PS)	The 0° raster angle imparts the highest strength when compared with 45° and 90°. An independent relationship between Lt, ET, and PS with UTS could not be established. These parameters are significant but need to be studied independently as analyses could only be done based on the effects observed by the interactions of Lt, PS, and ET. As for lower Lt, ET is insignificant and PS has a weakening effect whereas for higher values of Lt, ET is significant but PS strengthens the specimen.	[216]
ABS	Build orientation (BO)	Flat orientation has superior UTS as compared to the upright orientation as the layers in the former are horizontal and are parallel to the loading direction	[217]
ABS	Raster angle (RA) (0°/90° and 45°/-45°)	The 0°/90° orientation has higher tensile strength than the 45°/-45° orientation as the surface structure of the former is along the direction of the applied force and the load is supported by the long road, which is in the same direction	[140]
PC	Raster-to-raster air gap (RRAG)	On introducing negative RRAGs, the inter-raster bonding gets stronger, which results in increased tensile strength	[218]

PEI	BO, Filament thickness (F_t)	For thick filaments, build orientation should be on-edge and upright, whereas, for thin filaments, the build direction should be flat, to achieve better tensile strength.	[219]
ABS	Layer thickness (L_t)	Minimum layer thickness leads to better tensile strength as it imparts additional bulk and cracks resistance to the structure	[220]
PEEK	Printing Speed (PS), L_t, Extrusion Temperatur e (ET), Infill density (ID %)	A relation cannot be established between PS and ET with the tensile strength. ID% is directly affecting the strength of the specimen, whereas L_t has an indirect relation with the tensile strength	[181]
PLA	BO, Feed rate (F_r)	On-edge (O) and flat (F) specimens had the highest tensile strength by trans-layer bond failure, whereas upright (U) specimens had the lowest strength due to inter-layer bond failure. F_r has no significant effect on O and F specimens but had an indirect effect on the strength of U specimens.	[215]

ABS	Surface roughness (SF), BO	SF values are contrasting for parallel and perpendicular directions. In the parallel direction, maximum SF is found for upright specimens, while in the perpendicular direction, flat specimens had the maximum SF values. On-edge specimens had nearly the same values of SF for both directions.	[214]
PLA	BO, Infill pattern (IP)	On-edge specimens displayed higher strength than Flat specimens. The IPs Honeycomb and grid have the highest strength and lower weight as compared to the solid, whereas the rectilinear and wiggle pattern has the weakest strength.	[200]
ABS	ID%, IP	Tensile strength has a direct relation with the infill percentage. Triangular, grid and hexagonal IPs have comparable strength, whereas honeycomb and wiggle have the minimum and the maximum tensile strength.	[221]

As can be seen in Table 2-5, the effect of some parameters, such as layer thickness (Lt), on the mechanical strength is difficult to analyze independently. These parameters often show their significance while interacting with other parameters. However, these parameters may be evaluated on other grounds. For example, in one of the studies conducted on PLA-wood composite material, it was concluded that Lt has a direct relation with surface quality and dimensional accuracy [222]. However, ET remains to be insignificant when its effects are observed on the surface quality but is quite significant when analyzed over dimensional accuracy [222]. The insignificance of ET has also been shown in a study conducted on PET-G, where no considerable changes were observed in the flexural strength of the specimens for different values of ET [223]. This indicates that ET still requires a lot of research for non-conventional plastics.

Finally, the color of the material is one underrated parameter on which few studies have been conducted [224], [225]showing its effect on the mechanical properties of the printed product [226]. It has been found for differently colored PLA materials that color influences the polymer's crystallinity and hence impacts the strength of the printed product [226]. However, some studies, such as the one conducted by *Montero M.* have disregarded color as a parameter influencing the quality of the FDM product as no significant effect was observed. This study was conducted on ABS P400 polymer and the color of the material had a minoreffect on influencing the printed parts' tensile strength [217].

Concerning the earlier text, the complexity of the FDM process can be explained by the fact that it involves a large number of factors, and only a specific combination of these parameters leads to optimized mechanical properties [215]. However, the lack of proper 3D printing standards also adds to this fact [220]. Different 3D printers may operate on different testing conditions to achieve the same quality. The intra-3D printer variability due to the presence of large printers is one reason why the comparison between the printed products from different printers operating at the same testing conditions is also complicated [227]. It is hence essential to set standards for AM processes. However, the complexities of the FDM process provided in this section cannot limit the potential uses of this technology; on the contrary, the main focal point is to adjourn the previous factors mentioned to reprocess the most common materials in FDM. The approaches used in FDM and their combination with the fabrication of multi-material units are equally important, which are discussed next.

2.4.3. Multi-material mixing of plastics - An interesting approach toward polymer blending

The majority of the FDM systems extrude a single material at the commercial level [228]. However, recent advancements in 3D printing have [102], [229] allowed the FDM setups to print multi-material units (MMUs) either by using multiple nozzle systems, such as the case of the RoVa3D setup manufactured by ORD solutions that can print five different filaments using five separate nozzles [228] or multi-in-one-out single nozzle systems [230] where polymer types pass through an entirely blending mechanism to print one mixed filament. These MMUs printed from varying nozzle systems come under the category of Functionally Gradient Materials (FGMs) [231]. For the case of the printing technology of FGMs, it is still a field that requires a lot of research, and the main studies that have been conducted are by [231], [232] but are considered insufficient.

For printing FGMs, both multi-in-one-out single nozzle systems and multi-nozzle systems, different efficiencies can vary, leading to a mismatch in the performance efficiencies of the final 3D printed multi-material part [233]. A multi-in-one-out single nozzle can be used to print mixed filaments and gradient materials by extruding multiple materials or multiple colors [233]. For the nozzle to melt multiple input filaments, it either works between a range of temperatures between different polymers or might even work at a single temperature value if the difference in the melting points of the polymers is not significant [234]. While using this multi-in-one-out single nozzle system, there are very few chances of any calibration error during material deposition [233], and hence this system is a preferred choice over multi-nozzle systems for printing gradient materials [233].

On the other hand, multi-nozzle systems are generally used in extrusion-based AM systems where for printing multi-colored or multi-material printing, two or more separate nozzles are mounted side-by-side on the same carrier [235]. However, this multi-nozzle system often contributes to calibration and oozing issues due to idle extruders [235]. These issues can be solved by two means- disabling one of the idle hot end nozzles while the other is printing or by enabling filament retraction for each polymer before it switches to another material to print a section [233]. A study [236] showed that a single nozzle system prints more consistent quality products, whereas multiple nozzle systems have better build time [236]. Table 2-6 shows the recent work done on polymer blending of different thermoplastics.

Table 2 - 6 Literature on polymer blending of different combinations of thermoplastics

Multi-materials mixed	Process involved	Remarks	Source
HIPS + ABS	Mechanical interlocking	The designed setup used a single nozzle for printing with the help of a static intermixer. This chaotic advection of flow inside the intermixer led to a proper mixing by mechanical interlocking of the molten polymeric liquids.	[231]
HIPS + ABS	Mechanical keying	Same methodology as above. The bond strength between adjacent deposited roads in side-by-side printing was 12 times lower than that of the fibers in intermixed printing	[232]
PA (Polyamide) + ABS	Compatibilization *(Compatibil*	For mixing the molten form of PA and ABS, first ABS was compounded with SMA, followed by compounding the SMA-activated ABS with PA. These compounding processes were carried out with the help of DSM Micro 5	[237]

	izer used- Poly(styrene -maleic anhydride) (SMA))	twin-screw micro-compounder at a temperature of 518 K with a residence time of 180 seconds and a screw speed of 100 RPM.	
PP + PET, PP + PS, PS + PET	Compatibilization *(Compatibilizer used- Styrene ethylene butylene styrene (SEBS))*	rPP and rPET blends formed a consistent and flexible filament that was easy to print. Blends of rPS and rPET yielded a brittle material, whereas the blends of PS and PP displayed good flexibility. It was also observed that the compatibilizers played an important role in enhancing the bonding between the phase boundaries. The glass transition temperatures also increased.	[155]
PP + PLA	Compatibilization *(Compatibilizer used- Maleated polypropylene (MAPP))*	The compatibilizer was used to mix blends of dried BF (bamboo fiber), PP, and PLA. These were then mixed in a co-rotating twin-screw extruder at high speed for 8 minutes. It was observed that the compatibility of a polymer-polymer interface should be considered over a fiber-polymer interface as it plays a more significant role in obtaining an ideal structure.	[238]
PLA + PA11	Compatibilization *(Compatibilizer used- Joncryl)*	For extrusion, PLA and PA11 pellets were first dried overnight under vacuum at 80°C. The compatibilizer was also dried at 80°C for 15 minutes. The first modified PLA pellets were developed by mixing with four wt% Joncryl. It was then mixed with PA11 and virgin PLA. For preparing the blend, a co-rotating twin-screw extruder was used.	[239]

The concept of multicomponent composite systems opens several doors for applications in areas that demand unique mechanical properties [240]. To benefit the environment and ensure a noble use of any recycled polymer, filament recycling plays a key role [241]. Since the mechanical properties of recycled polymers are known to deteriorate, a blend of recycled and virgin material is an acceptable trade-off to preserve that material's mechanical properties [135]. Some recycled polymers, when blended, show improved properties, while others are undisturbed and have the strength just like the original polymer [238]. The blending can be done with the help of compatibilizers keeping in mind the fact that the polymer pairs can be thermodynamically immiscible [238]. Compatibilized polymer blends offer a wide variety of feedstock materials along with a cost-effective method to reuse mixed plastic wastes [155]. For mixing two or more polymers, the solubility parameters of the polymers should be nearly equal; only then are the polymers miscible [239]. On the other hand, if the solubility parameters of the polymers are not compatible, they become immiscible, and also various compatibilization methods enhance the interfacial adhesion of two immiscible polymers [242]. These can include the incorporation of a co-polymer or areactive polymer [243]. For instance, to ensure better blending results with PLA, ABS was incorporated with 38% of polybutadiene content to ensure thermodynamic feasibility in the mixing of these two polymers [243]**.** The working of any compatibilizing additive (coupling agent) is that it operates at the multi-phase blend interface and enhances the adhesive bond strength [237]. Interfacial adhesion (bead-bead adhesion) is an essential factor linked to the uniformity of the mechanical properties in additive manufacturing [237]. However, there is still a lot to explore about the blending effects on the interfacial properties.

Co-extrusion through intermixing by mechanical interlocking has proved to be yet another efficient way of 3D printing FDM-style multi-materials using polymer blends [244]. Here, the working of the intermixing becomes crucial because the mixing of the polymers next to the nozzle orifice can significantly improve the bond strength between the polymer filaments [244]. The orientation of the intermixer blade should be such that it allows the molten polymeric liquids to split, combine, re-split, and eventually re-combine [244]. It has been observed that intermixed extrudates have better properties than side-by-side extrudates [231]. They have fewer delamination issues, better bonding strength between the two filaments, and also better strength during the transition of one material to another in printing FGM devices [231]. Even the composite sheets made from interlocking mechanisms exhibit higher breaking force when compared with those made through side-by-side co-extrusion mechanisms [231]. Figure 2-9 shows the different mechanisms of multi-material mixing.

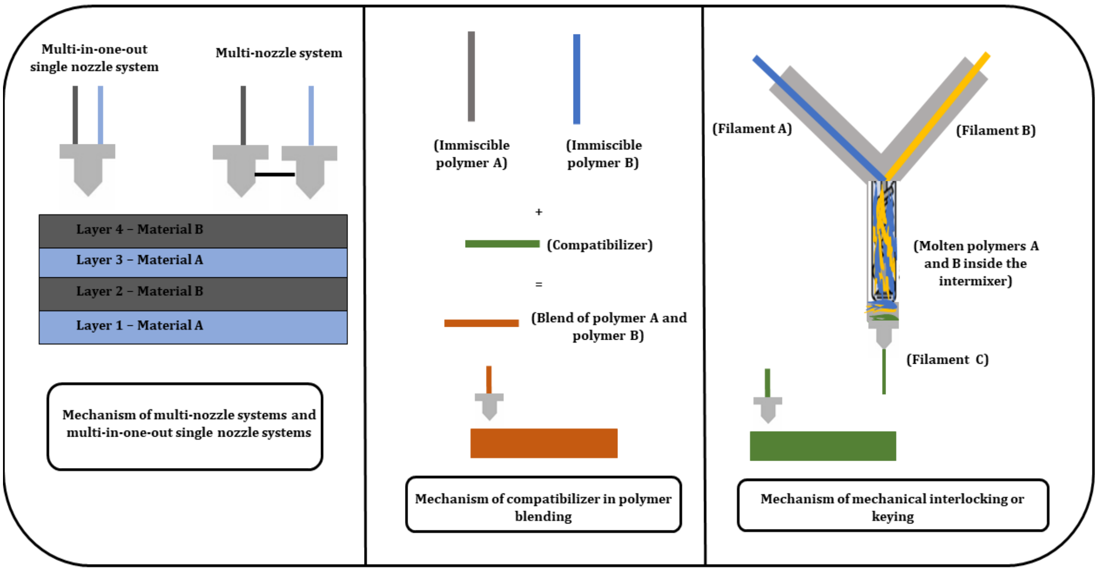

Figure 2 - 9 Different mechanisms of multi-material mixing of plastics

One significant example of multi-material AM technology is in the medical field as it contributes to developing tissue engineering structures for delicate human parts [245]. It also has applications in electronics as the different properties of materials can be integrated into a specific circuit [245]. Multi-material FDM technology does have some drawbacks, such as poor surface finish, poor resolution, lower interfacial bonding, and slow build speed [246]. The difference in the physical and chemical properties of the different materials in multi-material FDM justifies the lower interfacial bonding in the process [246]. Multi-material printing also has some areas to explore, such as printing efficiency [247]. The former can be achieved by employing higher energy power and faster scanning speeds. However, this often leads to low printing accuracy [247]. Another challenge in the multi-material domain is the weak bond strength between the adjacent layers of different materials by the defect formations due to the differences in the physical and chemical properties of the materials [236].

Multi-material AM technology is a complex process and offers several challenges during printing. It becomes highly essential to have a well-defined system that absorbs all the complications of this process and imparts good results, unlike the existing printer setups. An approach adopted in recent studies is designing direct deposition systems that directly make use of plastic pellets or shreds and save time by skipping the step of filament fabrication as in conventional FDM printers and promoting plastic reuse [248]. This is a current area of research as many custom designs are being proposed for direct deposition systems to upgrade the layer deposition 3D printing process and increase recycling rates. The next section describes a deep analysis of this technique and its main characteristics.

2.4.4. Direct FDM systems

Most of the FDM printing technologies follow the approach of FFF and rely on filaments. However, not all materials can be extruded in the form of filaments due to a lack of complex functionalities [248]. This restricts the use of FFF in manufacturing functional materials [249]. To overcome this limitation, many projects have been working on different print heads to extend the material feedstock options. Direct FDM systems have emerged as potential alternatives to conventional FFF systems and directly make use of plastic powder, pellets, flakes, granules, or shreds in 3D printing [250]. These systems have screw-based print heads, which consist of an auger screw that helps in the transportation of the molten material [248]. This section provides a short review of studies conducted on these systems' customized designs using different thermoplastics.

In the filament extrusion process, as the filament feedstock is pushed through the liquefier, any variation in the diameter of the filament may cause blocking [248]. A large-diameter filament may block the extrusion process, whereas a small-diameter filament may not touch the walls of the extruder and can lead to material rise between the filament and the wall [248]. Buckling of the filament can be another interruption in the building process. The limited availability of polymer feedstock materials is another drawback of the filament-based 3D printing process [249]. On the other hand, since the materials are no longer restricted by their mechanical properties in the filament form, the materials are widely available for the direct deposition process [251].

A direct FDM system includes many dimensions to study. This work is limited to screw-assisted systems working on extrusion additive manufacturing (EAM). Since these systems can be directly fed with granulated materials, EAM is emerging as an enabling technology that expands the range of 3D printing materials, reduces feedstock fabrication costs, and increases the rate of material deposition compared to the traditional FFF process [252].

As the name suggests, a screw-assisted system contains a screw extruder of different types. Single screw extruders are among the most common extruders having a smooth or grooved inside barrel surface [252]. It can also contain a degassing zone to extract any moisture that can form during the extrusion process [253]. A schematic diagram of a single screw extruder is shown in Figure 2-10. Another common extruder category is the twin-screw extruder [250]. This consists of co-rotating or counter-rotating screws which can be intermeshing or non-intermeshing. The essential use of these extruders is to mix and compound the polymers [250]. This process creates high shear and extension forces, leading to enhanced distributive mixing [250]. In general, there are three zones inside a plasticating extruder- the solids conveying zone, the Transition zone, and the Metering zone [254]. The solid pellets are transported from the hopper to the screw channel in the solids conveying zone. These pellets are then made compact and made to move down the channel. The process of compacting the materials is possible only if the friction at the barrel surface is more than the friction at the screw surface [255]. The barrel friction is responsible for moving the pellets in the axial direction. In the absence of barrel friction, the rotational speed of the pellets is less than that of the screw, due to which the pellets cannot attain an axial push. At last, the pellets are then melted and made into a homogenous mixture. This mixture is finally pumped through the die. This friction between the barrel and the pellets can be maintained at a higher value if the feed section inside the barrel is kept at a cold temperature [256]. This can be done with the help of cold water cooling lines. Higher friction ensures higher pressure rise. This pressure is utilized to compress the solid pellets, which melt as they travel down the channel in the transition zone. Another method to increase this friction is to groove the barrel surface in the axial direction [257]. Grooving leads to higher productivity and higher melt flow stability. However, surface grooving has some limitations. The length of the grooved barrel section should not exceed 3.5 D; otherwise, the excessive pressure may result in barrel or screw failure [258]. Inside the transition zone, the relative motion between the barrel surface and the solid bed conveys the freshly molten polymer from the melt film into the melt pool. This also results in the solid bed pushing against the leading flight of the screw. It is important to define the starting and end point of the melt zone in order to come out with an optimum design of the screw. This length of the zone depends on material properties, the geometry of the screw, and the processing conditions. The metering zone is responsible for generating sufficient pressure for pumping [52].

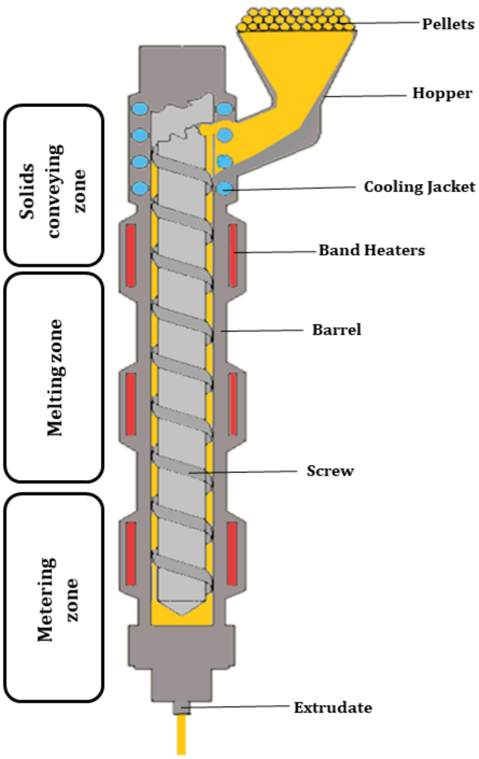

Figure 2 - 10 Schematic diagram of a single screw extruder (adapted from [259])

Since the mixing capability of a single screw extruder is limited due to the absence of specific mixing zones, it becomes essential to blend the powder before the start of the printing process. To create an internal pressure to extrude the material, the material is compressed along the length of the screw [260]. This compression is possible due to the linearly increasing core diameter of the screw. A stepper motor is used to rotate the screw in small increments to impart constant mass flow for a smooth printing process. Also, to prevent the possibility of any damage due to the misalignment of the screw and barrel, the latter is made from harder steel than the former [261].

As per the literature, there have been several proposals for screw extrusion designs and several modifications as well as revisions in the earlier existing models. Table 2-7 shows some literature on work done on direct FDM systems.

Table 2 - 7 Literature review on direct FDM systems

Material(s) used	Novelty in design	Remarks	Source
PS, PP, PLA, PCL (Polycaprolactone)	A three-section plastic processing screw was designed in the proposed extruder system and applied at the print head. This print head is mounted on the Cartesian frame of a retro-fitted Coordinate measuring machine (CMM)	The print obtained from the proposed extruder was a smooth surface without any trapped air.	[248]

Ethylene-vinyl acetate (EVA) and Poly(1-vinylpyrrolidone-co-vinyl acetate) (PVPVA)	A single screw hot-end of 8 mm had been designed and characterized in this work.	The materials used in this work are either difficult or unable to be processed in the form of filaments. For instance, PVPVA and EVA are brittle and frequently fracture during filament processing.	[261]
Thermoplastic polyurethane (TPU)	A large tapered conical screw was developed.	The conical screw-based extrusion deposition (CSBED) system had more plasticizing and extruding efficiency as compared to the conventional screw system.	[262]
Polyether-ether-ketone (PEEK)	Exchangeable printing head to implement line and plane-printing additive manufacturing.	To date there are no proper guidelines to 3D print highly viscous materials such as PEEK. This system allowed efficient layering of PEEK. Also, the printed parts had better surface roughness than conventional screw mechanism printed products.	[263]
ABS + 10% GF (Glass fiber)	The large-scale 3D printer used in this review had a double-stage screw extruder.	This system experienced issues such as unstable melt flow. The possible solution for this was to implement a pressure-stabilized extruder in the setup.	[264]

In the study conducted by *Woern A, L,*, an open-source RecycleBot version- Gigabot X, which is a large-scale direct deposition 3D printer, was used to print parts using FPF (Fused particle fabrication) technology [265]. To set the reference, the analysis of recycled PLA, ABS, PET, and PP was done for the already analyzed virgin PLA pellets [265]. It was observed that Gigabot X was able to print the material at a speed of 6.5X to 13X faster than the conventional 3D printers while maintaining nearly the same mechanical properties. This deposition system also utilized a wide range of recycled polymers and also required little post-processing [265]. Some common RecycleBot versions (direct deposition system) are Lyman, Filastruder, Filafab, EWE, Strooder, Felfil, etc. [265]**.** Another study by *Alexandre A.* analyzed the comparison of tensile strength of parts fabricated from both FFF and FGF (Fused granular fabrication) techniques using recycled as well as virgin PLA and showed that there was no statistical difference between the mechanical strength of the specimens made from both the techniques [266]. The shredded and pelletized materials had 74% and 36% less diameter as compared to the virgin materials [266]. Hence due to comparable properties, direct FDM systems are potential options for EAM.

2.5. Conclusions

The main idea of this chapter was to discuss the fused deposition modeling process in the context of plastic recycling. A scientometric analysis was done at the beginning to get a knowledge domain of the studies conducted in this field from 2013-2021. A total of 1452 relevant publications were filtered through the scientific-mapping approach. The number of publications per year on plastic recycling has been on increasing trend, which shows the growing interest of researchers in this field. Stats even showed that 'fused deposition modeling' and 'circular economy' had high connectivity with other keywords, highlighting the importance of this process and the economic model in the last decade. The analysis was done through network and density visualization techniques using VOSviewer software. The entire analysis formed a basis for amplifying the idea of forming a bridge between fused deposition modeling and plastic recycling processes. Finally, a critical review was done on various aspects of the FDM process in the recycling context. It was seen that various potential thermoplastics, mainly PLA, ABS, HIPS, PC, PET, etc. have material characteristics required for recycling purposes. However, materials like PP are not mechanically strong and have a chance to degrade on recycling. Hence PP was reinforced with PS or PET to make it mechanically strong enough to be able to use for recycling. However, since PP is not compatible with PS or PET, an external compatibilizer was used for this mixing. This generated the idea of multi-material mixing or polymer blending. Before discussing this idea broadly, some influencing parameters affecting the tensile strength of the parts printed from the FDM process were elaborated. The literature found that infill density and raster angle were important parameters as these had uniform conclusions. Although a relationship could not be established between the extrusion temperature and the tensile strength, it can be said to be an important parameter as it directly links the rheology of the material with the printing process. Other parameters, such as build orientation, showed that on-edge and flat specimens have higher tensile strength than upright specimens. After discussing the influence of the FDM parameters, the concept of multi-material mixing was highlighted. Out of the multi-nozzle systems and multi-in-one-out single nozzle systems, it was found that the latter had more consistent results, whereas the former displayed better results in build time. Another interesting method of multi-material mixing was through the blending of polymers. Various techniques were discussed in which immiscible polymers were blended either with the help of a static intermixer or compatibilizer. This method increased the variety of feedstock materials available for the FDM process.

Lastly, Direct FDM systems were discussed, which worked on the same ideology of increasing the variety of feedstock materials available for the FDM process as materials like PVPVA and EVA, which were earlier difficult to be processed in the form of filaments, could then be directly deposited from their pellet form. The mechanism of direct FDM systems was discussed, along with several studies on novel designs of these systems. From this literature, it is viable to conclude that there is a high potential to implement these systems applicable to the FDM process and execute multi-material printing. The review was finally concluded by discussing some future directions and scopes based on the literature survey. Where the main conclusion leads to a necessary set of research and experimental work on data to correlate reprocessablity factors, FDM parameters, and end mechanical properties.

Chapter 3 Design of Experiments to Compare the Reprocessing effect with FDM printing parameters on Mechanical Properties of PLA specimens towards Circular Economy

3.1. Introduction

Recycling plastics is a necessary step toward the reduction of new plastic feedstock and minimizing the amount of energy required for its production [40]. The process of plastic recycling gets difficult when it reaches the end of its life [267], and hence it is important to recycle them at an early stage in order to prevent their disposal in oceans and landfills. The main threat is not the usage of plastics, but the disposal of plastics after their use [268], and this generates an urgent need to develop mechanisms for recycling polymeric wastes economically and sustainably following the environmental safety and plastic waste management rules [269]. A serious concern is that polymeric materials consume around 4% of the global production of oils and gas in the form of feedstock, whereas another 3-4% is used in their energy transformation [270]. This deduces that it is important to use the polymeric materials efficiently in order to ensure minimal wastage [271]. However, at the same time, it has been estimated that there is an annual consumption of 18500 tons of plastics used in 3D printing [272]. Out of this, almost 70% contributes to plastic waste and gets accumulated in the environment [59]. This raises the need for 'Circular Economy', which makes the after-life use of plastics and contributes to the supply chain [273]. Recycling plastic is one such action that promotes this strategy [274]. The plastic circular economy promotes the flow of plastics in a closed cycle, which leads to a sustainable economy with optimized production costs and minimal plastic pollution [275]. It tends to avoid harmful emissions and, at the same time, harness all the extraordinary properties of plastic material [276].

3D printing technologies have widened their applications to various fields because of their efficiency, precision, and accuracy [141] and have provided ways to utilize recycled plastics and convert them to useful items [63]. However, despite having good material efficiency, the material sustainability is a threat to the 3D printing process [277]. To handle this issue of sustainability, closed-loop recycling, which is a key to a circular economy [278], can be a potential measure that can restrict the need to explore more commercially viable materials for the 3D printing process as it is way ahead of other processing methods like down-cycling and to landfill [277].

The feedstock materials used for 3D printing are fairly expensive and cost around 19-80 USD/kg [145]. These high material costs also promote the concept of plastic recycling [145]. Many extruders such as Felfil filament extruder, Filabot, Filafab, Protocycler^{+}, 3Devo, Noztek, Robotdigg etc., have started utilizing both recycled and virgin pellets to produce filaments [279]–[284]. On the other hand, organizations such as Plastic bank, ProjectSeafood, Perpetual Plastics Project etc., also work dedicatedly on waste plastic recycling for 3D printing filaments [145]. Several studies have aimed toward developing and utilizing biodegradable and recycled filaments in 3D printing technologies [285]–[287]. Utilizing recycled plastic wastes and transforming them into plastic filaments suitable for FFF (Fused Filament Fabrication) or FDM (Fused Deposition Modeling) printers has become a need of the current scenario [145].

As discussed in Chapter 1, Distributed Recycling via Additive Manufacturing (DRAM) is one potential solution for improving sustainability and promoting a circular economy worldwide [270]. The closed loop DRAM chain comprises six stages: recovery, preparation, compounding, feedstock, printing, and quality [72]. It is essential to know that, to date, there are several gaps in the DRAM literature. For instance, the printing parameters of recycled material are still not defined in the printing phase. Only few materials have been tested for their recycling ability, leaving a huge literature gap in the feedstock phase. Additionally, there is still a lack of information on the material properties after recycling and its effect on the 3D printing process.

The literature signifies that FDM is one of the most critical methods which is associated with plastic recycling. It is a complex process as it is associated with multiple parameters while only a specific parametric combination yields optimum results [288]. Many studies have been conducted in the past which have shown the influence of a specific set of parameters on the mechanical properties of the FDM printed parts [289]–[291]. Likewise, the scope of this work is limited to analyzing the effect of FDM parameters - Infill Density (ID), Raster Angle (RA), and Extrusion temperature (ET) on the tensile strength of virgin and up to 3 times recycled PLA. As per the literature, RA is a critical FDM parameter that can be defined as the direction of roads (beads material) relative to the direction of loading of the part [292]. RA governs the anisotropy of the printed product [293]. It has been found that longitudinally aligned rasters display higher tensile strength than transversally aligned raster orientation [294]. There are typically four types of raster angles- 0° or axial, 45°/-45° or crisscross, 0°/90° or cross, and 90° or transverse [140]. The majority of the studies have been conducted for these values of raster angles which signifies a gap in the literature. ID is yet another parameter that plays a critical role in ensuring a good bonding strength between the rasters and the layers [246]. This parameter indicates the quantity of material with which the component is 3D printed [198]. The modulus and the tensile strength of the FDM product are significantly affected by the ID [295]. Low ID contributes to low load-bearing capacity, whereas high ID contributes toward higher tensile strength

[296]. Hence to obtain low weight and high strength for a product, it becomes necessary to have an optimum ID [297]. Lastly, the third FDM parameter considered in this work is ET. Since the FDM process is prone to thermal degradation, it involves high temperature, which often leads to a loss of viscosity in the filaments by virtue of increased fluidity [298]. Hence an over-excessive temperature can lead to void generation in the final printed product, which attributes to low strength and dimensional inaccuracy [299], [300]. On the other hand, if the ET is low, the material will not melt properly, eventually clogging the nozzle [301]. It is, therefore, a critical parameter and has a governing role in the strength of the ABS and PLA fabricated parts [302]. Although PLA has a linear relation with the tensile strength for a temperature range of 200-220°C [303], literature shows that studies have failed to form a generic relationship between the ET and the tensile strength.

FDM processes generally demand materials that have bulk strength and elastic moduli in the range of 30-100 MPa and 1.3-3.6 GPa, respectively [165]. The material properties govern the type of recycling process to be used for plastics [304]. Some common thermoplastics, such as PLA and ABS, are mainly treated by physical recycling methods [72]. These thermoplastics are first shredded and reprocessed after melting [141]. ABS has excellent properties of heat resistance, high impact resistance, and toughness [233]. 3D printing, when done with ABS, generates harmful fumes of ultra-fine aerosols [305]. However, despite being a very common 3D printing thermoplastic, there are varying findings associated with the properties of ABS and hence there is a requirement for more studies to be conducted in order to utilize ABS for widespread applications [188]. On the other hand, PLA is a linear aliphatic thermoplastic polyester that is extracted from natural sources and has superior thermos-physical properties

[306]. High brittleness and poor thermal stability are some of the few demerits which limit its uses [238]. Since PLA is biodegradable, it is often preferred over other printing materials as it does not contaminate the environment upon degradation [233]. As far as the scope of this work, PLA has been used to compare the abovementioned mechanical properties. This will establish a base study for other potential thermoplastics such as ABS, PC, HIPS, etc.

Recycled material is cheaper than new virgin material, brings less energy consumption, and is environmentally friendly as the carbon footprint is reduced by at least 80% [307]. However, when it comes to utilizing recycled materials for 3D printing, it should be noted that many 3D printing technologies still lack information on the mechanical properties of reprocessed materials, and to increase the viability of using recycled materials for 3D printing purposes, there is a need for profound analysis in terms of material defects, processing conditions, end quality, and performance properties after recycling [308]. Hence, a novel idea of including the 'number of reprocessing cycles' as the fourth influencing factor has been considered in this work. In this way, this chapter aims to serve as a base study for filling several literature gaps of the DRAM approach, which are discussed earlier in this section. Finally, using the Design of Experiments - Taguchi Analysis, the four parameters have been ranked based on their severity in affecting the tensile strength of PLA printed ASTM standard D-638 Type 1 tensile specimens. The results have been analyzed, and suitable inferences have been derived.

3.2. Experimental details

This section provides an in-depth idea of various experimental aspects such as the material used, FDM process parameters, machines used, ASTM standard used, speed test, execution of design of experiments, and the time analysis.

3.2.1. Materials

As mentioned in the earlier section, PLA has been used in this work. The commercial 3D printing PLA filaments have been acquired from Innofil^{3D}, which is a Canadian filament store. The standard extrusion temperatures have been maintained to avoid warping and stringing issues during printing. Similarly, an optimum bed temperature well above the material's glass transition temperature has been maintained to ensure a reduced surface tension between the material and the bed surface, which leads to proper adhesion [309]. Lastly, in order to avoid inconsistencies in the print and jamming of the FDM extruders, it is necessary to remove any possible atmospheric moisture absorbed by the filaments when exposed to the environment [310]. Hence, the filaments are dried at a specific temperature for a specific time, depending on the material type. The specifications for PLA are shown in Table 3-1.

Table 3 - 1 Material specifications [311]

Material	Filament Diameter	Standard Extrusion Temperature Range	Standard Bed Temperature Range	Drying Temperature	Drying Time
PLA	1.75 mm	210-230°C	50-70°C	80°C	4 hours

3.2.2. Methodology

This section discusses in detail the methodology followed in this work. The flowchart shown in Figures 3-21 and 3-3 describes the entire process of printing, shredding, filament making, reprocessing, and tensile testing of specimens.

3.2.2.1. Design of experiments and Taguchi Analysis

Taguchi analysis has been employed in this work for analyzing the effect of process parameters. This method has been given preference over other statistical methods as it gives the flexibility to analyze numerous parameters simultaneously with fewer experimental trials [312]. The upcoming sections describe this process in detail.

Introduction to Taguchi Analysis

Taguchi analysis is a statistical method that investigates the effect of different process parameters by analyzing the mean and the variance of the process performance characteristic or the target value ('Ultimate Tensile Strength' (UTS) value in this work) [313]. These process parameters are variables that affect the process performance (tensile strength).

The central idea of Taguchi's philosophy is to reduce the variability or changes around the target value [314] caused by the process parameters. For reducing the variation, the analysis employs statistical experimental design methods [314].

According to Taguchi, the quality of a product is the measure of all the losses associated with that product. These losses are defined by variations or deviations in their function by uncontrollable factors [315]. Uncontrollable factors are defined as the process parameters which vary the performance characteristics of a process and cannot be controlled. The product quality attained is maximum when the product is immune to these uncontrollable factors, and the deviation from the targeted mean value is minimum [316]. This means that high losses reduce product quality. In other words, the process parameter which attributes to large deviations in the process performance characteristics from its mean value reduces the product quality. The ratio of product quality (signal) and the uncontrollable factors (noise) is termed as Sn ratio (Signal/noise ratio) [316]. It is mathematically given as –

$$SNi = 10\log\frac{yi^{2}}{si^{2}}$$

From the mathematical relation, it can be seen that fewer deviations (small variance) yield high SN values. Hence, it can be inferred that the high Sn ratio results in good product quality [316]. In the above equation, SNi denotes the signal-to-noise ratio of the ith experiment. yi and si^2 denote the average and variance of all the data values of the ith experiment [317].

Step-wise procedure for implementing Taguchi Analysis

There are some basic steps involved in the Taguchi methodology [316] which are described below. A detailed description of these steps has been shown in the upcoming sections.

i. Defining a process objective or a target value for analyzing the performance of the process. The deviation of the performance characteristic from the mean value is used to determine the loss function of the process.
ii. Identifying the process factors affecting the process performance and specifying the number of levels for these factors.

iii. Creating orthogonal arrays according to the number of parameters and the level of variation for each of these parameters. The concept of Taguchi orthogonal arrays is based on the design matrix proposed by Dr. Genichi Taguchi. The proposed matrix works in a way that allows only a subset of combinations of multiple factors at multiple levels for analysis.

iv. Conducting experiments as per the combinations provided by the orthogonal arrays and collecting the data of the process performance characteristic.

v. Analyzing the data to determine the effect of different parameters on the process performance. Figure 3 – 1 shows the flowchart of the steps involved in the Taguchi analysis. It also contains some additional steps (not included in this literature as out of scope) depending on the complexity of the analysis.

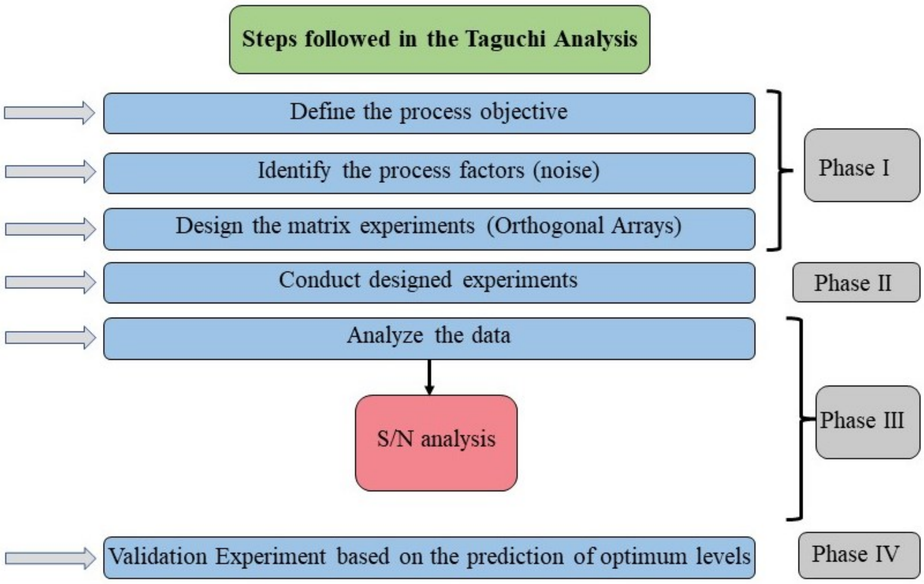

Figure 3 - 1 Taguchi Analysis Flowchart (adapted from [316])

Working of Taguchi Analysis

The Taguchi method analyzes the effect of multiple parameters with very few tests with the help of orthogonal arrays which distribute the variables in a balanced way and hence reduce the number of experiments. These arrays are based on general fractional factorial design [318], which means that a Taguchi Orthogonal array only considers a selected subset of all the possible combinations of different factors at multiple levels [318]. The size of the orthogonal array is determined by the number of parameters and the number of levels. In Taguchi analysis, the level of a parameter signifies the value of that entity. On increasing the number of levels, the Taguchi experiment size increases as the parameters are then assessed at a greater number of values. The unit of levels might change as per the parameter. For example, in Table 3-4, the levels 1, 2, and 3 for raster angle are 0°/90°, 30°/-60°, and 45°/-45°, respectively.

The SN values are calculated for each experiment using the mean and the variance values of the experimental data. These SN values are then averaged as per the levels and the SN values are calculated for each parameter at each level (refer to Section 4 of Appendix).

For finding the rank of the parameters, it is important to find the range value (Δ) of all the parameters. Δ for any parameter is defined as the difference between the maximum SN and the minimum SN value for that parameter [316].

$$\Delta = \max(SNi) - \min(SNi)$$

The larger Δ parameter signifies a larger impact on the process outcome (UTS) [316]. This is because on switching at different levels, there is a significant change in the SN values. In other words, if the same change in signal or the same deviation is implemented to all the parameters, the one with the highest Δ would bring a more impactful change to the output variable (UTS) being targeted [316]. The parameter having the largest Δ is ranked first [316].

Advantages and limitations of the Taguchi Method

Taguchi Analysis is a very useful method. The parameters are organized in such a way that minimum possible tests have to be conducted instead of conducting all the test combinations in the factorial design. Through this technique, it becomes possible to analyze the most significant factor which affects the product quality (ultimate tensile strength of the specimens) with minimum experimentation and saves plenty of time and resources.

However, at the same time, there are limitations of the Taguchi method. Firstly, the Taguchi analysis is relative; hence, it does not provide an exact conclusion as to which parameter has the highest effect on performance characteristics. Secondly, the orthogonal array does not consider all the variable combinations. This restricts its use at places where the interaction of variables is to be considered [317].

Example of Taguchi Analysis (derived from literature survey)

There have been several studies done in the past where Taguchi analysis has been used to analyze the effect of noise parameters on the process performance. A study conducted by *Qureshi* analyzed thirteen FDM parameters at three levels each based on their effect on the tensile stress and elastic modulus as shown in Table 3 – 2 [172]. Another study conducted by *Wankhede* showed the analysis of three FDM parameters at two levels each based on their effect on the build time and surface roughness values of ABS specimens as shown in Table 3 – 3 [319]. The use of Taguchi analysis has also been validated by several other studies conducted in the past [320]–[324].

Table 3 - 2 Parameters and Control levels in study conducted by *Qureshi* (adapted from [172])

Experiment number	Factor	Level 1	Level 2	Level 3
1	Component Scale (thickness h)	2 mm	4 mm	6 mm
2	Print location	Left	Center	Right
3	Extruder Temperature (°C)	218.5	230	241.5
4	Raster angle (°)	90	45	0
5	Speed while travelling (mm/s)	120	150	180
6	Speed while extruding (mm/s)	72	90	108
7	Build plate temperature (°C)	104.5	110	115.5
8	Peeling temperature (°C)	38.0	40.0	42.0
9	Layer thickness (mm)	0.16	0.20	0.24
10	Infill density	8%	10%	12%
11	Number of shells	1	2	3
12	Infill pattern	linear	hexagonal	moroccanstar
13	Infill Shell Spacing	0.64	0.80	0.96

Till date no research has been done which included recycling as one of the noise parameters in Taguchi analysis. An attempt has been made in this work to compare some selected FDM process parameters with recycling based on their effect on the tensile properties of the PLA specimens.

Table 3 - 3 Parameters and Control levels in study conducted by *Wankhede* (adapted from [319])

Experiment number	Factor	Level 1	Level 2
1	A - Layer thickness	0.254 mm	0.3302 mm
2	B – Infill density	Sparse low density	Sparse low density
3	C – Support style	Sparse	Smart

Taguchi Analysis in the present work

In the present work, the Ultimate Tensile Strength (UTS) value is defined as the process objective of the Taguchi analysis. Four process factors which are Infill density, Raster angle, Extrusion temperature, and Number of reprocessing cycles, have been identified that can affect the tensile strength of the 3D printed specimens. These factors have a significant effect on the tensile strength of 3D printed specimens and are derived from the literature survey done in Section 2.4.2.

Two different Taguchi analyses have been conducted for result validation purposes. In Taguchi analysis-I (TA1) the four parameters have been investigated with three-level responses. As per Taguchi, for four parameter-three level analysis, a 9-run array or L-9 array should be selected [316]**.** An L-9 array signifies that only 9 different parametric combinations need to be 3D printed and tested. These nine combinations are shown in Table 3-4.

Table 3 - 4 Parameters and Control levels as per Taguchi L-9 array

Experiment number	A (Raster Angle) [Levels]	B (Infill Density) [Levels]	C (Extrusion Temperature) [Levels]	D (Number of reprocessing cycles) [Levels]	Specimen nomenclature (used in this work)	Tensile Strength (X)
1	1 (0°/90°)	1 (30%)	1 (200°C)	1 (1)	P.0.1.3.1	X1
2	1 (0°/90°)	2 (60%)	2 (210°C)	2 (3)	P.0.2.6.3	X2
3	1 (0°/90°)	3 (90%)	3 (220°C)	3 (4)	P.0.3.9.4	X3
4	2 (30°/-60°)	1 (30%)	2 (210°C)	3 (4)	P.3.2.3.4	X4
5	2 (30°/-60°)	2 (60%)	3 (220°C)	1 (1)	P.3.3.6.1	X5
6	2 (30°/-60°)	3 (90%)	1 (200°C)	2 (3)	P.3.1.9.3	X6
7	3 (45°/-45°)	1 (30%)	3 (220°C)	2 (3)	P.4.3.3.3	X7
8	3 (45°/-45°)	2 (60%)	1 (200°C)	3 (4)	P.4.1.6.4	X8
9	3 (45°/-45°)	3 (90%)	2 (210°C)	1 (1)	P.4.2.9.1	X9

From Table 3-4, the three levels of parameter A are 0°/90°, 30°/-60° and 45°/-45° raster angle configurations. The three levels of parameter B are 30%, 60% and 90% infill densities. Whereas for parameter C, the three levels are 200°C, 210°C and 220°C. Similarly, the three levels for parameter D are 1, 3, and 4 reprocessing cycles. However, it should be noted that parameter D is quite a complex parameter when it comes to the analysis of the total number of specimens to be 3D printed and the time taken to print them over four reprocessing cycles. It considers the efficiencies of the shredder and the filament maker, making the analysis a bit complex. Due to this efficiency issue, more specimens need to be printed in the initial stages as compared to the later stages. It should be noted that the nomenclature of specimens has been described in the third section of the appendix.

Similarly, in the second Taguchi analysis (TA2), the four parameters were investigated with two-level responses. As per Taguchi, for four parameter-two level analysis, an 8-run array or L-8 array should be selected [316]. An L-8 array signifies that only 8 different parametric combinations need to be 3D printed and tested. These eight combinations are shown in Table 3-5.

Table 3 - 5 Parameters and Control levels as per Taguchi L-8 array

Experiment number	A (Raster Angle) [Levels]	B (Infill Density) [Levels]	C (Extrusion Temperature) [Levels]	D (Number of reprocessing cycles) [Levels]	Specimen nomenclature (used in this work)	Tensile Strength (X)
1	1 (0°/90°)	1 (30%)	1 (200°C)	1 (1)	P.0.1.3.1	X1
2	1 (0°/90°)	1 (30%)	1 (200°C)	2 (2)	P.0.1.3.2	X2
3	1 (0°/90°)	2 (90%)	2 (220°C)	1 (1)	P.0.2.9.1	X3
4	1 (0°/90°)	2 (90%)	2 (220°C)	2 (2)	P.0.2.9.2	X4
5	2 (45°/-45°)	1 (30%)	2 (220°C)	1 (1)	P.4.2.3.1	X5
6	2 (45°/-45°)	1 (30%)	2 (220°C)	2 (2)	P.4.2.3.2	X6
7	2 (45°/-45°)	2 (90%)	1 (200°C)	1 (1)	P.4.1.9.1	X7
8	2 (45°/-45°)	2 (90%)	1 (200°C)	2 (2)	P.4.1.9.2	X8

From Table 3-5, the two levels of parameter A are 0°/90°, and 45°/-45° raster angle configurations, for parameter B are 30% and 90% infill densities, whereas, for parameter C, the two levels are 200°C and 220°C. Lastly, the two levels for parameter D are 1 and 2 reprocessing cycles. The calculations of the experimental results using Taguchi Analyses I and II are shown in section 3.3.4, whereas the number and time analyses for specimens are shown in section 3.3.1.

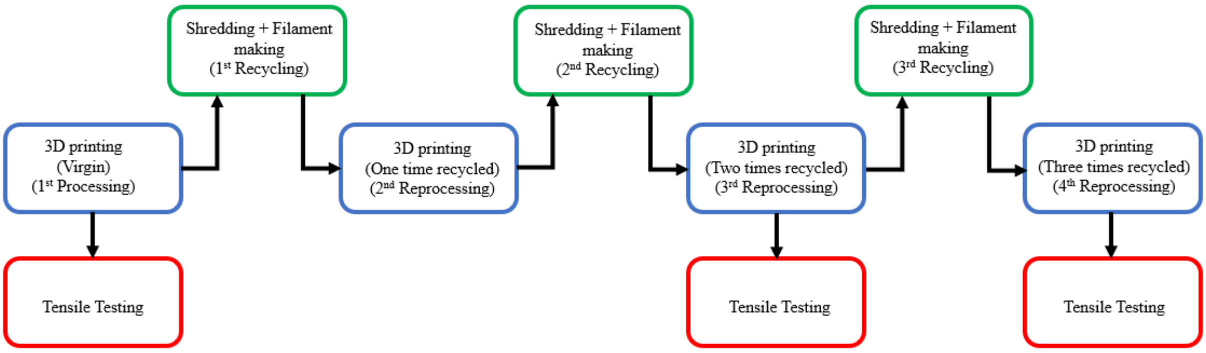

Figure 3 - 2 Research methodology flowchart- Taguchi Analysis I

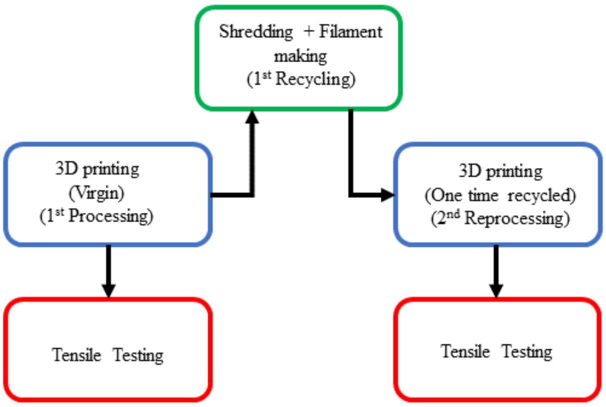

Figure 3 - 3 Research methodology flowchart- Taguchi Analysis II

Figures 3-2 and 3-3 show the research methodology flowchart for TA1 and TA2, respectively. The tensile specimens are 3D printed as per the batch size required (as per the analysis shown in section 3.3.1) at each processing cycle. As per the number analysis, for TA1, tensile testing is conducted for three of the specimens at this first processing stage, and then the required number of specimens are shredded to get sufficient material to make filaments for printing the specimens for the second reprocessing cycle. This process continues, and tensile testing is conducted for the specimens of the third and the fourth reprocessing cycles, whereas for TA2, the process stops at the second reprocessing cycle. Hence to conclude, among TA1 and TA2, the former involves reprocessing effect at first (Virgin), third (two times recycled), and fourth (three times recycled) reprocessing cycle. In contrast, the latter involves the reprocessing effect at the first (Virgin) and second (one-time recycled) reprocessing cycle. For both TA1 and TA2 analyses, three specimens of each combination are tested in order to avoid uncertainty in the results.

3.2.2.2. 3D printing of Specimens

A large-scale 3D printer-Modix BIG-60 V3, shown in Figure 3-4, has been used in this work. It has a print volume of 600 X 600 X 660 mm (XYZ), making printing large-sized objects and multiple objects feasible. It leads to less material wastage and reduced printing time, which results in cheap printing costs.

Figure 3 - 4 Modix 3D printer

Since this thesis aims to compare the effect of Infill density, Raster Angle, and Extrusion temperature along with a non-FDM parameter (number of reprocessing recycles) on the tensile strength of 3D printed PLA specimens, the other parameters are kept constant, and their most optimum values have been derived from the literature. The FDM parameters are mentioned in Table 3-6.

Table 3 - 6 Description of FDM parameters

Parameter	Value	Source
Infill Density	30%, 60%, 90%	-
Raster Angle	0°/90°, 45°/-45°, 30°/-60°	-
Extrusion Temperature	200°C, 210°C, 220°C	-
Infill Pattern	Grid	[200]
Build Orientation	Flat	[217]

Layer Height	0.2 mm	[220]
Retraction distance	3.5 mm	Based on initial printing trials
Build plate Adhesion type	Brim (Width = 3 mm)	Based on initial printing trials

In this work, the layer height has been set at 0.2 mm, which makes the specimen a print of 16 layers. All the specimens in this work are printed using a 0.4 mm nozzle. Additional important FDM parameters include the speed parameters. These parameters mainly include printing speed, traveling speed, and retraction speed. All these parameters have a direct relationship with the printing time. Traveling speed denotes the extruder's motion when it is not extruding the filament. Although increasing the traveling speed significantly decreases the print time, an excessive speed might result in a ringing effect on the printed part [325]. For this work, the traveling speed has been set at 80 mm/s. Retraction speed signifies how quickly an extruder pulls back the filament just before traveling. It plays an important role as higher retraction speeds can result in stringing issues, whereas lower speeds can lead to the generation of blobs within the print [326]. A retraction speed of 25 mm/s has been adopted for this work. Lastly, Printing speed depicts the motion of the axes motors as well as the extruder motors. Low printing speed forces the nozzle to rest on the printed plastic layer for more than the required time, which results in print deformation. In contrast, excessive printing speed may result in insufficient cooling, ringing issues, and weak interlayer adhesion [327]. Hence it is important to have an optimum printing speed to ensure a good quality product.

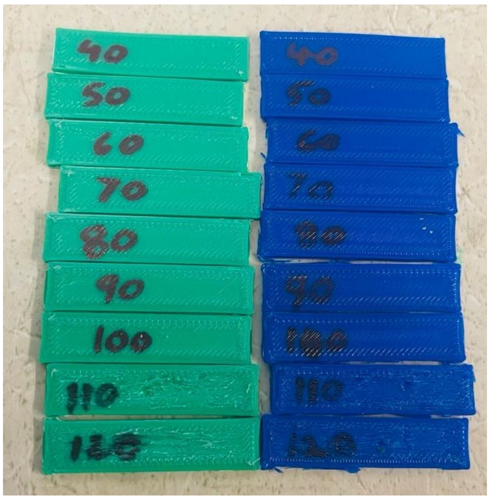

Figure 3 - 5 Speed test specimens (Green - virgin PLA, Blue – one-time recycled PLA)

For this, a print speed test was conducted on both virgin and recycled PLA specimens. A test specimen of dimension 10 X 40 X 2 mm was designed and printed at speeds of 40,50,60,70,80,90,100,110 and 120 mm/s. It can be seen from Figure 3-5 that at speeds above 100 mm/s, there were issues of layer shifting in the test specimens. Hence all the tensile specimens have been printed at a printing speed of 100 mm/s in this work. Separate tests were conducted for two- and three-times recycled PLA, and 100 mm/s was again found to be the optimum speed.

3.2.2.3. Tensile testing of Specimens

The tensile specimens are 3D printed as per the ASTM D638 (Type I) standard. The CAD model of this standard was designed on Autodesk Fusion 360 and is shown in Figure 3-6. This 3D CAD model is then exported to the slicing software Ultimaker Cura. This software processes the part in STL file format, tessellates it into several basic triangular components, and further slices it into several horizontal sections. The FDM process then generates these two-dimensional contours and stacks them above each other [328]. The final 3D printed PLA specimen is shown in Figure 3-6.

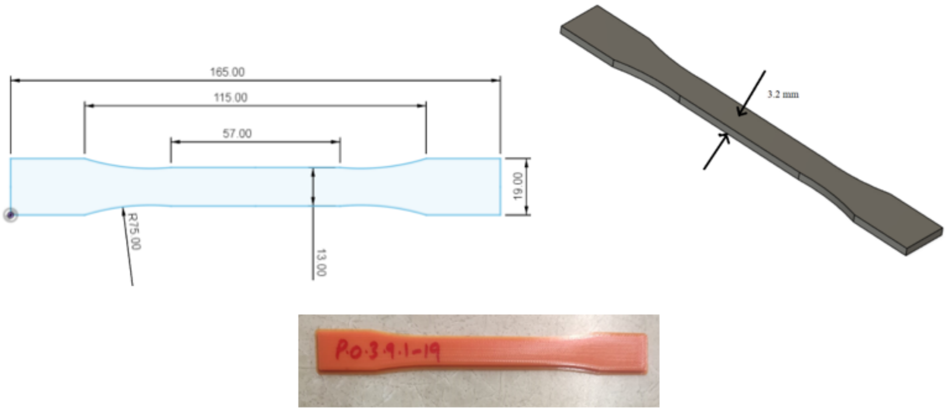

Figure 3 - 6 ASTM D638 Type I design, designed tensile specimen and final 3D printed tensile specimens

Once the specimens are 3D printed, tensile strength analysis of the specimens is done using Instron 5966 machine at a stroke rate of 2 mm/min. The machine uses a load cell of 10 kN and a gripper of a maximum load 5 kN. The Instron machine used in this work is a product of a US based firm 'Instron' and can be seen in Figure 3-7.

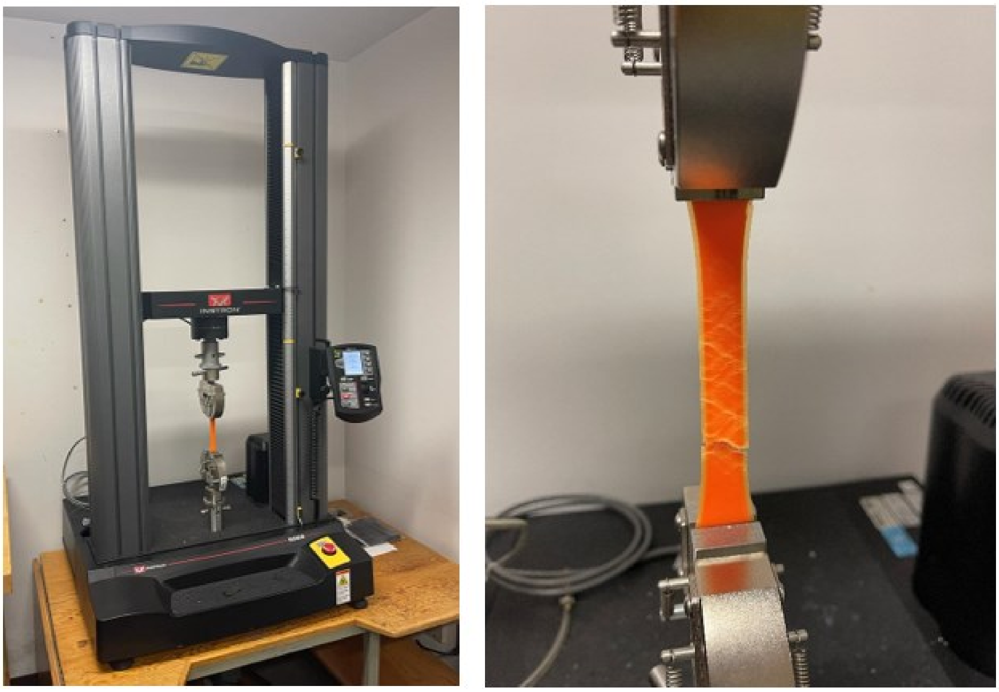
Figure 3 - 7 Instron 5966 machine used for tensile testing

3.2.2.4. Shredding specimens and converting into filaments

The specimens which are not tensile tested are shredded and made into filaments. The ProtoCycler+ machine manufactured by ReDeTec, Canada, shown in Figure 3-8, has been used in this work. It is an advanced desktop extruder having arrangements for both the grinding and filament-making process. The grinder has a 32:1 gearing system which provides high torque to the extruder screw. To ensure good quality extrusion of filaments, the shredded particles' size is kept between 3mm - 5mm. The grinder as well as the grinded PLA particles, are shown in Figure 3-9. Uniform particle shape and size lead to good extrusion. After grinding, the shredded particles are dried and then fed to the extruder chamber. Shredded PLA specimens are dried at 80°C for 4 hours. ProtoCycler+ has the capacity to extrude a maximum throughput of 500 grams per hour.

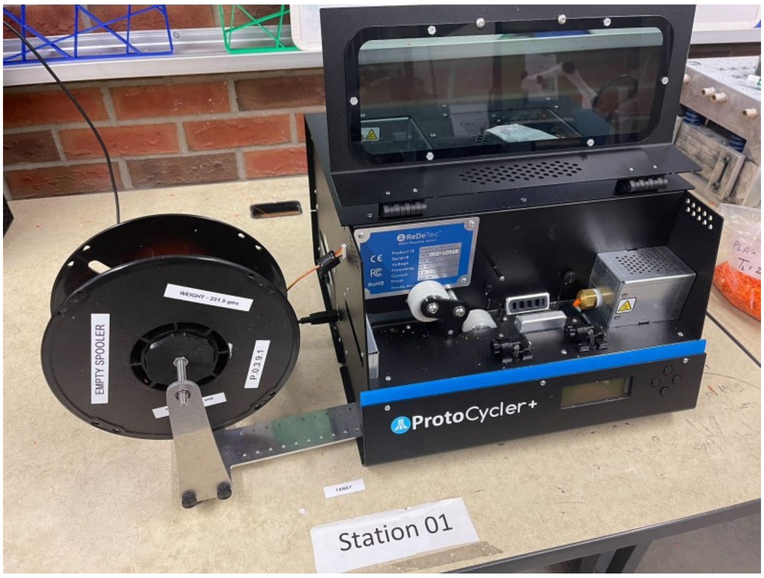

Figure 3 - 8 ProtoCycler+ setup used for shredding and filament making

Also, the diameter of the extruded filament has a measurement precision of 0.01 mm. Although 1.75 mm diameter has been chosen as a standard measure for the extruded filaments in this work, the output diameter was in the range of 145-185 mm, which was suitable enough to be 3D printed using Modix. This device can be operated at a maximum temperature of 250°C. Figure 3-10 shows the filament getting extruded from the ProtoCycler+ setup.

An interesting observation during the process of filament make was the color shifting property of the material by virtue of mechanical and thermal degradation [329]. Figure 3-11 shows the visible change in color of a virgin PLA filament as well as the filament made from two-time processed PLA material.

Figure 3 - 9 ProtoCycler+ grinder and grinded PLA particles

Figure 3 - 10 ProtoCycler+ filament maker

From various trials, it was estimated that for PLA, the filament maker mass efficiency was around 70% for virgin or one-time processed material, and this efficiency dropped by around 5% for every subsequent processing cycle. On the other hand, the grinder mass efficiency for PLA was found to be 89% for all the processing cycles. These efficiencies have a very crucial role in estimating the number of specimens that need to be 3D printed at every reprocessing stage and have been discussed elaborately in section 3.3.4. The fifth section of the appendix shows the grinder as well as the filament maker efficiency calculations in detail.

Figure 3 - 11 Color shift in PLA filament by virtue of recycling (left – filament made from two times reprocessed PLA material, right – virgin PLA filament)

3.3. Result Analysis

3.3.1. Observations on experiments (Time challenges)

A systematic analysis has been done in this section to calculate the total number of specimens to be printed and the total number of days required to complete the printing based on the machine efficiencies, print time for a single specimen and machine as well as human tolerances. Based on the printing speed, which is 100 mm/s, the time taken for a single specimen to print is shown in Figure 3-12.

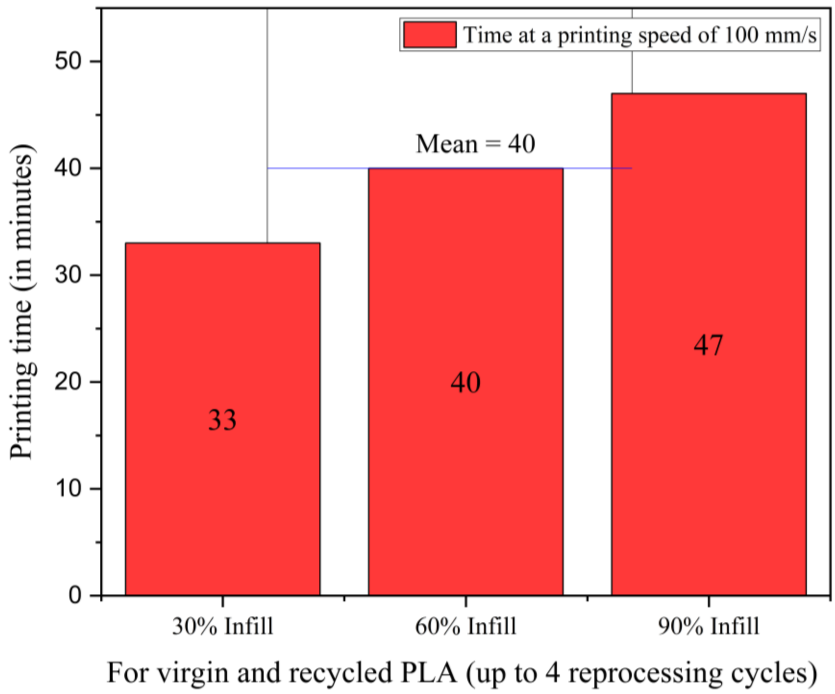

Figure 3 - 12 Results for time to print one specimen

The 3D printing was conducted at the LIMDA lab at the University of Alberta from 10 am to 4 pm (an average of 6 hours duration) on all working days. Considering the time taken for a single specimen to print and the time slot available for printing in a single day, an average of 9 specimens were printed per working day. Table 3-7 shows the calculation for number analysis, whereas Table 3-8 shows the results of the time analysis for PLA specimens as per TA1.

Table 3 - 7 Calculation for number analysis for PLA specimens in TA1

RA	ID%	ET	RP	Nomenclature	Specimens for tensile test (specimens)	Specimens for next processing (specimens)	Output Required (specimens)	Filament maker efficiency	Calculation for filament maker input (specimens)	Filament maker input (specimens)	Shredder efficiency	Calculation for shredder input (specimens)	Input to be given (specimens)
0°/90°	30%	200°C	1	P.0.1.3.1	**3**	0	3	1	3	3	1	3	3
0°/90°	60%	210°C	3	P.0.2.6.3	**3**	0	3	0.65	4.615	5	0.89	5.618	**6**
0°/90°	60%	210°C	2	P.0.2.6.2	0	6	6	0.7	8.571	9	0.89	10.112	**11**
0°/90°	60%	210°C	1	P.0.2.6.1	0	11	11	1	11	11	1	11	11
0°/90°	90%	220°C	4	P.0.3.9.4	**3**	0	3	0.6	5	5	0.89	5.618	**6**
0°/90°	90%	220°C	3	P.0.3.9.3	0	6	6	0.65	9.231	10	0.89	11.236	**12**
0°/90°	90%	220°C	2	P.0.3.9.2	0	12	12	0.7	17.143	18	0.89	20.225	**21**
0°/90°	90%	220°C	1	P.0.3.9.1	0	21	21	1	21	21	1	21	21
30°/-60°	30%	210°C	4	P.3.2.3.4	**3**	0	3	0.6	5	5	0.89	5.618	**6**
30°/-60°	30%	210°C	3	P.3.2.3.3	0	6	6	0.65	9.231	10	0.89	11.236	**12**
30°/-60°	30%	210°C	2	P.3.2.3.2	0	12	12	0.7	17.143	18	0.89	20.225	**21**
30°/-60°	30%	210°C	1	P.3.2.3.1	0	21	21	1	21	21	1	21	21
30°/-60°	60%	220°C	1	P.3.3.6.1	**3**	0	3	1	3	3	1	3	3
30°/-60°	90%	200°C	3	P.3.1.9.3	**3**	0	3	0.65	4.615	5	0.89	5.618	**6**
30°/-60°	90%	200°C	2	P.3.1.9.2	0	6	6	0.7	8.571	9	0.89	10.112	**11**

30°/-60°	90%	200°C	1	P.3.1.9.1	0	11	11	1	11	11	1	11	11
45°/-45°	30%	220°C	3	P.4.3.3.3	**3**	0	3	0.65	4.615	5	0.89	5.618	**6**
45°/-45°	30%	220°C	2	P.4.3.3.2	0	6	6	0.7	8.571	9	0.89	10.112	**11**
45°/-45°	30%	220°C	1	P.4.3.3.1	0	11	11	1	11	11	1	11	11
45°/-45°	60%	200°C	4	P.4.1.6.4	**3**	0	3	0.6	5	5	0.89	5.618	**6**
45°/-45°	60%	200°C	3	P.4.1.6.3	0	6	6	0.65	9.231	10	0.89	11.236	**12**
45°/-45°	60%	200°C	2	P.4.1.6.2	0	12	12	0.7	17.143	18	0.89	20.225	**21**
45°/-45°	60%	200°C	1	P.4.1.6.1	0	21	21	1	21	21	1	21	21
45°/-45°	90%	210°C	1	P.4.2.9.1	**3**	0	3	1	3	3	1	3	3

Table 3 - 8 Calculation for time analysis for PLA specimens in TA1

Total specimens to be printed across 4 cycles	Rate of specimen printing (per day)	Calculation for days	Weekend days	Other Holidays	Machine and Human Allowance	Sum of calculations	Number of days required
195	9	21.667	6.190	4	5	36.857	**37**

The best way to understand the number analysis is to study the process in reverse order. For example, in Table 3-7, for conducting tensile tests on 3 specimens of P.0.3.9.4 combination, sufficient filament for 3 specimens should be obtained as an output from the filament maker. Hence, an efficiency of 60% for the filament maker at the fourth processing cycle means that shredded material of 5 specimens needs to be fed as input to the filament maker. On carrying forward this analysis, the shredder efficiency of 89% signifies that in order to obtain a shredded material output of 5 specimens, 5.618 or approximately 6 specimens need to be shredded. Hence, 6 specimens need to be printed as an output from the third processing cycle. Following the same concept and going into further reverse analysis, it can be observed that for providing sufficient material to print 6 specimens, 12 specimens need to be shredded at the start of the third processing cycle. Hence, 12 specimens need to be printed at the end of the second processing cycle. Again, to provide sufficient material to print 12 specimens, 21 specimens need to be shredded at the start of the second processing cycle. Hence, 21 specimens need to be printed at the end of the first processing cycle. Now since the first processing cycle involves virgin material and does not involve any shredding or filament making, it means that 21 specimens need to be printed at the start of the first cycle. To conclude, to test the required 3 specimens of P.0.3.9.4 combination, 21 specimens need to be printed at the starting. Similarly, for all the combinations, the numerical analysis is done based on the efficiencies of the equipment. The example of P.0.3.9.4 combination can be seen in Figure 3-13.

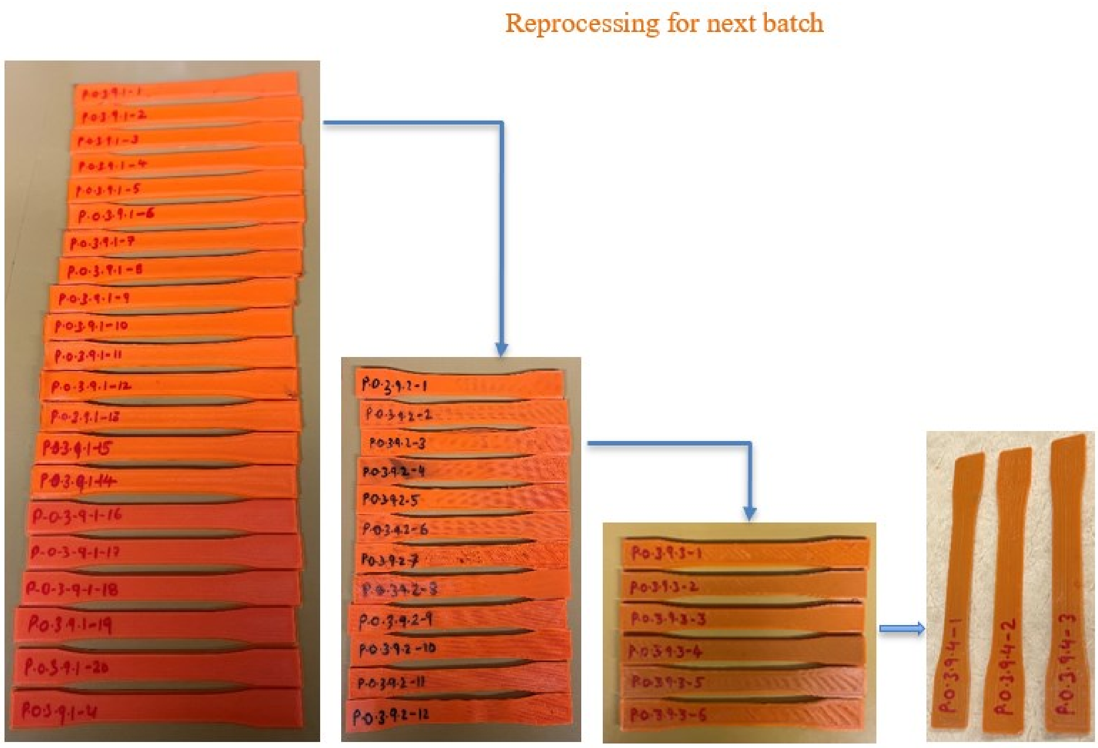

Figure 3 - 13 Number analysis for P.0.3.9.4 specimens

From Table 3-8, a total of 195 specimens need to be 3D printed over four reprocessing cycles. On moving further, at a rate of 9 specimens/day, it takes 21.667 days (around 22 days) to print all the specimens. However, in a practical scenario, it is not possible to use the machine daily. Also, it is always a good idea to include machine and human allowances so that both man and machine fatigue are taken into consideration. In this analysis, weekends are considered as non-working days, and around 25% of the total days have been excluded as machine and human allowances. A margin of 4 extra days has been considered since the workplace for conducting this research is a university laboratory, which must follow the University holiday closure. To sum up, it will take around 37 days (6 hours daily) to finish the job of printing 195 desired PLA specimens.

Table 3 - 9 Calculation for number analysis for PLA specimens in TA2

RA	ID%	ET	RP	Nomenclature	Specimens for tensile test (specimens)	Specimens for next processing (specimens)	Output Required (specimens)	Filament maker efficiency	Calculation for filament maker input (specimens)	Filament maker input (specimens)	Shredder efficiency	Calculation for shredder input (specimens)	Input to be given (specimens)
0°/90°	30%	200°C	2	P.0.1.3.2	**3**	0	3	0.7	4.286	5	0.89	5.618	6
0°/90°	30%	200°C	1	P.0.1.3.1	3	6	9	1	9	9	1	9	**9**
0°/90°	90%	220°C	2	P.0.2.9.2	**3**	0	3	0.7	4.286	5	0.89	5.618	6
0°/90°	90%	220°C	1	P.0.2.9.1	3	6	9	1	9	9	1	9	**9**
45°/-45°	30%	220°C	2	P.4.2.3.2	**3**	0	3	0.7	4.286	5	0.89	5.618	6
45°/-45°	30%	220°C	1	P.4.2.3.1	3	6	9	1	9	9	1	9	**9**
45°/-45°	90%	200°C	2	P.4.1.6.2	**3**	0	3	0.7	4.286	5	0.89	5.618	6
45°/-45°	90%	200°C	1	P.4.1.6.1	3	6	9	1	9	9	1	9	**9**

Table 3 - 10 Calculation for time analysis for PLA specimens in TA2

Total specimens to be printed across 4 cycles	Rate of specimen printing (per day)	Calculation for days	Weekend days	Other Holidays	Machine and Human Allowance	Sum of calculations	Number of days required
48	9	5.333	1.523	1	1	8.857	**9**

Similarly, for TA2, by following the same methodology as in TA1, it can be concluded from Tables 3-9 and 3-10 that it will take around 9 days to finish the job of 3D printing the required 48 PLA tensile specimens over two reprocessing cycles. Hence the total number of days utilized for 3D printing of all the specimens (TA1 + TA2) in this entire research work is 37 + 9 = 46 days, which is approximately 1.5 months.

However, it should be made clear that the time analysis is done in this work only considers the time for 3D printing of the specimens. The time for shredding and filament making is not included in this work as both the tasks were done simultaneously along with 3D printing of the specimens and hence did not add any extra time.

3.3.2. Specimen weight analysis

Recycling plastic degrades its mechanical and rheological properties [40]. Most thermoplastics often experience a drop in density under recycling [330]. In this work, since the analysis was done on the dog bone specimens (constant volume), a drop in mass or weight was observed with the increase in reprocessing cycles. Figure 3-14 shows the specimens' weight drop as per their infill density and reprocessing cycle combination.

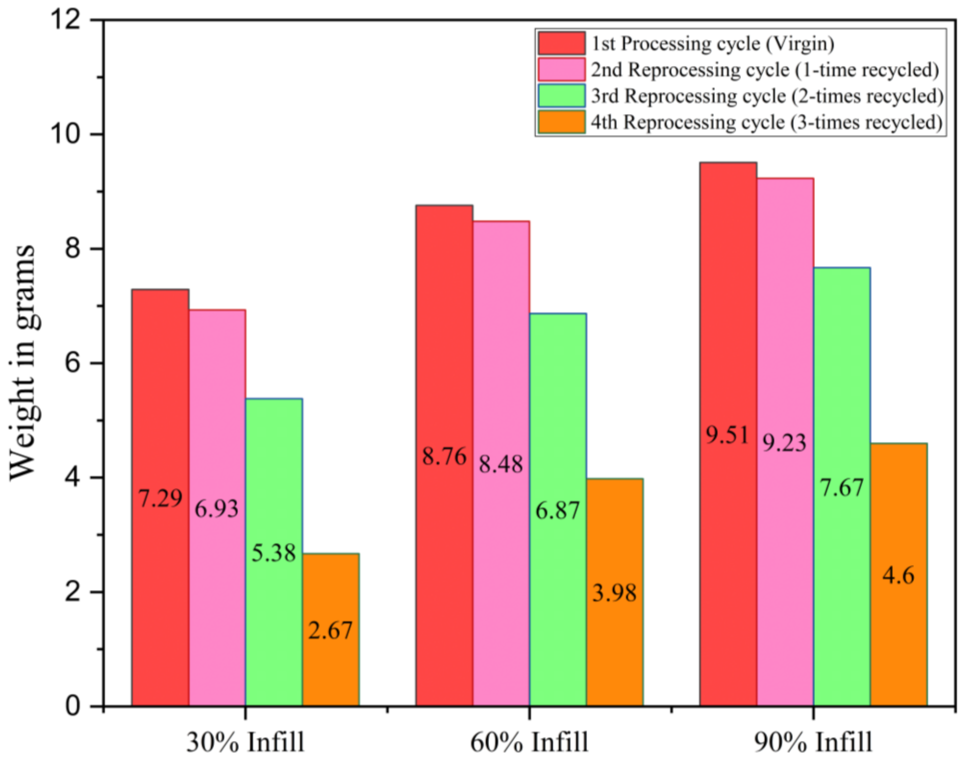

Figure 3 - 14 Average weight of specimens (in grams) as per the infill density-recycling stage combination

From the results in Figure 3-14, it can be seen that the weight of the specimens had a significant drop consistently till the fourth processing cycle. Although the percentage drop varied for different infill densities, a similar pattern of increase in the percentage reduction of weight with increasing reprocessing cycles was common for all the infill density specimens. 30% of infill density specimens experienced a drop in weight by around 5%, 22%, and 50% with every increasing reprocessing cycle. In contrast, for 60% of infill specimens, the percentage reduction in weight was around 3%, 19%, and 42% for every subsequent reprocessing cycle. Lastly, for 90% infill density, the percentage drop was around 3%, 17%, and 40% for subsequent reprocessing cycles.

3.3.3. Mechanical test results

Once all the required specimens were printed, tensile testing was carried out. The stress-strain curves were plotted as shown in Figures 3-15 to 3-18, and the Ultimate Tensile Strength (maximum stress in the stress-strain curve [331]) was targeted. The UTS values of all the specimen combinations are shown in Tables 3-11 and 3-112. The tables also contain variance and the signal-to-noise ratio values, which will be used in the calculations for Taguchi Analysis in Section 3.3.3.

Table 3 - 11 Tensile test results along with Taguchi Analysis 1

Experiment Number	A	B	C	D	Specimen	Ultimate Tensile Strength (MPa)			Taguchi Analysis 1		
	RA	ID%	ET	RP		Sample 1 (T1)	Sample 2 (T2)	Sample 3 (T3)	Average (y_i)	Variance (s_i^2)	Signal-to-noise ratio (SN_i)
1	1	1	1	1	P.0.1.3.1	22.239	19.821	20.101	20.720	1.749	23.900
2	1	2	2	2	P.0.2.6.3	16.702	11.011	13.728	13.813	8.102	13.720
3	1	3	3	3	P.0.3.9.4	9.436	9.273	9.186	9.298	0.016	37.290
4	2	1	2	3	P.3.2.3.4	8.100	6.812	6.759	7.224	0.576	19.569
5	2	2	3	1	P.3.3.6.1	24.576	24.826	22.540	23.981	1.573	25.629
6	2	3	1	2	P.3.1.9.3	11.456	15.342	19.085	15.294	14.552	12.062
7	3	1	3	2	P.4.3.3.3	12.595	10.535	9.777	10.969	2.127	17.527
8	3	2	1	3	P.4.1.6.4	8.796	8.511	8.457	8.588	0.033	33.469
9	3	3	2	1	P.4.2.9.1	24.853	24.996	25.266	25.038	0.044	41.535

Table 3 - 12 Tensile test results along with Taguchi Analysis 2

Experiment Number	A	B	C	D	Specimen	Ultimate Tensile Strength (MPa)			Taguchi Analysis 2		
	RA	ID%	ET	RP		Sample 1 (T1)	Sample 2 (T2)	Sample 3 (T3)	Average (y_i)	Variance (s_i^2)	Signal-to-noise ratio (SN_i)
1	1	1	1	1	P.0.1.3.1	22.239	19.821	20.101	20.720	1.749	23.900
2	1	1	1	2	P.0.1.3.2	12.189	17.978	11.271	13.813	13.220	11.593
3	1	2	2	1	P.0.2.9.1	25.941	27.177	26.481	26.533	0.384	32.635
4	1	2	2	2	P.0.2.9.2	23.500	19.565	23.721	22.262	5.468	19.573
5	2	1	2	1	P.4.2.3.1	18.382	17.854	24.868	20.368	15.259	14.343
6	2	1	2	2	P.4.2.3.2	18.510	10.894	10.373	13.259	20.748	9.281
7	2	2	1	1	P.4.1.9.1	24.371	24.446	23.537	24.118	0.254	33.595
8	2	2	1	2	P.4.1.9.2	22.613	23.937	18.252	21.600	8.847	17.221

From the results, it can be seen that the UTS of the specimens of first processing cycle was in the range of 20-26 MPa. This range of UTS reduced to 13-22 MPa for the second reprocessing cycle. While there was a significant drop to 12-16 MPa and 7-9 MPa for the third and the fourth reprocessing cycles, respectively. It was observed that specimens with higher infill densities had a better UTS when compared within a reprocessing cycle. This analysis was supported by [196], [332], in which it has already been shown that higher infill densities result in better tensile strength. It was also observed that the UTS of the specimens was more for 0°/90° raster orientation, followed by 30°/-60° and 45°/-45° orientation. This analysis was supported by [192], [323], and [324], which showed that cross orientations (0°/90°) show better tensile strength than crisscross orientations (45°/-45°). Also, 30°/-60° has shown better tensile strength than 45°/-45°orientations for PLA samples. However, the results contradicted the work proposed in [335]. It was deduced that for samples printed with 0.2 mm layer thickness, 30°/-60° orientation displayed maximum UTS followed by the crisscross and the cross orientations.

Lastly, it was observed that for the samples of a specific reprocessing cycle, Extrusion temperature (ET) had a direct relationship with the UTS. Samples at 220°C exhibited the highest UTS, followed by samples at 210° and 200°. This analysis was supported by [291], in which it was mentioned that for a temperature range of 200-220°C in PLA, ET has a direct relation with the tensile strength.

Here, it is important to clarify that the combination of parameters was a result of the Design of Experiments and hence each specimen is an experiment of the Taguchi analysis. Every graph represents a unique experiment and a specific set of parametric combinations. The graphs cannot be classified on the basis of any one parameter and hence were not merged and were drawn separately.

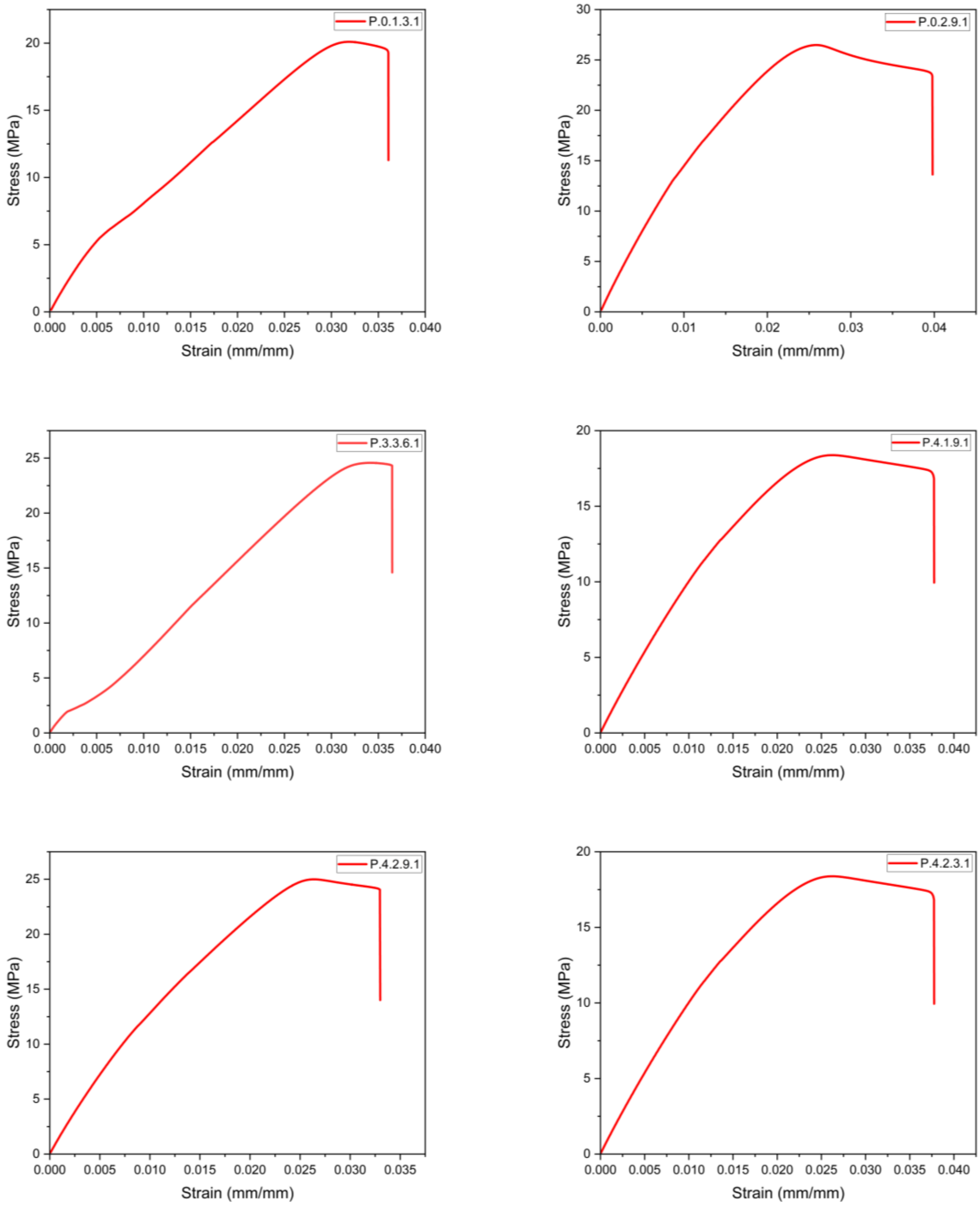

Figure 3 - 15 Stress-Strain analysis for specimens of 1st reprocessing cycle

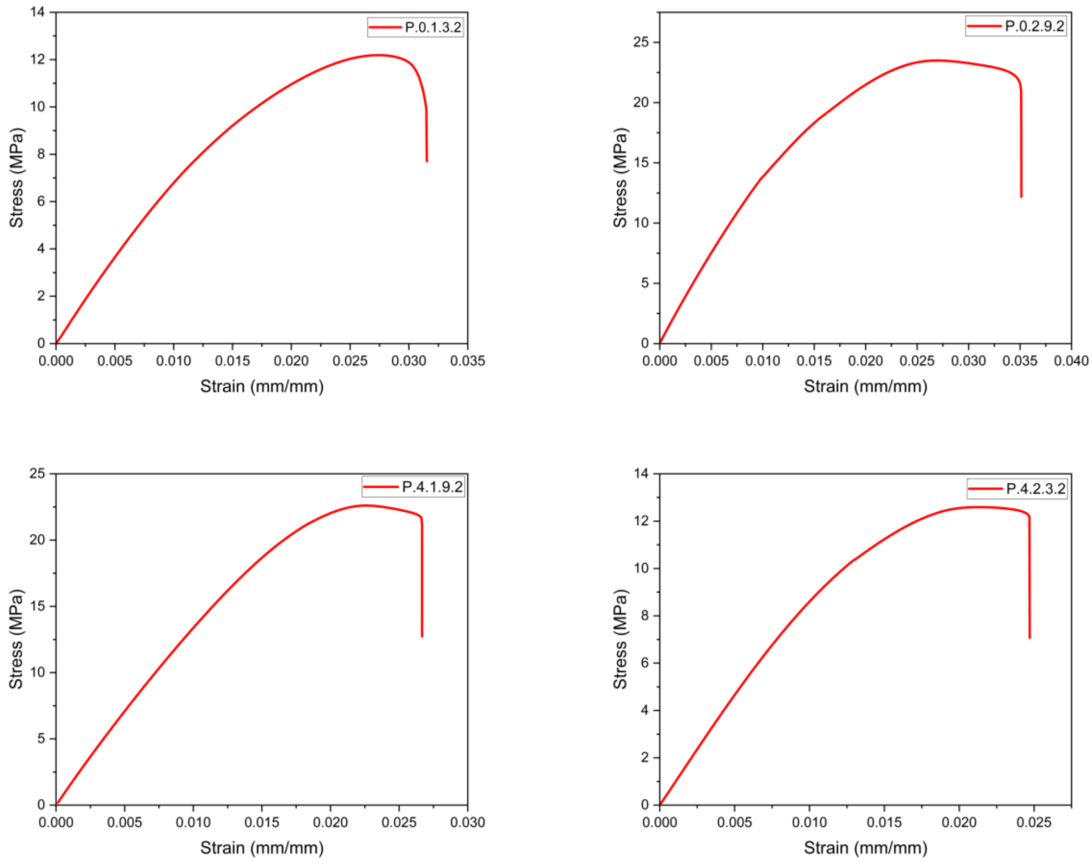

Figure 3 - 16 Stress-Strain analysis for specimens of 2nd reprocessing cycle

Table 3 – 13 shows the UTS values of all the combinations analysed in this work. The combinations from both TA1 and TA2 analyses are arranged in decreasing order of their UTS values which shows the effect of recycling, infill density, raster angle and extrusion temperature on the tensile strength values.

Table 3 - 13 Conclusion for UTS values of specimens from TA1 and TA2 analyses

Specimen Type	Ultimate Tensile Strength (UTS) in MPa
P.0.2.9.1	26.5
P.4.2.9.1	25
P.4.1.9.1	24.1
P.3.3.6.1	24
P.0.2.9.2	22.3
P.4.1.9.2	21.6
P.0.1.3.1	20.7
P.4.2.3.1	20.4
P.3.1.9.3	15.3
P.0.2.6.3	13.8
P.0.1.3.2	13.8
P.4.2.3.2	13.3
P.4.3.3.3	11
P.0.3.9.4	9.3
P.4.1.6.4	8.6
P.3.2.3.4	7.2

3.3.4. Taguchi Analysis

As mentioned earlier, two Taguchi analyses (TA1 and TA2) have been conducted in this work to compare the impact of FDM printing parameters (RA, ID%, and ET) and the recycling effect (RP) on the tensile properties of PLA dog bone specimens. Since Taguchi targets the mean and variance of the process performance characteristic, these values are tabulated in Tables 3-11 and 3-12. Also, to calculate the effect of each of the four parameters on the output, the SN values have also been tabulated in these tables for every type of specimen. Tables 3-14 and 3-15 show the results for TA1 and TA2, respectively.

From Table 3-14, it can be seen that the highest Δ is for parameter D (RP), followed by RA, ID%, and ET. Hence for TA1, reprocessing cycle is the most influencing parameter on the tensile strength of PLA specimens, followed by the raster angle orientations, infill density, and the extrusion temperature.

Table 3 - 14 Taguchi Analysis I results

Level	A (RA)	B (ID%)	C (ET)	D (RP)
1	24.970	20.332	23.143	30.355
2	19.087	24.273	24.941	14.436
3	30.843	30.295	26.815	30.109
Δ	11.757	9.963	3.672	15.919
Rank	2	3	4	1

Table 3 - 15 Taguchi Analysis II results

Level	A (RA)	B (ID%)	C (ET)	D (RP)
1	21.925	14.779	21.578	26.118
2	18.610	25.756	18.958	14.417
Δ	3.315	10.977	2.620	11.701
Rank	3	2	4	1

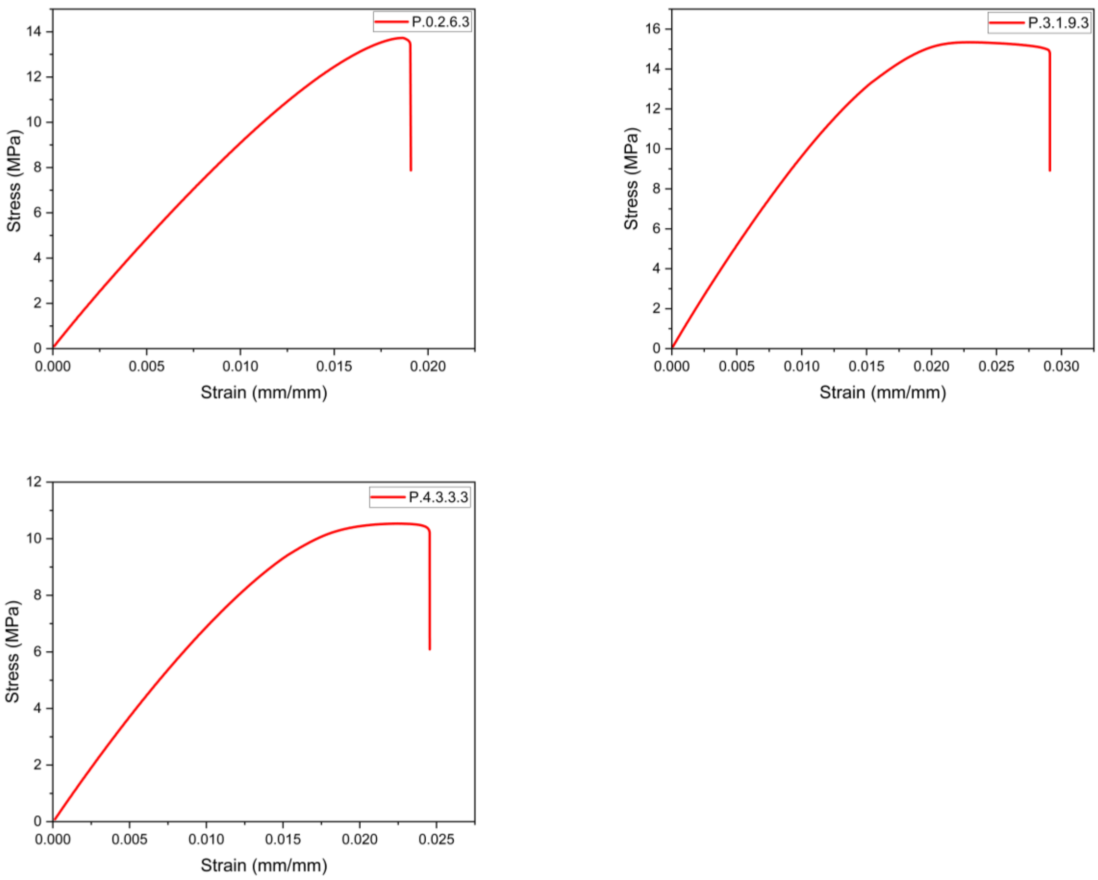

Figure 3 - 17 Stress-Strain analysis for specimens of 3rd reprocessing cycle

Similarly, from Table 3-15, it can be seen that yet again, the highest range value is for parameter D (number of reprocessing cycles), which confirms that at least up to four reprocessing cycles, recycling has the most impactful effect on the tensile properties of

PLA specimens when compared with printing parameters such as RA, ID%, and ET. However, ID% is the second most influencing factor this time, followed by RA and ET. This infers that this order of impact for the four parameters can vary if the analysis is done for different levels or different processing conditions.

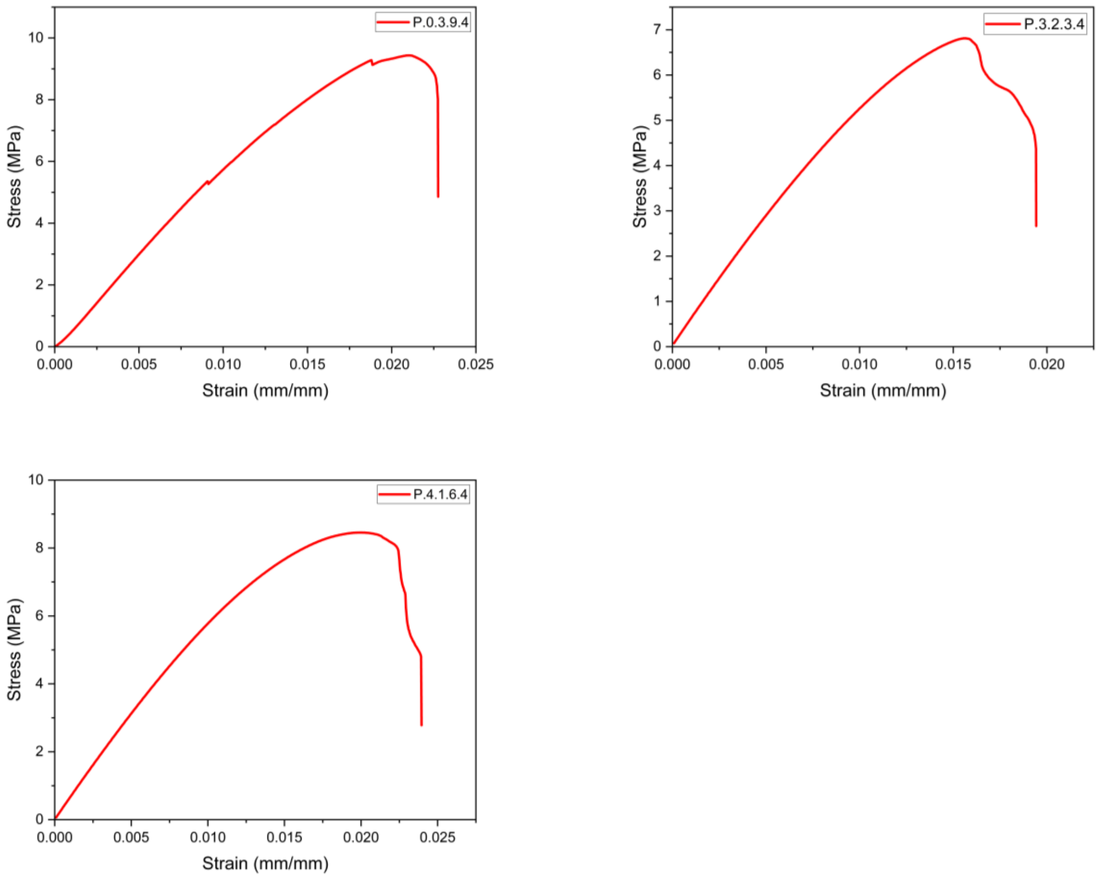

Figure 3 - 18 Stress-Strain analysis for specimens of 4th reprocessing cycle

The fourth section of the appendix shows the descriptive calculation of Taguchi analysis done in this work.

3.4. Discussions

Several aspects of this work related to recycling effect on material properties, printing as well as machine parameters that have an impact on the DRAM process can be discussed in this section. In relevance to the product design and its mechanical properties, DRAM is yet to give concrete data as to how significantly a material degrades once it is recycled. This degradation varies according to the type of plastic and the number of reprocessing cycles. In this work, it was observed that PLA could degrade up to 75% in the course of four reprocessing cycles (P.0.2.9.1-2 = 27.2 MPa, whereas P.3.2.3.4-3 = 6.8 MPa). There was a change in color observed when the PLA material was recycled due to mechanical and thermal degradation. Another interesting analysis was the drop in weight of the specimens on subsequent recycling. This was due to the fact that the density of PLA was reduced on reprocessing, which resulted in a loss in weight as the volume of the samples was constant (ASTM D638 Type 1 standard). Hence, there is a scope of a huge database that can be created, including the type of plastic which actually can be recycled, its extent of recycling, and the change in mechanical properties it encounters during this recycling. In relevance to processing energy consumption, DRAM still fails to deliver information about the energy consumed in the 3D printing process under recycling. This is dependent on machine efficiencies as well as the recycled material properties. This work showed that the grinder and filament maker had efficiencies of around 89% and 60-75%, respectively, as per the reprocessing cycle. These efficiencies had an important role in determining the number of specimens to be 3D printed and the time taken to print them. Pre-known material properties such as temperature requirements at different reprocessing cycles can help determine the energy requirements for 3D printing of that recycled material. In relevance to the circular economy, DRAM lacks information about the life cycle assessment of the material. As mentioned earlier, there is a big literature gap in the context of how many times a particular plastic can be recycled. This work provides literature that PLA can be reprocessed at least four times, and there is a scope for recycling it even more. Adding to this, the effect of recycling on the printing parameters is yet to be explored completely. It is important to analyze the critical printing parameters for any recycled material. An attempt has been made in this work to rank the important parameters up to four reprocessing cycles for PLA.

3.5. Conclusions

In this chapter, the Design of experiments via Taguchi analysis was conducted to reduce the amount specimens to be printed and analyzed. Due to this, it was possible to compare the recycling property (reprocessing cycles) with FDM printing parameters (raster angle, infill density, and extrusion temperature) up to three levels. Each of these properties had its own impact on the tensile strength of the specimens. For instance, as the number of reprocessing cycles increased, the tensile strength of the PLA samples decreased significantly. There was a drop of 33% in the tensile strength for 30% infill density samples when moving from the first reprocessing cycle to the second reprocessing cycle. This drop decreased to 23% and then 30% for the third and fourth reprocessing cycles. Likewise, there was a significant drop in tensile strength for 60% and 90% infill density specimens with each subsequent reprocessing cycle. Now, within a specific reprocessing cycle, it was observed that Infill density had a direct relationship with the tensile strength of the specimens. In the first reprocessing cycle, the tensile strength increased to 15% when moving from 30% infill to 60% infill and further increased by around 8.7% from 60% to 90%. This trend in infill densities was common in all reprocessing cycles. Similarly, in the case of raster angle orientation, it was observed that at all the reprocessing cycles, 0°/90° orientation showed the best tensile strength, followed by 30°/-60° and 45°/-45° orientations. Lastly, there was a direct relation observed between Extrusion temperature and the tensile strength of the samples at each reprocessing cycle. On conducting the two Taguchi analyses, it was seen that reprocessing effect was the most critical parameter among the four. Whereas at two-level analysis, infill density emerged as the second most influencing factor, while at three-level analysis, raster angle was the second most impactful parameter. The extrusion temperature was the least critical parameter in both analyses. Lastly, the number and time analysis was conducted, which gave an idea of the number of specimens to be printed at the initial stages to reach the desired number of specimens at a later reprocessing stage. This analysis was dependent on the efficiencies of the grinder and filament maker as well as the speed of 3D printing the specimens. For this, a separate speed test was conducted, which is also a part of this work.

Chapter 4 Design of a hybrid high-throughput Fused Deposition Modeling System for Circular Economy Applications

4.1. Introduction

The plastic recycling process face challenges such as high transportation and collection costs of waste plastics as well as the low value of recycled content [336]. This has limited the execution of this much-required process to the extent that the plastic recycling rate has been estimated to be only around 9% [337]. Hence, there is a need to compensate for these constraining factors in the long run. DRAM is an economically viable approach to plastic recycling. It utilizes local plastic wastes for 3D printing [338]. This approach has ultimately resulted in an inclination of material extrusion AM technologies towards the use of recycled plastics to ensure reduced costs and a low carbon footprint [282]. Many polymers, when recycled, still have mechanical properties comparable to their virgin counterpart [339]. Hence, material extrusion AM technologies such as Fused Deposition Modelling (FDM) and Direct-FDM (DFDM) technologies [340] aim toward recycled materials to promote zero waste manufacturing. While FDM technology uses filament for layer-by-layer material deposition, DFDM technology directly uses shredded or pelletized plastics for 3D printing [340]. These concepts of DRAM save approximately 130 million kJ of energy per ton of plastic getting recycled [341].

AM has been considered a slow manufacturing process when compared to conventional manufacturing technologies [342]. Typical FDM systems can deposit layers within the range of 0.4mm up to 0.8mm thickness [343], which increases the number of layers that need to be deposited in order to print the product. The use of bigger nozzle diameters in the system can lead to increased layer thickness which reduces the number of layers in a print and hence reduce the printing time. This can result in a high throughput as well as reduced 3D printing time. Hence there needs to be an exploration of a novel design that can result in high throughputs and an increased rate of recycling. The lack of available materials for 3D printing an object, the type of extrusion heads to print any specific plastic material, the limited speed, printing parameters, control, performance, and building volume in existing machines, and the high cost of materials are some other downsides that this emerging technology is still facing and that discourages the industry from implementing it into their manufacturing processes [344]. In addition, multi-materials parts design is another insufficiently explored field where several configurations have been analyzed, and multiple gaps exist to make components of this process with multiple materials optimal and more competitive [345]. Different AM processes have different mechanisms and have their own limitations. For instance, some polymers are not readily available in filaments, which restricts their use as an ideal printing material in the FDM process [252]. The extra step of heating causes filament formation usually unfavorable for these materials. Hence they are most suitable for the direct extrusion process or DFDM process [252]. Many commercial DFDM systems work on extrusion additive manufacturing (EAM). These systems contain screw-based print heads, which have an auger screw that helps transport the molten material [340]. These print heads also have a screw having either a decreasing pitch or a decreasing channel depth, or both, which leads to efficient polymer plastification and mixing [250]. Since these systems can be directly fed with shredded or pelletized materials, EAM is emerging as an enabling technology that expands the range of 3D printing materials as these are no more restricted by their mechanical properties in the filament form or by their performance in the filament extrusion process or even by the tolerance requirements [261]. EAM also reduces feedstock fabrication costs and increases the rate of material deposition when compared to the traditional FDM process [252]. However, although DFDM systems do not need filaments and work directly with pellets or shredded plastics, it is always a challenge to ensure uniform extrusion while using a plastic feedstock of irregular shape and size [346].

As per the literature, there have been several proposals of screw extrusion designs and several modifications as well as revisions have been done and are still done on the existing designs to make the process more efficient [347]–[349]. For instance, to eliminate the feeding problems, *Reddy* included a separate granule feeding unity and a screw having variable channel depth and pitch [350]. A conical crew has also been designed to enhance plastification and material homogenization over a short length [351]. A successful attempt has also been made to adjust the design in order to achieve a better volumetric rate of the extrusion flow [352]. In yet another interesting study, the deposition surface was attached to a robotic arm having movement in six different axes and had a fixed printhead [353]. Another study on Gigabot X, which is a large-scale direct deposition 3D printer, uses FPF (Fused particle fabrication) technology for 3D printing. The system was able to print the material at a speed of 6.5X to 13X faster than the conventional 3D printers while maintaining nearly the same mechanical properties [354].

Since hybrid 3D printers are not very popular but are at an evolving phase in the current time, the design of the system in this work aims toward the development of a novel approach for 3D printing by utilizing the benefits of both FDM and DFDM systems. This makes the system hybrid and suitable for multicomponent as well as multi-material printing of a broad range of thermoplastic materials, where the latter is one of the future objectives of this work. The entire system proposed is designed on the basis of extrusion theory and includes features such as cooling, temperature control, and speed control [251] and aims toward high throughput. The system's capabilities will also employ raw materials from 3D printed waste parts and other conventional plastic manufacturing processes. Furthermore, in terms of the environmental problems generated by plastic waste, the system promotes the "Circular Economy" strategy for part production where material after life-use can be easily reincorporated into the supply chain to avoid plastic accumulation.

4.2. The System Design

In this proposed hybrid system, the design of the screw extruder unit was a big challenge. The thermoplastic polymer granules are fed into the hopper, which ensures a controlled and correct feeding rate of material quantity [251]. The feed material is then transported from the barrel to the nozzle via a three-section screw which makes the polymer granules heat into a viscoelastic melt [248]. The trapped air between the granules is expelled by virtue of the pressure developed by the screw geometry [355]. It also helps to overcome the back pressure induced by the nozzle geometry [356]. The design also comprises a heating and cooling system, a driving motor, temperature sensors, and encoders [251].

4.2.1. Mechanical design of the screw and selection

The screw is a very important component of the extrusion system and is often referred as the heart of the extruder [357]**.** The geometry of the screw is very critical in terms of the efficiency of the entire extrusion system [357]**.** The parameters involved in a screw geometry are channel depth, channel width, pitch, helix angle, etc. Varying any of these parameters can change the physical properties of the screw. Figure 4-1 shows the various components of screw geometry.

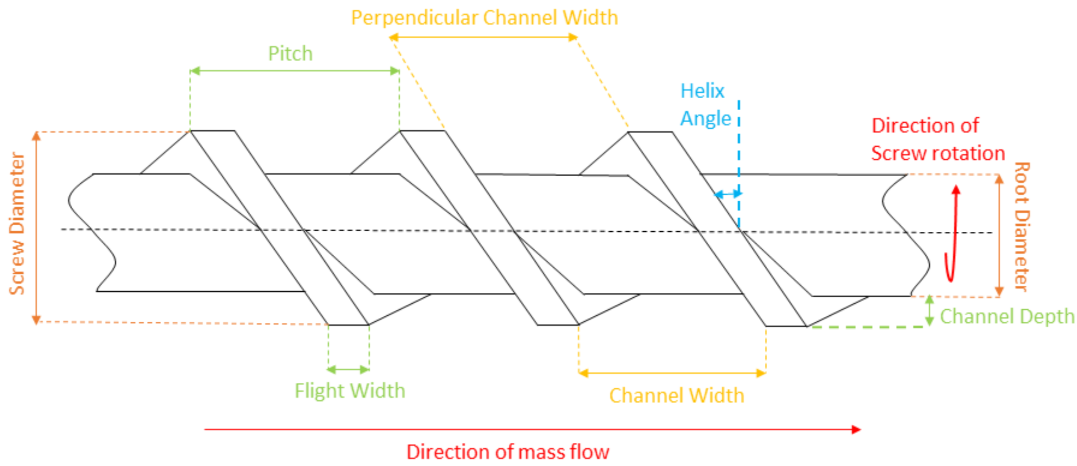

Figure 4 - 1 Components of Screw Geometry (adapted from [358])

The screw length (L) and diameter (D) are two other important parameters of a screw extrusion system. Some studies have shown that the L/D ratio should be less than or equal to 20 for melt extruders for an efficient extrusion [52]. Table 4-1 shows the standard values of different screw parameters.

To minimize the gravity induced deflections in the shaft, the screw is placed in a vertical position. On the other hand, to reduce the lateral deflections, the rotation speed of the screws is intended to be low. The symmetrical sustentation provided by the molten polymers too helps in reducing the lateral deflections [359]. Inside the screw geometry, the transportation of material takes place through conveying elements. These elements have a varying pitch, which leads to the required flow compression [359]**.** Figure 4-2 shows the sectional view of the screw and the barrel arrangement used in this work.

Table 4 - 1 Screw Parameters [52]

Screw Parameters	Standard values (from literature)
Length to Diameter ratio (L/D)	20 or less for melt extruders
Diameter (D)	20, 25, 30, 35, 40, 50, 60, 90, 120, 150, 200, 250, 300, 350, 400, 450, 500 and 600 mm
Helix Angle (ϕ)	17.65° or 0.308 rad, for $0.8<L_S/D<1.2$ (where L_S is pitch length)
Channel Depth (h) in metering section	0.05D-0.07D for D < 30 mm, 0.02D-0.05D for D > 30 mm
Clearance between screw and barrel (δ)	0.1 mm for D < 30 mm, 0.15 mm for D > 30 mm

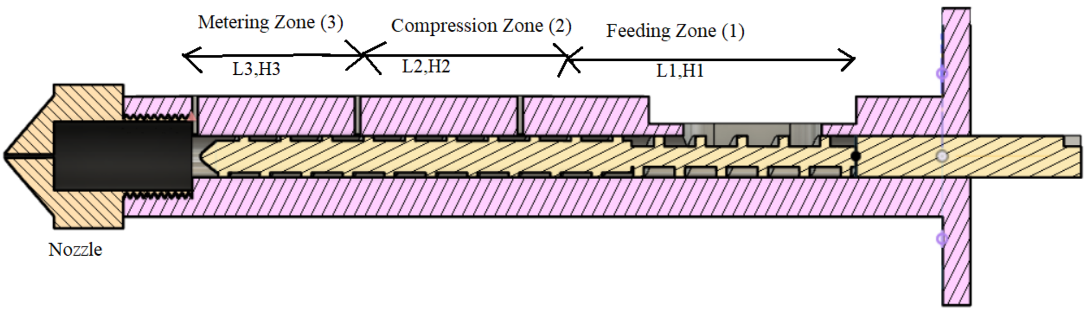

Figure 4 - 2 Sectional view of the Barrel and Screw Arrangement

The screw has a diameter of 11.75 mm, whereas the barrel has an inner diameter of 11.8 mm, leaving a small clearance of 0.025 mm in between. Table 4-2 shows all the remaining dimensions of the screw used in this work. The nozzle has a diameter of 1.75 mm. The screw, barrel, and nozzle are made of stainless steel and hence have good corrosion resistance and long service life.

Some studies have shown that irrespective of the L/D ratio, the length of the feed zone should be constant throughout, and the remainder of the length should be dedicatedly used for melting and pumping [360]. While more channel depth results in higher specific output (lb/rpm), a larger length of the screw is taken into account in order to create the pressure required to push out the polymer from the nozzle [361]. This excessive length for the overall processing situation limits the output of the system [362]. It results in excessive melt temperature, which leads to color shift, polymer degradation, loss of adhesiveness, etc., [329]. Also, the length of the melting zone should be less if the polymer melts easily [363].

Excessive length can compromise the melting rate [364]. Lastly, for the metering zone, the length can be reduced on using proper melt pumps which can withstand the discharge pressure [361].

To increase the output, the L/D ratio can be increased [365]. However, the feed section is able to deliver polymer only up to a certain quantity limit which in turn limits the increment of ratio L/D [366]. For screws having a smaller diameter, this limit is determined by the screw strength [367]. The channel depth can be increased up to a point where the screw can bear the torque generated from the rotation [368]. On the other hand, for larger extruders, the channel depth can be increased till there is an increment in the output [369]. Increasing the channel depth beyond this point often reduces the efficiency of feeding [370]. Hence, the L/D ratio is an important parameter as larger values of it may penalize the overall performance of the system [362].

Table 4 - 2 Screw geometry dimensions

S.No.	Screw Geometry Parameter	Value
1	Channel Width (W)	9.5 mm
2	Channel Depth (H)	H1 = 3.5 mm, H2 = 3 mm, H3 = 2 mm, H = $H_{avg.}$ = 2.83 mm
3	Diameter of Screw (D_s)	11.75 mm
4	Inner Diameter of Barrel (D)	11.80 mm
5	Outer Diameter of Barrel (Do)	35.60 mm
6	Thickness of Barrel (t)	11.90 mm
7	Clearance between screw and barrel	0.025 mm
8	Helix Angle of screw (ϕ)	0.359 rad
9	Length of the screw (L)	L1 = 65 mm, L2 = 65 mm, L3 = 60 mm, L = 190 mm

To create an internal pressure to extrude the material, the material is compressed along the length of the screw [371]. This compression is possible due to the linearly increasing core diameter of the screw [372]. A stepper motor is used to rotate the screw in small increments to impart constant mass flow for a smooth printing process [373]. Also, to prevent any damage due to the misalignment of the screw and barrel, the latter is made from harder steel than the former [261].

Another important aspect is the size of the extruder. For higher throughput, which is also one of the objectives of this work, often larger extruders are preferred. However, at the same time, it should also be noted that while an oversized extruder provides the flexibility of having a higher output, it also results in higher daily operating costs [374].

The capital investment can increase up to double on moving up one extruder size [375]. Large extruders have more residence time for a specific output, increasing the chance of polymer degradation [376]. Additionally, the heat-up and temperature requirements are proportional to the mass of the extruder [375]. The time required for heating the extruder can double on increasing one size of the extruder [375].

Even at low speed, the AC and DC drives extract high power per unit mass of the output [377]. Due to poor power factors at low speed, DC drives are costlier than AC drives [378]. The large surface area of a big-sized heated extruder also results in increased thermal losses to the environment, which may be beneficial in cold weather but significantly increases the cost in warm weather [375]**.** This was the motivation for going with a small-sized extruder. Figure 4-3 shows the extruder assembly consisting of the screw, barrel, and the nozzle.

Figure 4 - 3 Screw extruder assembly

Yet another important component of the screw extruder assembly is the nozzle as it is responsible for shaping the output of the polymer as well as generating pressure inside the extruder [379]. It was also observed that the smaller the nozzle size, the more pressure is required by the screw to extrude the material [380]. The end barrel section implements a detachable nozzle tip configuration with diameters ranging from 1.75 to 2.5 mm. The system design can reach up to 2 mm thickness deposition layer, which makes the system able to print higher throughputs that reduce printing time and consequently increase the efficiency of the printing process. However, the use of the 2.5 mm nozzle resulted in unstable prints due to Die-Swelling issues during extrusion, which has been discussed in Section 4.5.1. Hence, a 1.75 mm nozzle has been used in this work throughout. On the other hand, a 1.4 mm nozzle has been used for the FDM system.

4.2.2. Hopper Design

Since the material is gravity assisted, it becomes important to design the hopper in such a way that there is precise control of the material feed rate to avoid jamming, possibly leading to inconsistencies in print [380]. Figure 4-4 shows the design and the machined hopper used in this work.

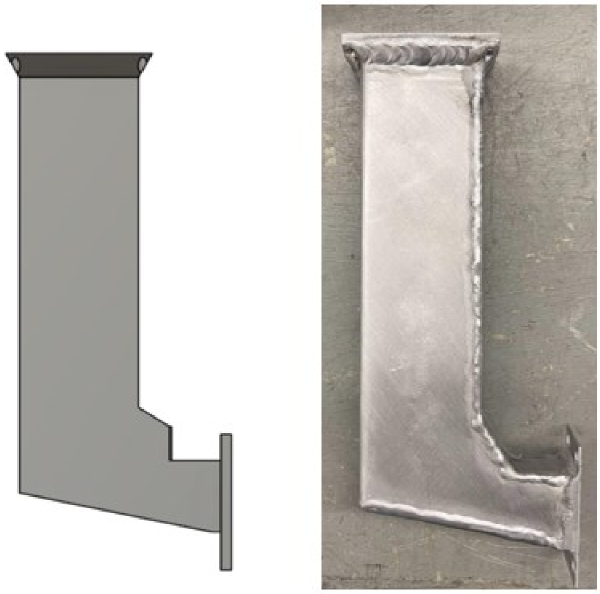

Figure 4 - 4 Hopper design and machined part

A concerning issue in the hopper system is the agglomeration of the material near the screw-hopper assembly [381]. As the screw passes through the center of the barrel, the pellets or shredded pieces in large numbers present inside the hopper act like a barrier to the rising heat and do not allow it to escape, resulting in the heat absorption by pellets and forming agglomerates [382] as shown in Figure 4-5. These large groups can stall the screw and prevent the downward movement of material, eventually starving the extruder. To transport the pellets at a fixed rate, an auger screw can also be used inside the hopper [380].

Figure 4 - 5 Agglomerates of PLA pellets

4.2.3. Thermal Band Heaters and Sensors

To get the screw filled with melted polymer at an initial stage, it is important to heat the barrel to obtain a temperature suitable for the polymer to stick to the surface [383]. The angle of the screw flights then pushes the polymer forward. After the barrel heating, the energy provided to the polymer comes entirely from the screw rotation relative to the barrel, which leads to the polymer's melting by shear [384]. The polymer inside the extruder gets heated to a viscoelastic melt when subjected to shear forces. The trapped air between the melted polymer is expelled by virtue of the pressure developed by the screw geometry [385]. It also helps to overcome the back pressure induced by the nozzle geometry [248]. The screw rotation speed and the object thickness directly affect the shear rate [386]. Hence polymers experience zero shears at the screw root and maximum shear at the barrel surface. The compression section of a screw comprises a gradually reducing channel depth which forces any unmelted polymer towards the barrel wall to impart maximum shear [387].

Out of the many ways of supplying heat, an electric band heater is used in this work as it was easy to use and made it possible to control the heat characteristics. The temperature of the heaters was controlled using temperature sensors. Four band heaters have been used in the system. These band heaters have a power of 225 W operating at 120V, a maximum heat output of 350°C, and have been placed at various locations at the barrel surface. A PT1000 temperature sensor has been installed for each of the heaters to control their temperature individually if required. It can measure temperature up to 400°C. Figure 4-6 shows the arrangement of the heaters as well as the temperature sensor.

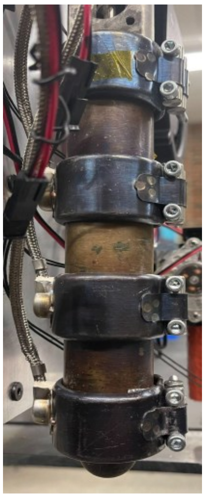

Figure 4 - 6 Arrangement of band heaters and thermistor

Although heating is an important and essential aspect of the extrusion process, there is a possibility of an upward flow of heat through the screw and the hopper, which can be detrimental as it can lead to the partial melting of the material and convert them into agglomerates [382]. Hence, to prevent this backward flow of heat, a cooling system must be installed close to the neck of the extruder [380]. Hence the current design consists of a cooling fan installed at the junction of the hopper and the barrel of the extruder, as shown in Figure 4-7.

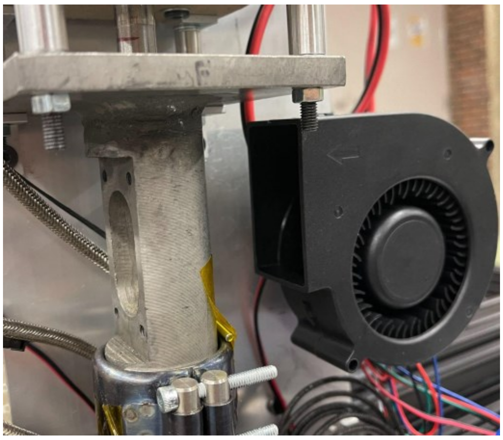

Figure 4 - 7 Cooling fan to control backflow of heat

Lastly, to improve the thermal insulation of the extruder in order to avoid the premature melting of the small-sized particles [252], the walls of the barrel are insulated with mineral wool, as shown in Figure 4-8.

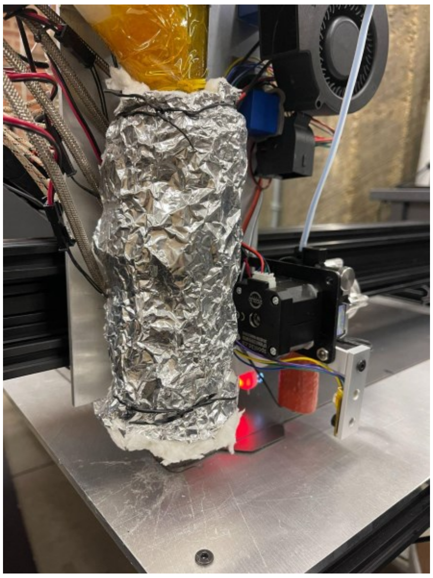

Figure 4 - 8 Mineral wool applied on barrel wall for thermal insulation

4.2.4. Stepper Motor and Encoder

Apart from the screw geometry, the rotation of the screw is another important aspect of a screw extrusion system. The rotation of the screw pressurizes the plastic, due to which it moves and gains heat from the barrel under friction [388]**.** An appropriate amount of power is needed to rotate the screw to carry on the screw extrusion mechanism. This power required is dependent on many factors, and the calculation for power requirement has been discussed in Section 4.3.3. As for the case of the Direct Fused Deposition element, the target to reach 5 mm^3/s as a maximum flow rate serves as the baseline to select the electric engine which can push the melted material at a continuous rate. The dependency of the volumetric flow rate of plastics on the screw rotation speed is shown in section 4.3.2.

A large fraction of the drive power (almost 85%) is used for the screw rotation, and the remaining power is used for mixing, pressurizing, and forwarding the melted polymer [389]. During the screw rotation process, the barrel heaters are in a cooling mode for a large duration and have almost no contribution to melting the polymers [390]. However, the initial barrel heating decreases the power requirement from the drive [391]. The viscosity of the polymer during shearing is directly related to the energy imparted by the screw drive [392]. As preheated polymers have less viscosity, less power is required for melting and remainder processes [389].

Figure 4 - 9 Closed loop servo motor with encoder and drivers

In the current design, a closed loop NEMA 23-sized stepper servo motor has been used. It has a 1.8-degree step angle, up to 3 N-m holding torque, and maximum current consumption of 4 A and operates at a DC voltage of 24-50 V [393]. Hence, the maximum power output is around 200 Watts. It has a built-in encoder having a high resolution of 4000 pulses per revolution. The encoder ensures high precision and no loss of step. In addition, the motor also has a stepper driver with a maximum step count of 40,000 steps and 16 types of micro steps, which allows the accurate functioning of encoder feedback. The motor shaft has a diameter of 8 mm; hence, an 8 X 12 mm coupler has been used to connect the motor and the screw. Figure 4-9 shows the NEMA 23 motor, inbuilt encoder, and motor driver.

4.2.5. Controlling systems

While the screw-extruding configuration is the mechanism to melt and deposit the material, the driven force required to deposit printed layers at specifically extrusion velocity at a controlled melting temperature requires the selection of integrated sensors and control components to push, and heat and move both the FDM and DFDM systems selectively. In the current hybrid system, it is essential to have an appropriate controlling system to regulate all the electronic components. Hence for this purpose, a Duet 3 6HC mainboard, a Duet 3 3HC expansion board, and a Duet 3 1XD expansion board have been used to form a connection between all the entities. These boards allow customized expansion of modules and provide good flexibility for machine design. This hardware system is enabled with RepRap Firmware which runs on a single board computer (SBC). The sequential arrangement of all the control boards used in the current design is shown in Figure 4-10.

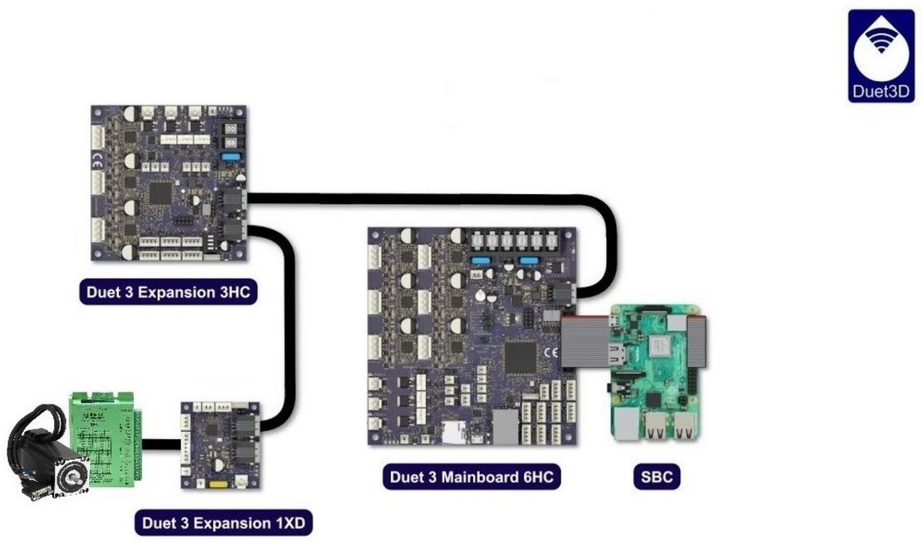

Figure 4 - 10 Sequential arrangement of control boards

The Duet 3 6HC mainboard is a high-power controller and includes 6 high current stepper drivers, 4 high current loads, and up to 6 fans. It has the capability to add more IO channels on board through CAN-FD-connected expansion boards. In the current design, the five stepper motors (one NEMA 17 for x-direction, two NEMA 23 for y-direction, and two NEMA 23 for z-direction) for movement in the three axes, one end stop sensor each for x and y-direction, two-bed platform heaters as well as two Solid state relays for the heaters and two thermocouples are connected. The Duet 3 3HC expansion board has been connected to the 6HC mainboard with the CAN bus cable. It is a high current expansion board that contains 3 stepper drivers, 3 current loads, 6 fans, and 6 IO channels. In the current design, four band heaters (DFDM), temperature sensors for these heaters (DFDM), cooling fan (DFDM), extruder fan for the conventional FDM system, cooling fan (FDM), heater (FDM), and temperature sensor (FDM) are connected to this expansion board. Finally, the Duet 3 1XD expansion board is connected to the 3HC expansion board with the help of a CAN bus cable. This board is responsible for providing a connection to an external stepper driver and can accept up to 48 V input. In the current design, the stepper servo driver of the NEMA 23 motor (for screw rotation) is connected with this expansion board. Figure 4-11 shows the connections made within the Duet 3 6HC mainboard, SBC (Raspberry Pie), Duet 3 3HC, and 1XD expansion boards.

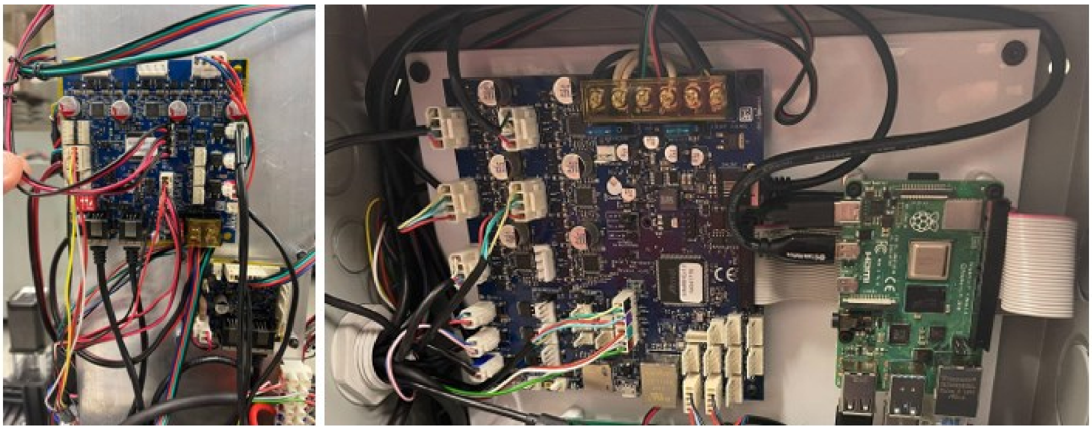

Figure 4 - 11 Connections of different control boards

This entire hardware arrangement is controlled by RepRap Firmware (version 3.4). It is an object-oriented C++ control program for self-replicating 3D printers. The G codes are sent to the software using a Duet3 Web interface through Wi-Fi. Figure 4-12 shows the Duet3 web interface.

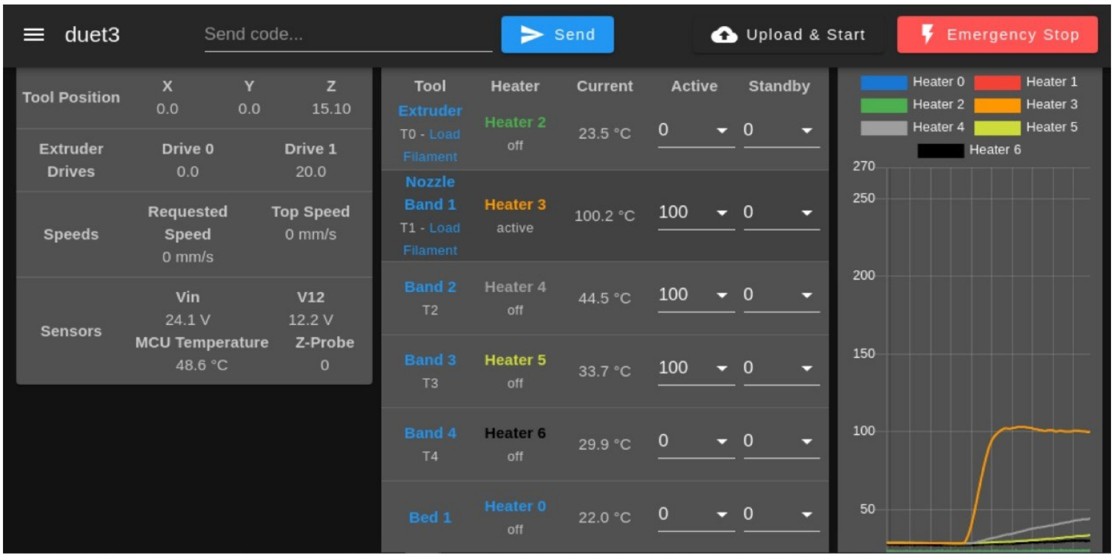

Figure 4 - 12 Duet 3 web interface

4.2.6. Hybrid Configuration Design and Assembly

One of the future objectives of this work is to print multi-material 3D objects which is possible only through the concept of hybrid 3D printing, which integrates multiple 3D printing technologies onto a single manufacturing platform. It has the combined advantages of each 3D printing technique's unique processing capability, making it feasible for many materials [236]. The components and the complete assembly were designed on Fusion 360, as shown in Figure 4-13. The actual system is shown in Figure 4-14.

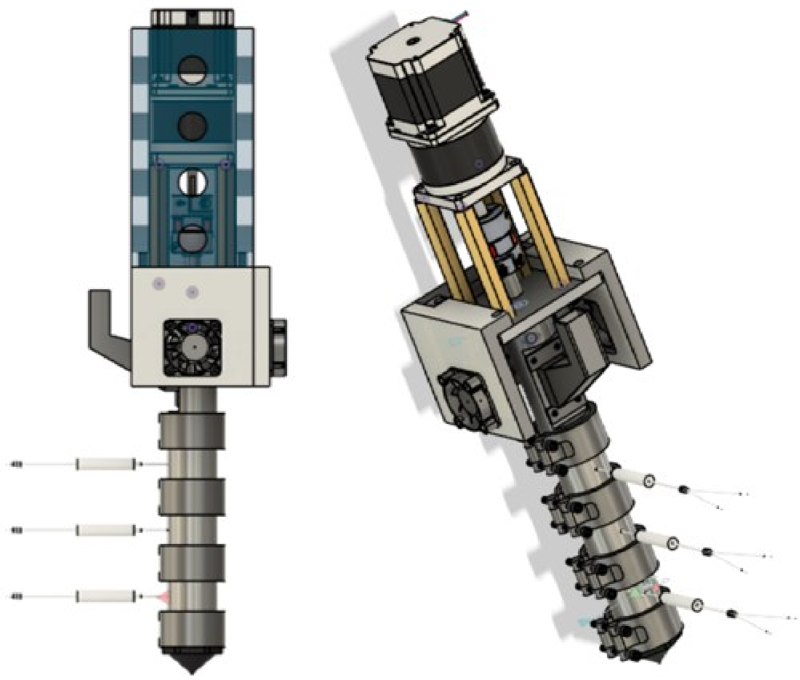

Figure 4 - 13 CAD model of DFDM system

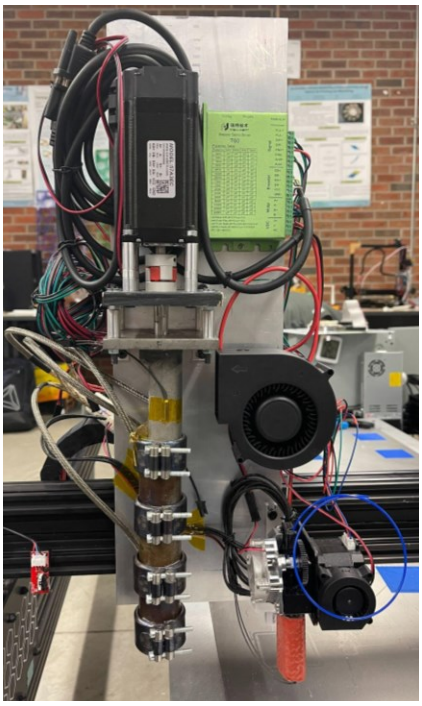

Figure 4 - 14 Hybrid system consisting of both FDM and DFDM systems

4.3. Technical Modeling

4.3.1. Barrel Material Selection

Any cylindrical body, such as a tube or a pipe, develops stresses at the circumference when pressure is applied [394]. To avoid bursting by virtue of pressure, these internal stresses act in the transverse direction and are tensile in nature. These are called Hoop stresses [395]. The barrel used in the DFDM system is cylindrical, and a Hoop stress analysis has been done to analyze the material that can be used for the barrel in this work. As mentioned earlier, PLA has been used in this work, and Table 4-3 shows the viscosity values of PLA at different temperatures. The calculations are derived from [394], [396].

$$\text{Hoop stress } (\sigma_H) = (P*d)/(2*t)$$

where, P = internal pressure in Pa

d = internal diameter of cylinder (here barrel) (mm)

and t = wall thickness (mm)

$P = (\mu*Q)/K$, where $K = (\pi*R^4)/8L = (\pi*D^4)/(128*L)$ {here, L is the length of the barrel, and μ is the viscosity of the material}

$$P =(128*\mu*Q*L)/(\pi*D^4)$$

Also, d = D (Barrel inner diameter)

$$\sigma_H = [(128*\mu*Q*L) *(D)]/[2*t*(\pi*D^4)] = (64*\mu*Q*L)/(\pi*D^3*t)$$

Therefore, $\sigma_{H(max)}= (64*\mu_{(max)}*Q_{(max)}*L)/(\pi*D^3*t)$

Now, $Q_{(max)} = 5\ mm^3/s$, L = 190 mm, D = 11.8 mm, t = 11.9 mm

Table 4 - 3 Viscosity values at different temperatures for PLA [397]

Temperature	Viscosity of PLA in Pa-s
180°C	3037
190°C	2360
200°C	1232
210°C	733

$\mu_{(max)}$ = 3037 Pa-s (at 180°C)

or $\mu_{(max)}$ (PLA) = 3037 $N\text{-}s/m^2$ = 3.037 kg/mm-s

$$\sigma_{H(max)}= (64*3.037*5*190)/(\pi*11.8^3*11.9) = 3.008\ kg/mm\text{-}s^2$$

$$\sigma_{H(max)} = 3008 \text{ N/m}^2, \text{ Factor of safety} = 5 \text{ [398]}$$

$$\sigma_{H(max)} = (3008*5) \text{ N/m}^2 = 15{,}040 \text{ N/m}^2$$

$$\text{Therefore, } \sigma_{H(max)} \text{ (PLA)} = 15 \text{ kN/m}^2$$

$$\sigma_{H(max)} \text{ (Barrel)} = 15 \text{ kN/m}^2 = 0.015 \text{ MPa}$$

From calculations, it can be deduced that any material that can withstand stresses equivalent to 0.015 MPa is an ideal material for a barrel, which is insignificant when compared to the strength of commercial metals. For the current hybrid system, a barrel made of stainless steel (tensile strength of around 600 MPa [399]) has been used to handle all the stresses generated by internal pressure.

4.3.2. Flow Rate Calculations

For initial trials, it becomes necessary to have a base value for screw rotation speed to ensure that a safe input value of rotation is fed to the control system. These calculations aim to form a relation between the screw rotation speed (N) and the volumetric flow rate (Q). A Q value of 5 mm^3/s has been targeted; accordingly, the corresponding value of N has been determined for initial trials. This relation between Q and N is based on Screw extrusion theory and has been completely derived from [396] and is shown below.

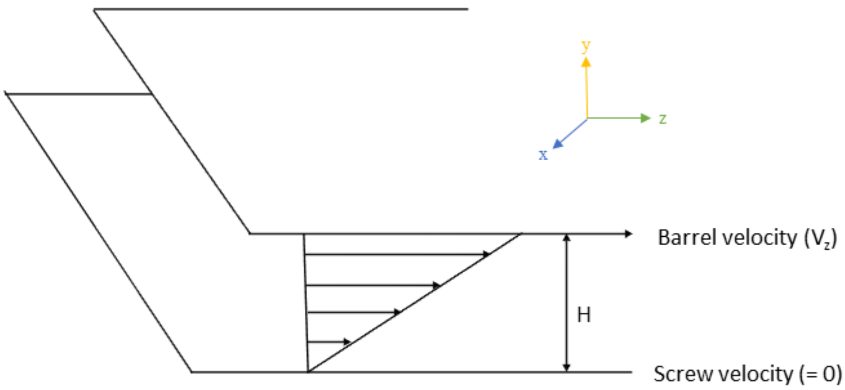

Figure 4 - 15 Drag Flow Mechanism (adapted from [396])

From Figures 4-15 and 4-16, the down Channel Velocity Component of the material, 'V_z', can be expressed in terms of the tangential velocity 'V' as: $V_z = V^*\cos ø$

Volumetric Flow Rate from drag (Q_D) is given as:

$$Q_D = W\int_0^H v(y)dy$$

Since the velocity profile for a Newtonian fluid is linear, $v(y) = V_z * y/H$

$$Q_D = W^*(V_z/H)\int_0^H ydy$$

$$Q_D = (W^*V_{z^*} H)/2$$

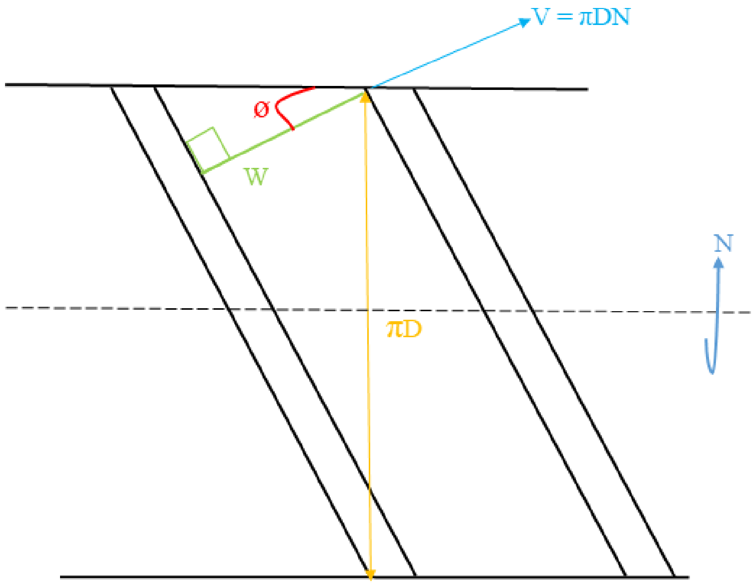

Figure 4 - 16 Unrolled Single Turn of the Extruder Screw Helix (adapted from [396])

From Figure 4-16, the tangential velocity at the barrel surface is related to the rotational speed of the screw and is given by: $V = \pi * D * N$

Therefore, the down channel velocity component can be given as: $V_z = \pi * D * N * \cos ø$

Hence, Q_D simplifies to: $Q_D = (\pi/2) * W * H * D * N * \cos ø$

An important point about the screw mechanism which needs to be considered is that the total pressure along the length of the screw is the sum of pressure changes across all the three zones which can be described by: Back pressure (**Δ**P) = $\Delta P_{feed.} + \Delta P_{comp.} + \Delta P_{meter.}$ [380]**.** This back pressure creates some flow restrictions that works against the flow through the screw. This volumetric flow rate by virtue of the back pressure generated can be given as:

$$Q_P = - (W/12) * H^3 * (\Delta P / \mu * L)$$

The net volumetric flow rate is the sum of Q_D and Q_P, and is derived below:

$$Q = Q_D + Q_P$$

$$Q = [(\pi /2) *W*H*D*N*\cos\o] + [- (W/12) *H^3*(\Delta P/ \mu*L)]$$

The net volumetric flow rate (Q) and pressure drop (ΔP) can be related as –

$Q = (K*\Delta P)/\mu$, where $K = (\pi*R^4)/8L$ {for a circular die according to Hagen-Poiseuille Law}

Here μ is the viscosity of the material present in the system, which is PLA in this work.

$$\Delta P = (\mu*Q)/K, \text{ where } K = (\pi*R^4)/8L = (\pi*D^4)/(128*L)$$

$$\Delta P =(128*\mu*Q*L)/(\pi*D^4)$$

$$(\Delta P/ \mu*L) =(128*Q)/(\pi*D^4)$$

$$Q = [(\pi /2) *W*H*D*N*\cos\o] + [- (W/12) *H^3*(128*Q)/(\pi*D^4)]$$

$$Q [1 + (W/12) *H^3*(128*Q)/(\pi*D^4)] = (\pi /2) *W*H*D*N*\cos\o$$

$$Q [(32W*H^3 +3\pi*D^4)/(3\pi*D^4)] = (\pi /2) *W*H*D*N*\cos\o$$

$Q = (3\pi^2*W*H*D^5*N*\cos\o)/(6\pi*D^4+64W*H^3)$ {here Q is in mm^3/min}

For mm^3/s, dividing by 60 on both the sides of the equation:

$$Q = (\pi^2*W*H*D^5*N*\cos\o)/(120\pi*D^4+1280W*H^3)$$

On substituting values of screw geometry parameters, the relation between the volumetric flow rate and screw rotation speed is found to be –

$Q = 7.5*N$, where N is in rpm and Q is in mm^3/s

Conversely, $N = 0.133*Q$

Hence for the DFDM system in this work, the rotational speed required for a screw in rpm is mathematically 0.133 times the volumetric flow rate in mm^3/s. To get the targeted volumetric flow rate of 5 mm^3/s, the screw should have a speed of 0.67 rpm, which is quite insignificant compared to realistic values.

4.3.3. Power Calculations

As discussed earlier, inside the extruder, the polymers are melted almost entirely by virtue of viscous dissipation due to the rotation of the screw inside the barrel. The polymer melt film adhered to the barrel surface experiences a shear force by the turning screw, which causes it to stretch [400]. The resistance offered to the screw rotation while stretching the melt film is overcome by the power provided to the screw by the extruder drive [401]. This energy from the drive increases the melt film temperature and melts any unmelted material in the vicinity by virtue of transferred heat. Different polymers have different energy requirements based on the energy requirements for reaching the processing temperature [402].

Several parameters affect the power required to melt the polymer, such as the specific heat of the polymer, output mass flow rate, and the final melt temperature. Additionally, there are several energy losses in the system due to thermal losses, driver efficiency, gearbox efficiency, and power required for melting pressurization. From studies, it has been found that around 35% of additional energy is required to compensate for these losses [403]. As per the calculations, Btu/hr should be multiplied by 1.35 and a conversion factor of 0.000393 to get the horsepower (hp) [403].

From [403], the equation for Power required to melt the polymer is given below.

Power (hp) = (0.000393*1.35) *(ṁ (lb/hr)) *(specific heat © (Btu/lb-°F)) *(temperature rise in the barrel)

Since the current design has been tested on PLA, the required material properties are derived from [404] and used in the equation. Also, as mentioned earlier for the case of the Direct Fused Deposition element, the target to reach 5 mm^3/s as a maximum flow rate serves as the baseline to select the electric engine. The mass flow rate value has been found accordingly. The calculations are shown below.

$$\dot{m} = \text{Volumetric flow rate } (= 5\ mm^3/s) * \text{Density } (= 1.24*10^{-6}\ kg/mm^3) = 6.2*10^{-6}\ kg/s = 0.0492\ lb/hr$$

$$\text{Max } T_{req} = 220°C = 428°F,\ T_{room} = 25°C = 77°F,\ C = 1800\ J/Kg\text{-}K = 0.429922\ Btu/lb\text{-}°F$$

$$P = 0.00053*0.0492*0.429922*(428-77)\ hp$$

$$P = 3.93*10^{-3}\ hp = 2.93\ watts$$

A power of around 3 W is required to melt PLA and achieve a volumetric flow rate of 5 mm^3/s. The NEMA 23 stepper motor used in this work can provide up to 200 W of power output, which makes the input power requirement of 3 W quite insignificant.

4.4. Materials

As far as this work is concerned, the proposed hybrid system has been tested only for PLA. Multi-material printing using other potential thermoplastics such as ABS, HIPS, and PC using this hybrid system is one of the future objectives of this work. Virgin PLA pellets (grade 4043D) have been used for trials. The pellet size was in the range of 2-5 mm. For the recycling counterpart, 3D printed PLA parts were shredded using a shredder and reduced to a size ranging from 2-3 mm. Here, it is important to clarify that the shredded PLA parts were printed from virgin PLA on the FDM system of this proposed hybrid system. The parts were similar and made from the same grade of PLA throughout to avoid material contamination. Additionally, the proposed hybrid system has been tested only for one-time recycled PLA, and printing with multiple times recycled materials is yet another future objective of this work.

Based on the literature survey and the trials conducted, some material properties for the current DFDM system are shown in Table 4-4.

Table 4 - 4 Material specifications

Material	Material Size	Standard Extrusion Temperature Range	Standard Bed Temperature Range	Drying Tempera ture	Dryin g Time
PLA (4043D)	2-5 mm	210-230°C	60-80°C	175°F	4 hours

4.5. Experimental Results

Since FDM is a conventional method, this technology's printing parameters for PLA are known. However, in the case of DFDM, print parameters were unknown and needed to be found out. For this, the pellets were loaded into the hopper, keeping the initial temperature the same as FDM. The DFDM experimental setup needed a high temperature to obtain a homogeneous melt; hence, the temperature was constantly increased by a margin of 5°C to have stable extruding. Various trials were conducted both for virgin and recycled PLA. Parameters such as temperature, screw rotation speed, layer height and nozzle diameter were adjusted as per the results obtained from the print.

4.5.1. Layer Deposition Testing

To ensure a good value of layer height, the DFDM system was made to extrude in a linear direction. After several trials, a layer height of 1.4 mm was found to be the most optimal one as it resulted in uniform and better extrusion. Figure 4-17 shows the trials on layer height is done.

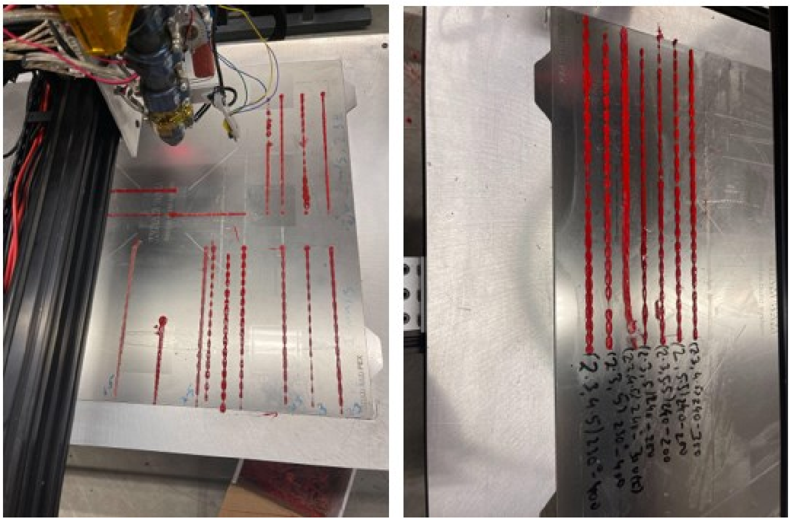

Figure 4 - 17 Layer Deposition Testing

Nozzle diameter was another factor that affected the quality of the print. The use of a 2.5 mm nozzle resulted in Die-swelling issues. This is a phenomenon in which the extrudate diameter becomes larger than the channel size or the nozzle diameter [405]. This created irregularities on the walls of the print, as shown in Figure 4-18.

Figure 4 - 18 Irregular Print due to Die-swelling issue

4.5.2. Printing Trials

A box geometry was printed using the DFDM system using both virgin and recycled PLA, one at a time. Several print trials were done to develop optimized printing parameters for both virgin and recycled material. Figure 4-19 shows the DFDM system printing virgin PLA.

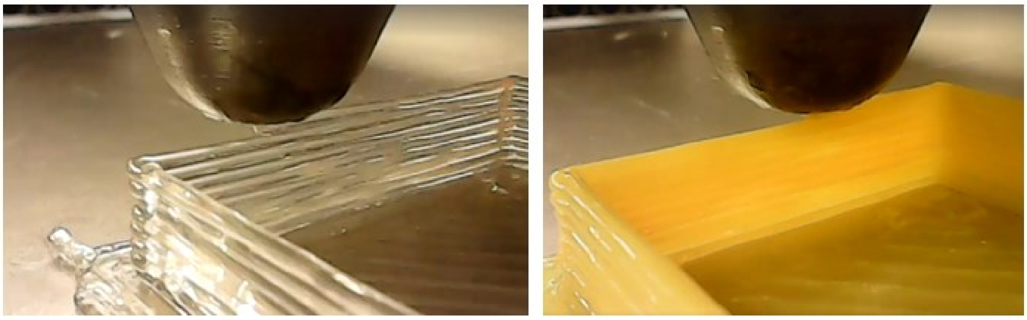

Figure 4 - 19 Printing trial with virgin PLA using DFDM system

The print parameters for virgin PLA pellets used in the trials are shown in Table 4-5.

Table 4 - 5 Printing parameters for virgin PLA

S.No.	Print Parameter	Value
1	Screw Speed	2 mm/s
2	Layer Height	1.4 mm
3	Temperature Profile (band heater temperatures from bottom to top)	175°C, 165°C, 155°C, 150°C
4	Bed temperature	60°C

Figure 4-20 shows some failed as well as successful trials using virgin PLA pellets.

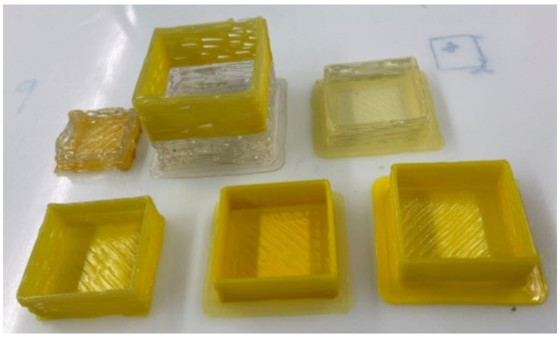

Figure 4 - 20 Print trials using virgin PLA

Figure 4 - 21 FDM printing of PLA parts

Once successful printing was achieved for virgin PLA, the next target was to make sure that the system works well with recycled PLA as well. The recycled PLA material was prepared by shredding the parts printed from the FDM setup of the hybrid system as shown in Figure 4-21.

For this, the trials were initiated with the same printing parameters as used for virgin PLA. Although, some parameters such as screw speed and temperature were continuously changed to come up with an optimized set of parameters. The main challenge was the non-uniform size of the shredded PLA particles as shown in Figure 4-22.

Figure 4 - 22 Shredded PLA particles (recycled)

After several trials, it was concluded that particle size within the range of 2-4 mm suits the best for this system. Figure 4-23 shows many failed prints using recycled PLA before reaching the most optimized print. Since the scope of this work was just to design the system and not to come out with the most optimized set of parameters, there is a huge scope for improving the quality of the prints, which is also one of the future objectives of this work.

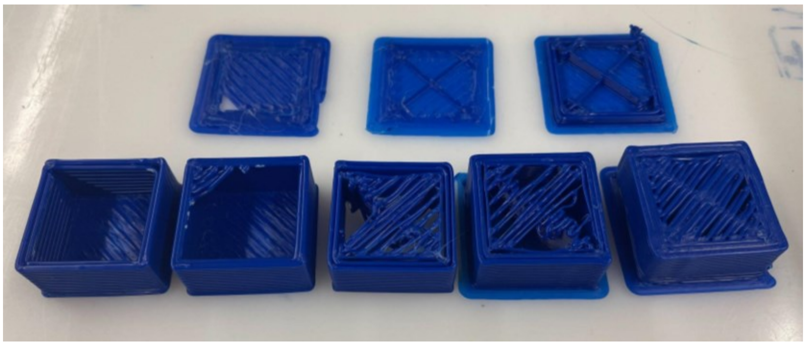

Figure 4 - 23 Print trials using recycled PLA

4.6. Conclusions

This chapter's main emphasis was printing using a high throughput hybrid system. For this, an existing FDM system was modified, and a DFDM system was installed alongside it. This DFDM system was designed after doing a literature survey on various aspects such as screw geometry, thermal requirement, electrical power requirement, and sensor analysis. A CAD file for the entire DFDM system was created first to visualize the system before machining the parts. The components were assembled mechanically, keeping in mind the electronics aspect as well. Calculations were done to ensure the right material for the barrel is being used, which can handle the hoop stresses generated on the inner walls of the barrel by virtue of the internal pressure created during the extrusion process. Further calculations were done to check the power requirements to melt the PLA in the proposed system having defined screw geometries. Apart from this, a relation between volumetric flow rate and screw rotation speed was also established. The aim of this relation was to analyze the initial speed requirements to get a targeted flow rate of 5mm^3/s. Finally, after all the electrical connections were made, the hybrid system was ready for trial. First, virgin PLA pellets ranging from 2-5 mm were tried, and based on trials, the printing parameters such as layer height, band heater temperatures, screw speed, etc., were continuously changed as per the requirement.

These trials were conducted till good, and stable print was obtained. Like virgin PLA, the trials were conducted for recycled shredded PLA material till a stable print was obtained.

Chapter 5 Conclusions

5.1. General Conclusion

Plastics indeed contribute significantly to society, but it happens at the cost of several essential factors, such as rigorous segregation methods and proper decomposition planning. However, at the same time, if not used wisely, plastics can even be a threat to the environment; hence, recycling plays a key role here. There can be many ways to recycle or reprocess plastic waste. The Circular Economy is one such economic growth model implemented to use or recycle plastic resources efficiently. In recent years, the recycling of plastics has opened several doors of advancements in the field of AM. This thesis also focuses on reprocessing plastics through additive manufacturing technology (particularly FDM) and on DRAM, a critical concept of utilizing plastic waste. The first task in the thesis was doing an intense literature survey and connecting the dots between plastic recycling and AM. For doing this, a Scientometric analysis was done on the previous studies and a total of 1452 relevant publications were sorted between 2013-2021. This analysis provided a gist of the topics and highlighted many trends such as leading countries working in this field, collaborations between authors, etc. However, for in-depth research, a critical review was also done, which discussed FDM parameters, multi-material, and muti-component 3D printing, as well as Direct FDM systems. The second part of the thesis involved some experimentations with an aim to address some literature gaps at different stages of the DRAM process. A novel approach was adopted by comparing the effect of recycling with the effect of FDM parameters on the tensile properties of PLA specimens. The results showed that the recycling effect was dominant when compared to other parameters. By recycling, several changes were observed in the specimens, such as a loss of weight, change in color and loss of strength. The analyses of time and number of specimens to be printed at the start of every reprocessing cycle were additionally included in this work. While talking about FDM throughout the thesis, it was also important to highlight the concept of Extrusion Additive Manufacturing (EAM) which has gained lots of attention recently. This process has been widely utilized for reprocessing waste plastics into filaments and finally printing them into useful products or even directly utilizing waste plastic for 3D printing. Hence as a final part of this thesis, a screw-assisted system based on EAM was designed and installed alongside a pre-existing FDM system. Throughout this work, this component was referred to as the Direct FDM (DFDM) system. The DFDM system used operated with a 1.75 mm nozzle and could give a high throughput. On the other hand, the pre-existing FDM system too worked with a 1.4 mm nozzle allowing it to give high throughputs. The resulting hybrid system was successfully printed with both virgin and recycled PLA material.

5.2. Research Contributions

There were three main research contributions from this thesis which are mentioned below.

- An optimal link between Plastic recycling and Additive Manufacturing is established, which ultimately served as a knowledge platform for the next two research objectives. A literature survey linking these two domains was missing, and hence the idea was to gather as much literature, which included a scientometric analysis of nearly 1500 papers from around the past ten years, followed by a critical review from over 250 research publications.
- Once the theoretical validation was done, the thesis contributed to Circular Economy by highlighting and also addressing the literature gaps at different stages

of the DRAM process. The analysis opened several scopes of future work and demanded a guideline for FDM parameters in the plastic recycling process.

- Design of a high-throughput hybrid system working on both FDM and DFDM technologies. The printer can utilize plastics in the form of pellets, flakes, shredded pieces, or filaments for 3D printing.

5.3. Research Limitations

The work done in this thesis does have several limitations, which are discussed below.

- This thesis has utilized Scientometric analysis and Critical review as two separate tools and used them parallelly for all the literature surveys. This limited the research to review 250 publications, as more time was invested in finding the relevant papers for critical review. A more productive and ideal way is to conduct a Scientometric analysis first and perform a critical review based on the results of the former analysis.
- Taguchi Analysis has been used in this work which is a relative method and hence does not conclude which parametric combination has the highest effect on the performance characteristics.
- This work is limited to only four reprocessing cycles. However, PLA has the potential to be reprocessed even more. All the inferences made in this thesis are valid only for four reprocessing cycles of PLA. Results might vary on increasing the reprocessing effect on the material.
- As far as the scope of this thesis is concerned, the designed hybrid system is validated and tested only for PLA and uses only one component (either FDM or DFDM) to print at a time.

5.4. Future Work

- The second research objective included a comparative analysis, and the end result was the ranking of parameters. However, the most optimized value of all the parameters is still not known. For doing so, further design of experiments can be conducted for parameters RP vs. ID% and RP vs. RA for up to four and two reprocessing cycles for Taguchi Analysis I and II, respectively. Since Extrusion temperature was the least critical parameter, it can be kept constant. Further, this research was only limited to PLA and can be conducted on conventional plastics such as ABS and other potential thermoplastics such as HIPS, PC, PETG, etc.
- As mentioned earlier, the FDM process itself is very complex. One of the reasons for this is the lack of 3D printing standards [73]. Different plastics have different recycling abilities and varying changes in properties. The criticality of printing parameters also changes with the varying reprocessing stages, as it was visible in TA1 and TA2 analysis. ID% was the second most influencing factor for two reprocessing cycles, but for four reprocessing cycles, RA replaced ID% to become the second most influencing factor. Hence it becomes essential that specific guidelines or rulebooks should be made for every recycled material and the change in its properties on recycling.
- One of the future goals of the proposed hybrid system (work already in progress) is to print multi-material structures using both FDM and DFDM technologies simultaneously. 3D printing using a combination of conventional or non-conventional materials or both at different reprocessing stages is yet another goal to be accomplished.
- With the analysis of mechanical properties of different materials, large amounts of data values can be obtained. The data set is extensive as it comes from multivariable

conditions and multi-processing cycles for multiple materials combinations. These data values can be used to train and validate the models working on Machine learning algorithms. For example, one approach can be the use of ANN (Artificial Neural Networks) and DNN (Deep Neural Networks), which are the subsets of machine learning and can be implemented on the data to train, validate and test the models. According to the accuracy of the models, the FDM manufacturing chain productions can then predict optimal product design for plastics having the most suitable strength.

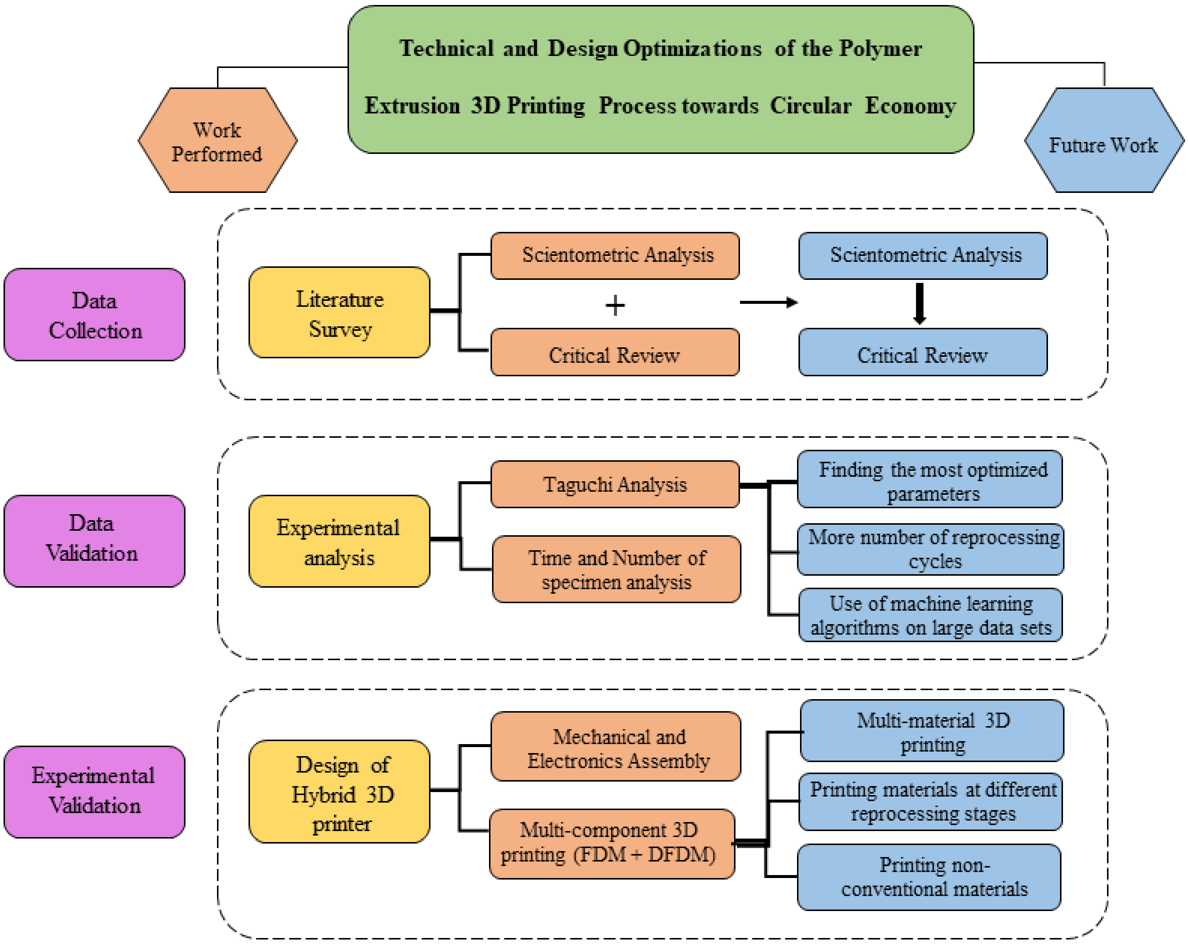

Figure 5 - 1 Future Work map

References

[1] A. L. Patrício Silva, "Future-proofing plastic waste management for a circular bioeconomy," *Curr. Opin. Environ. Sci. Heal.*, vol. 22, p. 100263, Aug. 2021, doi: 10.1016/J.COESH.2021.100263.

[2] K. Ghosh and B. H. Jones, "Roadmap to biodegradable plastics-current state and research needs," *ACS Sustain. Chem. Eng.*, vol. 9, no. 18, pp. 6170–6187, May 2021, doi: 10.1021/ACSSUSCHEMENG.1C00801/ASSET/IMAGES/ACSSUSCHEMENG.1C00801.SOCIAL.JPEG_V03.

[3] M. Degli Esposti *et al.*, "The role of biotechnology in the transition from plastics to bioplastics: an opportunity to reconnect global growth with sustainability," *FEBS Open Bio*, vol. 11, no. 4, pp. 967–983, Apr. 2021, doi: 10.1002/2211-5463.13119.

[4] S. Sikdar, A. Siddaiah, and P. L. Menezes, "Conversion of waste plastic to oils for tribological applications," *Lubricants*, vol. 8, no. 8, 2020, doi: 10.3390/LUBRICANTS8080078.

[5] S. Anandan and M. Alsubih, "Mechanical Strength Characterization of Plastic Fiber Reinforced Cement Concrete Composites," *Appl. Sci. 2021, Vol. 11, Page 852*, vol. 11, no. 2, p. 852, Jan. 2021, doi: 10.3390/APP11020852.

[6] J. Di, B. K. Reck, A. Miatto, and T. E. Graedel, "United States plastics: Large flows, short lifetimes, and negligible recycling," *Resour. Conserv. Recycl.*, vol. 167, p. 105440, Apr. 2021, doi: 10.1016/J.RESCONREC.2021.105440.

[7] M. I. Jahirul, M. G. Rasul, D. Schaller, M. M. K. Khan, M. M. Hasan, and M. A. Hazrat, "Transport fuel from waste plastics pyrolysis – A review on technologies, challenges and opportunities," *Energy Convers. Manag.*, vol. 258, p. 115451, Apr. 2022, doi: 10.1016/J.ENCONMAN.2022.115451.

[8] A. Lee and M. S. Liew, "Tertiary recycling of plastics waste: an analysis of feedstock, chemical and biological degradation methods," *J. Mater. Cycles Waste Manag.*, vol. 23, no. 1, pp. 32–43, Jan. 2021, doi: 10.1007/S10163-020-01106-2/TABLES/2.

[9] B. Sharma, Y. Goswami, S. Sharma, and S. Shekhar, "Inherent roadmap of conversion of plastic waste into energy and its life cycle assessment: A frontrunner compendium," *Renew. Sustain. Energy Rev.*, vol. 146, p. 111070, Aug. 2021, doi: 10.1016/J.RSER.2021.111070.

[10] C. Signoret *et al.*, "Degradation of Styrenic Plastics during Recycling: Accommodation of PP within ABS after WEEE Plastics Imperfect Sorting," *Polym. 2021, Vol. 13, Page 1439*, vol. 13, no. 9, p. 1439, Apr. 2021, doi: 10.3390/POLYM13091439.

[11] B. Baldassarre, T. Maury, F. Mathieux, E. Garbarino, I. Antonopoulos, and S. Sala, "Drivers and Barriers to the Circular Economy Transition: the Case of Recycled Plastics in the Automotive Sector in the European Union," *Procedia CIRP*, vol. 105, pp. 37–42, Jan. 2022, doi: 10.1016/J.PROCIR.2022.02.007.

[12] I. Čabalová, A. Ház, J. Krilek, T. Bubeníková, J. Melicherčík, and T. Kuvik, "Recycling of Wastes Plastics and Tires from Automotive Industry," *Polym. 2021, Vol. 13, Page 2210*, vol. 13, no. 13, p. 2210, Jul. 2021, doi: 10.3390/POLYM13132210.

[13] T. Osswald and N. Rudolph, "Introduction to Rheology," *Polym. Rheol.*, pp. 1–24, 2014, doi: 10.3139/9781569905234.001.

[14] K. R. Hart, J. B. Frketic, and J. R. Brown, "Recycling meal-ready-to-eat (MRE) pouches into polymer filament for material extrusion additive manufacturing," *Addit. Manuf.*, vol. 21, no. February, pp. 536–543, 2018, doi: 10.1016/j.addma.2018.04.011.

[15] S. Thakur, A. Verma, B. Sharma, J. Chaudhary, S. Tamulevicius, and V. K. Thakur, "SC," *Curr. Opin. Green Sustain. Chem.*, 2018, doi: 10.1016/j.cogsc.2018.03.011.

[16] Q. P. Xochitl, H. B. M. Del Consuelo, M. S. M. Del Consuelo, E. V. R. María, and V. M. Alethia, "Degradation of Plastics in Simulated Landfill Conditions," *Polym. 2021, Vol. 13, Page 1014*, vol. 13, no. 7, p. 1014, Mar. 2021, doi: 10.3390/POLYM13071014.

[17] C. A. Fletcher, R. St. Clair, and M. Sharmina, "A framework for assessing the circularity and technological maturity of plastic waste management strategies in hospitals," *J. Clean. Prod.*, vol. 306, p. 127169, Jul. 2021, doi: 10.1016/J.JCLEPRO.2021.127169.

[18] A. J. Martín, C. Mondelli, S. D. Jaydev, and J. Pérez-Ramírez, "Catalytic processing of plastic waste on the rise," *Chem*, vol. 7, no. 6, pp. 1487–1533, Jun. 2021, doi: 10.1016/J.CHEMPR.2020.12.006.

[19] Y. Chen, A. K. Awasthi, F. Wei, Q. Tan, and J. Li, "Single-use plastics: Production, usage, disposal, and adverse impacts," *Sci. Total Environ.*, vol. 752, p. 141772, Jan. 2021, doi: 10.1016/J.SCITOTENV.2020.141772.

[20] G. Suzuki *et al.*, "Mechanical recycling of plastic waste as a point source of microplastic pollution," *Environ. Pollut.*, vol. 303, p. 119114, Jun. 2022, doi: 10.1016/J.ENVPOL.2022.119114.

[21] M. S. Qureshi *et al.*, "Pyrolysis of plastic waste: Opportunities and challenges," *J. Anal. Appl. Pyrolysis*, vol. 152, no. February, 2020, doi: 10.1016/j.jaap.2020.104804.

[22] K. P. Gopinath, V. M. Nagarajan, A. Krishnan, and R. Malolan, "A critical review on the influence of energy, environmental and economic factors on various processes used to handle and recycle plastic wastes: Development of a comprehensive index," *J. Clean. Prod.*, vol. 274, p. 123031, 2020, doi: 10.1016/j.jclepro.2020.123031.

[23] S. Nanda and F. Berruti, "Municipal solid waste management and landfilling technologies: a review," *Environ. Chem. Lett.*, vol. 19, no. 2, pp. 1433–1456, Apr. 2021, doi: 10.1007/S10311-020-01100-Y/FIGURES/9.

[24] A. L. Patrício Silva, J. C. Prata, A. C. Duarte, D. Barcelò, and T. Rocha-Santos,

"An urgent call to think globally and act locally on landfill disposable plastics under and after covid-19 pandemic: Pollution prevention and technological (Bio) remediation solutions," *Chem. Eng. J.*, vol. 426, p. 131201, Dec. 2021, doi: 10.1016/J.CEJ.2021.131201.

[25] Closed Loop Partners, "CLP_Circular_Supply_Chains_for_Plastics_Updated," 2019, [Online]. Available: https://www.closedlooppartners.com/research/advancing-circular-systems-for-plastics/.

[26] S. L. Wright and F. J. Kelly, "Plastic and Human Health: A Micro Issue?," *Environ. Sci. Technol.*, vol. 51, no. 12, pp. 6634–6647, 2017, doi: 10.1021/acs.est.7b00423.

[27] M. R. Johansen, T. B. Christensen, T. M. Ramos, and K. Syberg, "A review of the plastic value chain from a circular economy perspective," *J. Environ. Manage.*, vol. 302, p. 113975, Jan. 2022, doi: 10.1016/J.JENVMAN.2021.113975.

[28] N. K. Sharma, K. Govindan, K. K. Lai, W. K. Chen, and V. Kumar, "The transition from linear economy to circular economy for sustainability among SMEs: A study on prospects, impediments, and prerequisites," *Bus. Strateg. Environ.*, vol. 30, no. 4, pp. 1803–1822, May 2021, doi: 10.1002/BSE.2717.

[29] A. Bellam Balaji, X. Liu, A. B. Balaji, and X. Liu, "Plastics in Circular Economy: A Sustainable Progression," *An Introd. to Circ. Econ.*, pp. 159–178, 2021, doi: 10.1007/978-981-15-8510-4_9.

[30] N. Mehta *et al.*, "Using regional material flow analysis and geospatial mapping to support the transition to a circular economy for plastics," *Resour. Conserv. Recycl.*, vol. 179, p. 106085, Apr. 2022, doi: 10.1016/J.RESCONREC.2021.106085.

[31] D. M. Mitrano and M. Wagner, "A sustainable future for plastics considering material safety and preserved value," *Nat. Rev. Mater. 2021 72*, vol. 7, no. 2, pp. 71–73, Dec. 2021, doi: 10.1038/s41578-021-00406-9.

[32] R. A. Ilyas *et al.*, "Reuse and Recycle of Biobased Packaging Products," *Bio-based Packag.*, pp. 413–426, May 2021, doi: 10.1002/9781119381228.CH23.

[33] D. Tonini, D. Schrijvers, S. Nessi, P. Garcia-Gutierrez, and J. Giuntoli, "Carbon footprint of plastic from biomass and recycled feedstock: methodological insights," *Int. J. Life Cycle Assess.*, vol. 26, no. 2, pp. 221–237, Feb. 2021, doi: 10.1007/S11367-020-01853-2/TABLES/3.

[34] R. Dhawan, B. M. S. Bisht, R. Kumar, S. Kumari, and S. K. Dhawan, "Recycling of plastic waste into tiles with reduced flammability and improved tensile strength," *Process Saf. Environ. Prot.*, vol. 124, pp. 299–307, 2019, doi: 10.1016/j.psep.2019.02.018.

[35] M. C. Mulakkal *et al.*, "Advancing mechanical recycling of multilayer plastics through finite element modelling and environmental policy," *Resour. Conserv. Recycl.*, vol. 166, p. 105371, Mar. 2021, doi: 10.1016/J.RESCONREC.2020.105371.

[36] F. R. Beltrán *et al.*, “Evaluation of the Technical Viability of Distributed Mechanical Recycling of PLA 3D Printing Wastes,” *Polym. 2021, Vol. 13, Page 1247*, vol. 13, no. 8, p. 1247, Apr. 2021, doi: 10.3390/POLYM13081247.

[37] A. E. Schwarz, T. N. Ligthart, D. Godoi Bizarro, P. De Wild, B. Vreugdenhil, and T. van Harmelen, “Plastic recycling in a circular economy; determining environmental performance through an LCA matrix model approach,” *Waste Manag.*, vol. 121, pp. 331–342, Feb. 2021, doi: 10.1016/J.WASMAN.2020.12.020.

[38] M. Y. Khalid, Z. U. Arif, W. Ahmed, and H. Arshad, “Recent trends in recycling and reusing techniques of different plastic polymers and their composite materials,” *Sustain. Mater. Technol.*, vol. 31, p. e00382, Apr. 2022, doi: 10.1016/J.SUSMAT.2021.E00382.

[39] N. Singh, D. Hui, R. Singh, I. P. S. Ahuja, L. Feo, and F. Fraternali, “Recycling of plastic solid waste: A state of art review and future applications,” *Compos. Part B Eng.*, vol. 115, pp. 409–422, 2017, doi: 10.1016/j.compositesb.2016.09.013.

[40] N. Rudolph, R. Kiesel, and C. Aumnate, *Understanding Plastics Recycling*. 2020.

[41] M. Imteaz, A. Mohammadinia, and A. Arulrajah, “Environmental suitability, carbon footprint and cost savings of recycled plastic for railway applications,” *https://doi.org/10.1080/19397038.2021.1929551*, vol. 14, no. 4, pp. 725–734, 2021, doi: 10.1080/19397038.2021.1929551.

[42] B. Jethy, S. Paul, S. K. Das, A. Adesina, and S. M. Mustakim, “Critical review on the evolution, properties, and utilization of plasticwastes for construction applications,” *J. Mater. Cycles Waste Manag.*, vol. 24, no. 2, pp. 435–451, Mar. 2022, doi: 10.1007/S10163-022-01362-4/TABLES/7.

[43] Z. O. G. Schyns and M. P. Shaver, “Mechanical Recycling of Packaging Plastics: A Review,” *Macromol. Rapid Commun.*, vol. 42, no. 3, pp. 1–27, 2021, doi: 10.1002/marc.202000415.

[44] F. Adel Ismael Chaqmaqchee, “Comparison of Various Plastics Wastes Using X-ray Fluorescence,” *Am. J. Mater. Synth. Process.*, vol. 2, no. 2, p. 24, 2017, doi: 10.11648/j.ajmsp.20170202.12.

[45] L. Pick, P. R. Hanna, and L. Gorman, “Assessment of processibility and properties of raw post-consumer waste polyethylene in the rotational moulding process,” *J. Polym. Eng.*, vol. 42, no. 4, pp. 374–383, Apr. 2022, doi: 10.1515/POLYENG-2021-0212/MACHINEREADABLECITATION/RIS.

[46] R. A. Muñoz Meneses, G. Cabrera-Papamija, F. Machuca-Martínez, L. A. Rodríguez, J. E. Diosa, and E. Mosquera-Vargas, “Plastic recycling and their use as raw material for the synthesis of carbonaceous materials,” *Heliyon*, vol. 8, no. 3, p. e09028, Mar. 2022, doi: 10.1016/J.HELIYON.2022.E09028.

[47] J. P. Lange, “Managing Plastic Waste-Sorting, Recycling, Disposal, and Product Redesign,” *ACS Sustain. Chem. Eng.*, vol. 9, no. 47, pp. 15722–15738, Nov. 2021, doi:

10.1021/ACSSUSCHEMENG.1C05013/ASSET/IMAGES/ACSSUSCHEMENG.1C05013.SOCIAL.JPEG_V03.

[48] G. Zhong and X. Peng, "Transport and accumulation of plastic litter in submarine canyons—The role of gravity flows," *Geology*, vol. 49, no. 5, pp. 581–586, May 2021, doi: 10.1130/G48536.1.

[49] S. K. Das *et al.*, "Plastic Recycling of Polyethylene Terephthalate (PET) and Polyhydroxybutyrate (PHB)—a Comprehensive Review," *Mater. Circ. Econ. 2021 31*, vol. 3, no. 1, pp. 1–22, Jun. 2021, doi: 10.1007/S42824-021-00025-3.

[50] D. S. Gabriel and H. Nasrullah, "Optical Properties Improvement of Recycled Polypropylene with Material Value Conservation Schemes Using Virgin Plastic Blends," *Mater. Sci. Forum*, vol. 1020, pp. 199–205, 2021, doi: 10.4028/WWW.SCIENTIFIC.NET/MSF.1020.199.

[51] S. M. Rajapaksha *et al.*, "Development of PP/Recycled-PET Blended Low Speed Wheels to Reduce the Virgin Plastic Usage in the Industry," *Adv. Technol.*, vol. 1, no. 1, pp. 7–24, May 2021, doi: 10.31357/AIT.V1I1.4893.

[52] T. A. Osswald, "Understanding Polymer Processing," *Underst. Polym. Process.*, Oct. 2017, doi: 10.3139/9781569906484.

[53] W. Li, H. Fan, Y. Bian, and F. Yang, "Plastic deformation and energy absorption of polycrystalline-like lattice structures," *Mater. Des.*, vol. 198, p. 109321, Jan. 2021, doi: 10.1016/J.MATDES.2020.109321.

[54] M. Rifai, E. Bagherpour, G. Yamamoto, M. Yuasa, and H. Miyamoto, "Transition of Dislocation Structures in Severe Plastic Deformation and Its Effect on Dissolution in Dislocation Etchant," *Adv. Mater. Sci. Eng.*, vol. 2018, 2018, doi: 10.1155/2018/4254156.

[55] L. Li *et al.*, "Dual-Mechanism and Multimotion Soft Actuators Based on Commercial Plastic Film," *ACS Appl. Mater. Interfaces*, vol. 10, no. 17, pp. 15122–15128, May 2018, doi: 10.1021/ACSAMI.8B00396/SUPPL_FILE/AM8B00396_SI_008.AVI.

[56] W. Zeng, J. He, and F. Liu, "Preparation and properties of antibacterial ABS plastics based on polymeric quaternary phosphonium salts antibacterial agents," *Polym. Adv. Technol.*, vol. 30, no. 10, pp. 2515–2522, Oct. 2019, doi: 10.1002/PAT.4653.

[57] S. H. Ahn, M. Montero, D. Odell, S. Roundy, and P. K. Wright, "Anisotropic material properties of fused deposition modeling ABS," *Rapid Prototyp. J.*, vol. 8, no. 4, pp. 248–257, 2002, doi: 10.1108/13552540210441166.

[58] I. Vollmer *et al.*, "Beyond Mechanical Recycling: Giving New Life to Plastic Waste," *Angew. Chemie Int. Ed.*, vol. 59, no. 36, pp. 15402–15423, Sep. 2020, doi: 10.1002/ANIE.201915651.

[59] G. Faraca and T. Astrup, "Plastic waste from recycling centres: Characterisation and evaluation of plastic recyclability," *Waste Manag.*, vol. 95, pp. 388–398, Jul. 2019, doi: 10.1016/J.WASMAN.2019.06.038.

[60] J. Hopewell, R. Dvorak, and E. Kosior, “Plastics recycling: challenges and opportunities,” *Philos. Trans. R. Soc. B Biol. Sci.*, vol. 364, no. 1526, p. 2115, Jul. 2009, doi: 10.1098/RSTB.2008.0311.

[61] M. W. M. Cunico, D. A. Kai, P. M. Cavalheiro, and J. de Carvalho, “Development and characterisation of 3D printing finishing process applying recycled plastic waste,” *https://doi.org/10.1080/17452759.2018.1521248*, vol. 14, no. 1, pp. 37–52, Jan. 2018, doi: 10.1080/17452759.2018.1521248.

[62] A. A. James, M. R. Rahman, M. K. Bin Bakri, and M. M. Matin, “Introduction to recycled plastic biocomposites,” *Recycl. Plast. Biocomposites*, pp. 1–27, Jan. 2022, doi: 10.1016/B978-0-323-88653-6.00005-5.

[63] K. Mikula *et al.*, “3D printing filament as a second life of waste plastics—a review,” *Environ. Sci. Pollut. Res.*, vol. 28, no. 10, pp. 12321–12333, 2021, doi: 10.1007/s11356-020-10657-8.

[64] C. Matthews, F. Moran, and A. K. Jaiswal, “A review on European Union’s strategy for plastics in a circular economy and its impact on food safety,” *J. Clean. Prod.*, vol. 283, p. 125263, Feb. 2021, doi: 10.1016/J.JCLEPRO.2020.125263.

[65] P. Santander, F. A. Cruz Sanchez, H. Boudaoud, and M. Camargo, “Closed loop supply chain network for local and distributed plastic recycling for 3D printing: a MILP-based optimization approach,” *Resour. Conserv. Recycl.*, vol. 154, p. 104531, Mar. 2020, doi: 10.1016/J.RESCONREC.2019.104531.

[66] S. Ügdüler *et al.*, “Towards closed-loop recycling of multilayer and coloured PET plastic waste by alkaline hydrolysis,” *Green Chem.*, vol. 22, no. 16, pp. 5376–5394, Aug. 2020, doi: 10.1039/D0GC00894J.

[67] M. K. Eriksen and T. F. Astrup, “Characterisation of source-separated, rigid plastic waste and evaluation of recycling initiatives: Effects of product design and source-separation system,” *Waste Manag.*, vol. 87, pp. 161–172, Mar. 2019, doi: 10.1016/J.WASMAN.2019.02.006.

[68] A. Behrens, “Time to Connect the Dots: What is the Link between Climate Change Policy and the Circular Economy?,” no. 337, pp. 1–7, 2016.

[69] P. O. Awoyera and A. Adesina, “Plastic wastes to construction products: Status, limitations and future perspective,” *Case Stud. Constr. Mater.*, vol. 12, p. e00330, Jun. 2020, doi: 10.1016/J.CSCM.2020.E00330.

[70] L. K. Ncube, A. U. Ude, E. N. Ogunmuyiwa, R. Zulkifli, and I. N. Beas, “An Overview of Plastic Waste Generation and Management in Food Packaging Industries,” *Recycl. 2021, Vol. 6, Page 12*, vol. 6, no. 1, p. 12, Feb. 2021, doi: 10.3390/RECYCLING6010012.

[71] F. M. AL-Oqla and M. T. Hayajneh, “A hierarchy weighting preferences model to optimise green composite characteristics for better sustainable bio-products,” *https://doi.org/10.1080/19397038.2020.1822951*, vol. 14, no. 5, pp. 1043–1048, 2020, doi: 10.1080/19397038.2020.1822951.

[72] F. A. Cruz Sanchez, H. Boudaoud, M. Camargo, and J. M. Pearce, “Plastic

recycling in additive manufacturing: A systematic literature review and opportunities for the circular economy," *J. Clean. Prod.*, vol. 264, 2020, doi: 10.1016/j.jclepro.2020.121602.

[73] H. A. Little, N. G. Tanikella, M. J. Reich, M. J. Fiedler, S. L. Snabes, and J. M. Pearce, "Towards distributed recycling with additive manufacturing of PET flake feedstocks," *Materials (Basel).*, vol. 13, no. 19, 2020, doi: 10.3390/MA13194273.

[74] D. M. B. Lopez and R. Ahmad, "Tensile mechanical behaviour of multi-polymer sandwich structures via fused deposition modelling," *Polymers (Basel).*, vol. 12, no. 3, 2020, doi: 10.3390/polym12030651.

[75] L. Li, J. Liu, Y. Ma, R. Ahmad, and A. Qureshi, "Multi-view feature modeling for design-for-additive manufacturing," *Adv. Eng. Informatics*, vol. 39, no. December, pp. 144–156, 2019, doi: 10.1016/j.aei.2018.12.004.

[76] Y. Zheng, J. Liu, and R. Ahmad, "A cost-driven process planning method for hybrid additive–subtractive remanufacturing," *J. Manuf. Syst.*, vol. 55, no. April, pp. 248–263, 2020, doi: 10.1016/j.jmsy.2020.03.006.

[77] H. Yu, H. Hong, S. Cao, and R. Ahmad, "Topology optimization for multipatch fused deposition modeling 3D printing," *Appl. Sci.*, vol. 10, no. 3, 2020, doi: 10.3390/app10030943.

[78] M. Alghamdy, R. Ahmad, and B. Alsayyed, "Material selection methodology for additive manufacturing applications," *Procedia CIRP*, vol. 84, pp. 486–490, 2019, doi: 10.1016/j.procir.2019.04.265.

[79] J. L. Pérez-Castillo *et al.*, "Curved layered fused filament fabrication: An overview," *Addit. Manuf.*, vol. 47, no. September, 2021, doi: 10.1016/j.addma.2021.102354.

[80] T. N. Azila *et al.*, "Recent Developments in Fused Deposition Modeling-Based 3D Printing of Polymers and Their Composites," *https://doi.org/10.1080/15583724.2019.1597883*, vol. 59, no. 4, pp. 589–624, Oct. 2019, doi: 10.1080/15583724.2019.1597883.

[81] C. Abeykoon, P. Sri-Amphorn, and A. Fernando, "Optimization of fused deposition modeling parameters for improved PLA and ABS 3D printed structures," *Int. J. Light. Mater. Manuf.*, vol. 3, no. 3, pp. 284–297, Sep. 2020, doi: 10.1016/J.IJLMM.2020.03.003.

[82] S. C. Daminabo, S. Goel, S. A. Grammatikos, H. Y. Nezhad, and V. K. Thakur, "Fused deposition modeling-based additive manufacturing (3D printing): techniques for polymer material systems," *Mater. Today Chem.*, vol. 16, p. 100248, Jun. 2020, doi: 10.1016/J.MTCHEM.2020.100248.

[83] A. Della Bona, V. Cantelli, V. T. Britto, K. F. Collares, and J. W. Stansbury, "3D printing restorative materials using a stereolithographic technique: a systematic review," *Dent. Mater.*, vol. 37, no. 2, pp. 336–350, Feb. 2021, doi: 10.1016/J.DENTAL.2020.11.030.

[84] M. Mukhtarkhanov, A. Perveen, and D. Talamona, "Application of

Stereolithography Based 3D Printing Technology in Investment Casting," *Micromachines 2020, Vol. 11, Page 946*, vol. 11, no. 10, p. 946, Oct. 2020, doi: 10.3390/MI11100946.

[85] B. Khatri, M. Frey, A. Raouf-Fahmy, M. V. Scharla, and T. Hanemann, "Development of a Multi-Material Stereolithography 3D Printing Device," *Micromachines 2020, Vol. 11, Page 532*, vol. 11, no. 5, p. 532, May 2020, doi: 10.3390/MI11050532.

[86] J. Zhang, Q. Hu, S. Wang, J. Tao, and M. Gou, "Digital Light Processing Based Three-dimensional Printing for Medical Applications," *Int. J. Bioprinting*, vol. 6, no. 1, pp. 12–27, 2020, doi: 10.18063/IJB.V6I1.242.

[87] X. Kuang *et al.*, "Grayscale digital light processing 3D printing for highly functionally graded materials," *Sci. Adv.*, vol. 5, no. 5, 2019, doi: 10.1126/SCIADV.AAV5790/SUPPL_FILE/AAV5790_SM.PDF.

[88] A. Awad, F. Fina, A. Goyanes, S. Gaisford, and A. W. Basit, "3D printing: Principles and pharmaceutical applications of selective laser sintering," *Int. J. Pharm.*, vol. 586, p. 119594, Aug. 2020, doi: 10.1016/J.IJPHARM.2020.119594.

[89] N. A. Charoo *et al.*, "Selective laser sintering 3D printing – an overview of the technology and pharmaceutical applications," *https://doi.org/10.1080/03639045.2020.1764027*, vol. 46, no. 6, pp. 869–877, Jun. 2020, doi: 10.1080/03639045.2020.1764027.

[90] S. F. Barakh Ali *et al.*, "Understanding the effects of formulation and process variables on the printlets quality manufactured by selective laser sintering 3D printing," *Int. J. Pharm.*, vol. 570, p. 118651, Oct. 2019, doi: 10.1016/J.IJPHARM.2019.118651.

[91] M. Mayyas, "Interpolation of tensile properties of polymer composite based on Polyjet 3D printing," *Prog. Addit. Manuf.*, vol. 6, no. 4, pp. 607–615, Dec. 2021, doi: 10.1007/S40964-021-00170-W/FIGURES/5.

[92] S. C. Das, R. Ranganathan, and N. Murugan, "Effect of build orientation on the strength and cost of PolyJet 3D printed parts," *Rapid Prototyp. J.*, vol. 24, no. 5, pp. 832–839, Sep. 2018, doi: 10.1108/RPJ-08-2016-0137/FULL/XML.

[93] R. Gupta, M. Dalakoti, and A. Narasimhulu, "A Critical Review of Process Parameters in Laminated Object Manufacturing Process," pp. 31–39, 2020, doi: 10.1007/978-981-15-4331-9_3.

[94] D. X. Luong *et al.*, "Laminated Object Manufacturing of 3D-Printed Laser-Induced Graphene Foams," *Adv. Mater.*, vol. 30, no. 28, p. 1707416, Jul. 2018, doi: 10.1002/ADMA.201707416.

[95] B. Dermeik and N. Travitzky, "Laminated Object Manufacturing of Ceramic-Based Materials," *Adv. Eng. Mater.*, vol. 22, no. 9, p. 2000256, Sep. 2020, doi: 10.1002/ADEM.202000256.

[96] S. D. Nath and S. Nilufar, "An overview of additive manufacturing of polymers and associated composites," *Polymers (Basel).*, vol. 12, no. 11, pp. 1–33, 2020,

doi: 10.3390/polym12112719.

[97] G. Palani, K. Kannan, G. Palani, and K. Kannan, “Introduction to Additive Manufacturing for Composites: State of the Art and Recent Trends,” pp. 1–24, 2022, doi: 10.1007/978-981-16-7377-1_1.

[98] A. Dey and N. Yodo, “A Systematic Survey of FDM Process Parameter Optimization and Their Influence on Part Characteristics,” *J. Manuf. Mater. Process. 2019, Vol. 3, Page 64*, vol. 3, no. 3, p. 64, Jul. 2019, doi: 10.3390/JMMP3030064.

[99] H. Zhao, X. Liu, W. Zhao, G. Wang, and B. Liu, “An Overview of Research on FDM 3D Printing Process of Continuous Fiber Reinforced Composites,” *J. Phys. Conf. Ser.*, vol. 1213, no. 5, p. 052037, Jun. 2019, doi: 10.1088/1742-6596/1213/5/052037.

[100] H. García-Martínez, E. Ávila-Navarro, G. Torregrosa-Penalva, A. Rodríguez-Martínez, C. Blanco-Angulo, and M. A. de la Casa-Lillo, “Low-Cost Additive Manufacturing Techniques Applied to the Design of Planar Microwave Circuits by Fused Deposition Modeling,” *Polym. 2020, Vol. 12, Page 1946*, vol. 12, no. 9, p. 1946, Aug. 2020, doi: 10.3390/POLYM12091946.

[101] D. Yadav, D. Chhabra, R. Kumar Garg, A. Ahlawat, and A. Phogat, “Optimization of FDM 3D printing process parameters for multi-material using artificial neural network,” *Mater. Today Proc.*, vol. 21, pp. 1583–1591, Jan. 2020, doi: 10.1016/J.MATPR.2019.11.225.

[102] J. Yin, C. Lu, J. Fu, Y. Huang, and Y. Zheng, “Interfacial bonding during multi-material fused deposition modeling (FDM) process due to inter-molecular diffusion,” *Mater. Des.*, vol. 150, pp. 104–112, Jul. 2018, doi: 10.1016/J.MATDES.2018.04.029.

[103] L. M. Clemon and T. I. Zohdi, “On the tolerable limits of granulated recycled material additives to maintain structural integrity,” *Constr. Build. Mater.*, vol. 167, pp. 846–852, 2018, doi: 10.1016/j.conbuildmat.2018.02.099.

[104] D. J. Byard, A. L. Woern, R. B. Oakley, M. J. Fiedler, S. L. Snabes, and J. M. Pearce, “Green fab lab applications of large-area waste polymer-based additive manufacturing,” *Addit. Manuf.*, vol. 27, pp. 515–525, May 2019, doi: 10.1016/J.ADDMA.2019.03.006.

[105] D. Rejeski, F. Zhao, and Y. Huang, “Research needs and recommendations on environmental implications of additive manufacturing,” *Addit. Manuf.*, vol. 19, pp. 21–28, Jan. 2018, doi: 10.1016/J.ADDMA.2017.10.019.

[106] K. Q. Nguyen, C. Mwiseneza, K. Mohamed, P. Cousin, M. Robert, and B. Benmokrane, “Long-term testing methods for HDPE pipe - advantages and disadvantages: A review,” *Eng. Fract. Mech.*, vol. 246, p. 107629, Apr. 2021, doi: 10.1016/J.ENGFRACMECH.2021.107629.

[107] R. Juan, C. Domínguez, N. Robledo, B. Paredes, and R. A. García-Muñoz, “Incorporation of recycled high-density polyethylene to polyethylene pipe grade resins to increase close-loop recycling and Underpin the circular economy,” *J. Clean. Prod.*, vol. 276, p. 124081, Dec. 2020, doi:

10.1016/J.JCLEPRO.2020.124081.

[108] S. Kumar and A. Czekanski, “Development of filaments using selective laser sintering waste powder,” *J. Clean. Prod.*, vol. 165, pp. 1188–1196, Nov. 2017, doi: 10.1016/j.jclepro.2017.07.202.

[109] P. Mägi, A. Krumme, and M. Pohlak, “Recycling of PA-12 in Additive Manufacturing and the Improvement of its Mechanical Properties,” in *Key Engineering Materials*, 2016, vol. 674, pp. 9–14, doi: 10.4028/www.scientific.net/KEM.674.9.

[110] V. Shanmugam *et al.*, “Polymer Recycling in Additive Manufacturing: an Opportunity for the Circular Economy,” *Mater. Circ. Econ. 2020 21*, vol. 2, no. 1, pp. 1–11, Nov. 2020, doi: 10.1007/S42824-020-00012-0.

[111] H. A. Colorado, E. I. G. Velásquez, and S. N. Monteiro, “Sustainability of additive manufacturing: the circular economy of materials and environmental perspectives,” *J. Mater. Res. Technol.*, vol. 9, no. 4, pp. 8221–8234, Jul. 2020, doi: 10.1016/J.JMRT.2020.04.062.

[112] N. Vidakis *et al.*, “Sustainable Additive Manufacturing: Mechanical Response of Polyamide 12 over Multiple Recycling Processes,” *Mater. 2021, Vol. 14, Page 466*, vol. 14, no. 2, p. 466, Jan. 2021, doi: 10.3390/MA14020466.

[113] N. Vidakis, M. Petousis, A. Maniadi, E. Koudoumas, A. Vairis, and J. Kechagias, “Sustainable Additive Manufacturing: Mechanical Response of Acrylonitrile-Butadiene-Styrene over Multiple Recycling Processes,” *Sustain. 2020, Vol. 12, Page 3568*, vol. 12, no. 9, p. 3568, Apr. 2020, doi: 10.3390/SU12093568.

[114] H. Kamioka, “Preferred reporting items for systematic review and meta-analysis protocols (prisma-p) 2015 statement,” *Japanese Pharmacol. Ther.*, vol. 47, no. 8, pp. 1177–1185, 2019.

[115] R. Alyousef, W. Ahmad, A. Ahmad, F. Aslam, P. Joyklad, and H. Alabduljabbar, “Potential use of recycled plastic and rubber aggregate in cementitious materials for sustainable construction: A review,” *J. Clean. Prod.*, vol. 329, p. 129736, Dec. 2021, doi: 10.1016/J.JCLEPRO.2021.129736.

[116] M. Wang, P. Liu, Z. Gu, H. Cheng, and X. Li, “A Scientometric Review of Resource Recycling Industry,” *Int. J. Environ. Res. Public Heal. 2019, Vol. 16, Page 4654*, vol. 16, no. 23, p. 4654, Nov. 2019, doi: 10.3390/IJERPH16234654.

[117] K. Chen, J. Wang, B. Yu, H. Wu, and J. Zhang, “Critical evaluation of construction and demolition waste and associated environmental impacts: A scientometric analysis,” *J. Clean. Prod.*, vol. 287, p. 125071, Mar. 2021, doi: 10.1016/J.JCLEPRO.2020.125071.

[118] D. He, K. Bristow, V. Filipović, J. Lv, and H. He, “Microplastics in Terrestrial Ecosystems: A Scientometric Analysis,” *Sustain. 2020, Vol. 12, Page 8739*, vol. 12, no. 20, p. 8739, Oct. 2020, doi: 10.3390/SU12208739.

[119] B. Zhang, W. Ahmad, A. Ahmad, F. Aslam, and P. Joyklad, “A scientometric

analysis approach to analyze the present research on recycled aggregate concrete," *J. Build. Eng.*, vol. 46, p. 103679, Apr. 2022, doi: 10.1016/J.JOBE.2021.103679.

[120] Y. Zhang, H. Liu, S. C. Kang, and M. Al-Hussein, "Virtual reality applications for the built environment: Research trends and opportunities," *Autom. Constr.*, vol. 118, no. June, p. 103311, 2020, doi: 10.1016/j.autcon.2020.103311.

[121] P. Martinez, M. Al-Hussein, and R. Ahmad, "A scientometric analysis and critical review of computer vision applications for construction," *Autom. Constr.*, vol. 107, no. May, 2019, doi: 10.1016/j.autcon.2019.102947.

[122] A. Andriamamonjy, D. Saelens, and R. Klein, "A combined scientometric and conventional literature review to grasp the entire BIM knowledge and its integration with energy simulation," *J. Build. Eng.*, vol. 22, pp. 513–527, Mar. 2019, doi: 10.1016/J.JOBE.2018.12.021.

[123] B. Zhong, H. Wu, H. Li, S. Sepasgozar, H. Luo, and L. He, "A scientometric analysis and critical review of construction related ontology research," *Autom. Constr.*, vol. 101, pp. 17–31, May 2019, doi: 10.1016/J.AUTCON.2018.12.013.

[124] N. Carl and M. A. Woodley of Menie, "A scientometric analysis of controversies in the field of intelligence research," *Intelligence*, vol. 77, p. 101397, Nov. 2019, doi: 10.1016/J.INTELL.2019.101397.

[125] D. Millenaar *et al.*, "Research in Atrial Fibrillation: A Scientometric Analysis Using the Novel Web Application SciPE," *Clin. Electrophysiol.*, vol. 6, no. 8, pp. 1008–1018, Aug. 2020, doi: 10.1016/J.JACEP.2020.05.010.

[126] Y. V. Granovsky, "Is it possible to measure science? V. V. Nalimov's research in scientometrics," *Scientometrics*, vol. 52, no. 2, pp. 127–150, 2001, doi: 10.1023/A:1017991017982.

[127] B. Sciences, "Mike, A., Harris, K., Roberts, B.W., Jackson, J.J., 2015. Conscientiousness. In: James D. Wright (editor-in-chief), International Encyclopedia of the Social & Behavioral Sciences, 2nd edition, Vol 4. Oxford: Elsevier. pp. 658–665.," vol. 4, pp. 658–665, 2015.

[128] S. Chavan, "Scientometric Analyses and Visualization of Scientific Outcome on Nipah Virus," doi: 10.18520/cs/v117/i10/1574-1584.

[129] M. Mustak, J. Salminen, L. Plé, and J. Wirtz, "Artificial intelligence in marketing: Topic modeling, scientometric analysis, and research agenda," *J. Bus. Res.*, vol. 124, pp. 389–404, Jan. 2021, doi: 10.1016/J.JBUSRES.2020.10.044.

[130] R. Iman, B. Reza, and A. Abdollah, "Scientometric Analysis of Scheduling in Renewable Energy: A Keyword and Citation Analysis," *J. Energy Power Technol. 2019, Vol. 1, Page 1*, vol. 1, no. 4, pp. 1–1, May 2019, doi: 10.21926/JEPT.1904004.

[131] S. K. Sood, N. Kumar, and M. Saini, "Scientometric analysis of literature on distributed vehicular networks : VOSViewer visualization techniques," *Artif.*

Intell. Rev., vol. 54, no. 8, pp. 6309–6341, Dec. 2021, doi: 10.1007/S10462-021-09980-4/TABLES/12.

[132] O. T. Oladinrin, M. Arif, M. Q. Rana, and L. Gyoh, "Interrelations between construction ethics and innovation: a bibliometric analysis using VOSviewer," *Constr. Innov.*, vol. ahead-of-print, no. ahead-of-print, Mar. 2022, doi: 10.1108/CI-07-2021-0130.

[133] D. Han and H. Lee, "Recent advances in multi-material additive manufacturing: methods and applications," *Curr. Opin. Chem. Eng.*, vol. 28, pp. 158–166, 2020, doi: 10.1016/j.coche.2020.03.004.

[134] N. J. van Eck and L. Waltman, "Software survey: VOSviewer, a computer program for bibliometric mapping," *Scientometrics*, vol. 84, no. 2, pp. 523–538, 2010, doi: 10.1007/s11192-009-0146-3.

[135] J. Pakkanen, D. Manfredi, P. Minetola and L. Iuliano, "About the Use of Recycled or Biodegradable Filaments for Sustainability of 3D Printing State of the Art and Research Opportunities," vol. 1, 2017, doi: 10.1007/978-3-319-57078-5.

[136] K. Ragaert *et al.*, "Design from recycling: A complex mixed plastic waste case study," *Resour. Conserv. Recycl.*, vol. 155, p. 104646, Apr. 2020, doi: 10.1016/J.RESCONREC.2019.104646.

[137] J. N. Hahladakis and E. Iacovidou, "An overview of the challenges and trade-offs in closing the loop of post-consumer plastic waste (PCPW): Focus on recycling," *J. Hazard. Mater.*, vol. 380, p. 120887, Dec. 2019, doi: 10.1016/J.JHAZMAT.2019.120887.

[138] F. Wagner, J. R. Peeters, J. De Keyzer, K. Janssens, J. R. Duflou, and W. Dewulf, "Towards a more circular economy for WEEE plastics – Part B: Assessment of the technical feasibility of recycling strategies," *Waste Manag.*, vol. 96, pp. 206–214, Aug. 2019, doi: 10.1016/J.WASMAN.2019.07.035.

[139] M. K. Eriksen, J. D. Christiansen, A. E. Daugaard, and T. F. Astrup, "Closing the loop for PET, PE and PP waste from households: Influence of material properties and product design for plastic recycling," *Waste Manag.*, vol. 96, pp. 75–85, Aug. 2019, doi: 10.1016/J.WASMAN.2019.07.005.

[140] A. W. Fatimatuzahraa, B. Farahaina, and W. A. Y. Yusoff, "The effect of employing different raster orientations on the mechanical properties and microstructure of Fused Deposition Modeling parts," *ISBEIA 2011 - 2011 IEEE Symp. Business, Eng. Ind. Appl.*, pp. 22–27, 2011, doi: 10.1109/ISBEIA.2011.6088811.

[141] C. Zhu *et al.*, "Realization of circular economy of 3D printed plastics: A review," *Polymers (Basel).*, vol. 13, no. 5, pp. 1–16, 2021, doi: 10.3390/polym13050744.

[142] K. S. Khoo, L. Y. Ho, H. R. Lim, H. Y. Leong, and K. W. Chew, "Plastic waste associated with the COVID-19 pandemic: Crisis or opportunity?," *J. Hazard. Mater.*, vol. 417, p. 126108, Sep. 2021, doi: 10.1016/J.JHAZMAT.2021.126108.

[143] M. W. Ryberg, M. Z. Hauschild, F. Wang, S. Averous-Monnery, and A. Laurent, "Global environmental losses of plastics across their value chains," *Resour. Conserv. Recycl.*, vol. 151, p. 104459, Dec. 2019, doi: 10.1016/J.RESCONREC.2019.104459.

[144] S. Nathaphan and W. Trutassanawin, "Effects of process parameters on compressive property of FDM with ABS," *Rapid Prototyp. J.*, vol. 27, no. 5, pp. 905–917, 2021, doi: 10.1108/RPJ-12-2019-0309.

[145] S. Chong, G. P. Mohammad, and K. Thomas, "Physical Characterization and Pre-assessment of Recycled High-Density Polyethylene as 3D Printing Material," pp. 136–145, 2017, doi: 10.1007/s10924-016-0793-4.

[146] P. Steinle, "Characterization of emissions from a desktop 3D printer and indoor air measurements in office settings," *J. Occup. Environ. Hyg.*, vol. 13, no. 2, pp. 121–132, Feb. 2016, doi: 10.1080/15459624.2015.1091957.

[147] "Choosing the right 3D printing materials for FDM - Opinion - Magigoo." https://magigoo.com/blog/choosing-the-right-3d-printing-materials-for-fdm-opinion/ (accessed Nov. 02, 2021).

[148] "Maximum Continuous Service Temperature - Plastic Properties." https://omnexus.specialchem.com/polymer-properties/properties/max-continuous-service-temperature (accessed Dec. 01, 2021).

[149] F. Awaja and D. Pavel, "Recycling of PET," *European Polymer Journal*, vol. 41, no. 7. pp. 1453–1477, Jul. 2005, doi: 10.1016/j.eurpolymj.2005.02.005.

[150] A. Majumdar, S. Shukla, A. A. Singh, and S. Arora, "Circular fashion: Properties of fabrics made from mechanically recycled poly-ethylene terephthalate (PET) bottles," *Resour. Conserv. Recycl.*, vol. 161, p. 104915, Oct. 2020, doi: 10.1016/J.RESCONREC.2020.104915.

[151] Krishanu Ghosal and Chinmaya Nayak, "Recent advances in chemical recycling of polyethylene terephthalate waste into value added products for sustainable coating solutions – hope vs . hype," *Mater. Adv.*, vol. 3, no. 4, pp. 1974–1992, Feb. 2022, doi: 10.1039/D1MA01112J.

[152] M. A. Kreiger, M. L. Mulder, A. G. Glover, and J. M. Pearce, "Life cycle analysis of distributed recycling of post-consumer high density polyethylene for 3-D printing filament," *J. Clean. Prod.*, vol. 70, pp. 90–96, May 2014, doi: 10.1016/j.jclepro.2014.02.009.

[153] J. Zhang, A. Panwar, D. Bello, J. A. Isaacs, T. Jozokos, and J. Mead, "The effects of recycling on the structure and properties of carbon nanotube-filled polycarbonate," *Polym. Eng. Sci.*, vol. 58, no. 8, pp. 1278–1284, Aug. 2018, doi: 10.1002/PEN.24692.

[154] T. S. Omonov, C. Harrats, G. Groeninckx, and P. Moldenaers, "Anisotropy and instability of the co-continuous phase morphology in uncompatibilized and reactively compatibilized polypropylene/polystyrene blends," *Polymer (Guildf).*, vol. 48, no. 18, pp. 5289–5302, Aug. 2007, doi: 10.1016/j.polymer.2007.06.043.

[155] N. E. Zander, M. Gillan, Z. Burckhard, and F. Gardea, "Recycled polypropylene blends as novel 3D printing materials," *Addit. Manuf.*, vol. 25, no. October 2018, pp. 122–130, 2019, doi: 10.1016/j.addma.2018.11.009.

[156] H. J. O'Connor and D. P. Dowling, "Evaluation of the influence of low pressure additive manufacturing processing conditions on printed polymer parts," *Addit. Manuf.*, vol. 21, no. May, pp. 404–412, 2018, doi: 10.1016/j.addma.2018.04.007.

[157] J. L. Walker and M. Santoro, "Processing and production of bioresorbable polymer scaffolds for tissue engineering," *Bioresorbable Polym. Biomed. Appl. From Fundam. to Transl. Med.*, pp. 181–203, 2017, doi: 10.1016/B978-0-08-100262-9.00009-4.

[158] "FFF vs FDM: Is there any difference? - Maker Industry." https://makerindustry.com/fff-vs-fdm/ (accessed Apr. 07, 2022).

[159] M. Pollak, M. Kocisko, A. Basistova, and S. Hlavata, "Production of fiber as an input material for the 3d printing process," *MM Sci. J.*, vol. 2021, no. June, pp. 4414–4419, 2021, doi: 10.17973/MMSJ.2021_6_2021031.

[160] L. Bergonzi and M. Vettori, "Mechanical properties comparison between new and recycled polyethylene terephthalate glycol obtained from fused deposition modelling waste," *Mater. Des. Process. Commun.*, vol. 3, no. 4, p. e250, Aug. 2021, doi: 10.1002/MDP2.250.

[161] C. Pascual-González *et al.*, "Processing and properties of PLA/Mg filaments for 3D printing of scaffolds for biomedical applications," *Rapid Prototyp. J.*, 2021, doi: 10.1108/RPJ-06-2021-0152/FULL/XML.

[162] M. Acevedo, L. Royano, A. I. Parralejo, J. Cabanillas, J. F. González, and J. González, "3D Printing Filaments from Kenaf, Poplar and Agricultural Residues," *Proc. 1st Int. Conf. Water Energy Food Sustain. (ICoWEFS 2021)*, pp. 489–494, 2021, doi: 10.1007/978-3-030-75315-3_53.

[163] H. Matsui *et al.*, "Poly(Lactic) Acid Reinforced with Alkaline Lignin Biocomposites Prepared by Thermal Extrusion for Sustainable 3D Printing Process," *J. Phys. Conf. Ser.*, vol. 2129, no. 1, p. 012003, Dec. 2021, doi: 10.1088/1742-6596/2129/1/012003.

[164] C. Baechler, M. Devuono, and J. M. Pearce, "Distributed recycling of waste polymer into RepRap feedstock," *Rapid Prototyp. J.*, vol. 19, no. 2, pp. 118–125, 2013, doi: 10.1108/13552541311302978.

[165] N. E. Zander, M. Gillan, and R. H. Lambeth, "Recycled polyethylene terephthalate as a new FFF feedstock material," *Addit. Manuf.*, vol. 21, no. March, pp. 174–182, 2018, doi: 10.1016/j.addma.2018.03.007.

[166] M. Hietala and K. Oksman, "Pelletized cellulose fibres used in twin-screw extrusion for biocomposite manufacturing: Fibre breakage and dispersion," *Compos. Part A Appl. Sci. Manuf.*, vol. 109, pp. 538–545, Jun. 2018, doi: 10.1016/J.COMPOSITESA.2018.04.006.

[167] T. L. Welker *et al.*, "Effects of feed processing method (extrusion and

expansion-compression pelleting) on water quality and growth of rainbow trout in a commercial setting," *https://doi.org/10.1080/10454438.2018.1433095*, vol. 30, no. 2, pp. 97–124, Apr. 2018, doi: 10.1080/10454438.2018.1433095.

[168] D. Deb and J. M. Jafferson, "Natural fibers reinforced FDM 3D printing filaments," *Mater. Today Proc.*, vol. 46, pp. 1308–1318, Jan. 2021, doi: 10.1016/J.MATPR.2021.02.397.

[169] S. Dinesh Kumar, K. Venkadeshwaran, and M. K. Aravindan, "Fused deposition modelling of PLA reinforced with cellulose nano-crystals," *Mater. Today Proc.*, vol. 33, pp. 868–875, Jan. 2020, doi: 10.1016/J.MATPR.2020.06.404.

[170] Y. Hong, M. Mrinal, H. S. Phan, V. D. Tran, X. Liu, and C. Luo, "In-situ observation of the extrusion processes of Acrylonitrile Butadiene Styrene and Polylactic Acid for material extrusion additive manufacturing," *Addit. Manuf.*, vol. 49, p. 102507, Jan. 2022, doi: 10.1016/J.ADDMA.2021.102507.

[171] C. A. Comelli, R. Davies, H. J. van der Pol, and O. Ghita, "PEEK filament characteristics before and after extrusion within fused filament fabrication process," *J. Mater. Sci.*, vol. 57, no. 1, pp. 766–788, Jan. 2022, doi: 10.1007/S10853-021-06652-0/FIGURES/19.

[172] A. J. Qureshi, S. Mahmood, W. L. E. Wong, and D. Talamona, "Design for scalability and strength optimisation for components created through fdm process," *Proc. Int. Conf. Eng. Des. ICED*, vol. 6, no. DS 80-06, 2015.

[173] R. B. Kristiawan, F. Imaduddin, D. Ariawan, Ubaidillah, and Z. Arifin, "A review on the fused deposition modeling (FDM) 3D printing: Filament processing, materials, and printing parameters," *Open Eng.*, vol. 11, no. 1, pp. 639–649, Jan. 2021, doi: 10.1515/ENG-2021-0063/MACHINEREADABLECITATION/RIS.

[174] M. Samykano, "Mechanical Property and Prediction Model for FDM-3D Printed Polylactic Acid (PLA)," *Arab. J. Sci. Eng.*, vol. 46, no. 8, pp. 7875–7892, Aug. 2021, doi: 10.1007/S13369-021-05617-4/TABLES/9.

[175] D. Syrlybayev, B. Zharylkassyn, A. Seisekulova, M. Akhmetov, A. Perveen, and D. Talamona, "Optimisation of strength properties of FDM printed parts—A critical review," *Polymers (Basel).*, vol. 13, no. 10, 2021, doi: 10.3390/polym13101587.

[176] L. Feng, Y. Wang, and Q. Wei, "PA12 Powder Recycled from SLS for FDM," *Polym. 2019, Vol. 11, Page 727*, vol. 11, no. 4, p. 727, Apr. 2019, doi: 10.3390/POLYM11040727.

[177] Y. Yang *et al.*, "3D-printed polycaprolactone-chitosan based drug delivery implants for personalized administration," *Mater. Des.*, vol. 214, p. 110394, Feb. 2022, doi: 10.1016/J.MATDES.2022.110394.

[178] G. S. Sivagnanamani, P. Ramesh, M. H. Kumar, and V. Arul Mozhi Selvan, "Fracture Analysis of Fused Deposition Modelling of Bio-composite Filaments," pp. 71–84, 2021, doi: 10.1007/978-981-16-0642-7_4/FIGURES/5.

[179] S. Xiaoyong, C. Liangcheng, M. Honglin, G. Peng, B. Zhanwei, and L. Cheng, "Experimental analysis of high temperature PEEK materials on 3D printing test," *Proc. - 9th Int. Conf. Meas. Technol. Mechatronics Autom. ICMTMA 2017*, pp. 13–16, 2017, doi: 10.1109/ICMTMA.2017.0012.

[180] M. Calì, G. Pascoletti, M. Gaeta, G. Milazzo, and R. Ambu, "A New Generation of Bio-Composite Thermoplastic Filaments for a More Sustainable Design of Parts Manufactured by FDM," *Appl. Sci. 2020, Vol. 10, Page 5852*, vol. 10, no. 17, p. 5852, Aug. 2020, doi: 10.3390/APP10175852.

[181] X. Deng, Z. Zeng, B. Peng, S. Yan, and W. Ke, "Mechanical properties optimization of poly-ether-ether-ketone via fused deposition modeling," *Materials (Basel).*, vol. 11, no. 2, 2018, doi: 10.3390/ma11020216.

[182] M. Spoerk, F. Arbeiter, I. Raguž, C. Holzer, and J. Gonzalez-Gutierrez, "Mechanical Recyclability of Polypropylene Composites Produced by Material Extrusion-Based Additive Manufacturing," *Polym. 2019, Vol. 11, Page 1318*, vol. 11, no. 8, p. 1318, Aug. 2019, doi: 10.3390/POLYM11081318.

[183] C. Parulski, O. Jennotte, A. Lechanteur, and B. Evrard, "Challenges of fused deposition modeling 3D printing in pharmaceutical applications: Where are we now?," *Adv. Drug Deliv. Rev.*, vol. 175, p. 113810, Aug. 2021, doi: 10.1016/J.ADDR.2021.05.020.

[184] J. Butt, R. Bhaskar, and V. Mohaghegh, "Investigating the effects of extrusion temperatures and material extrusion rates on FFF-printed thermoplastics," *Int. J. Adv. Manuf. Technol.*, vol. 117, no. 9–10, pp. 2679–2699, Dec. 2021, doi: 10.1007/S00170-021-07850-5/FIGURES/20.

[185] H. Attar, S. Ehtemam-Haghighi, N. Soro, D. Kent, and M. S. Dargusch, "Additive manufacturing of low-cost porous titanium-based composites for biomedical applications: Advantages, challenges and opinion for future development," *J. Alloys Compd.*, vol. 827, p. 154263, Jun. 2020, doi: 10.1016/J.JALLCOM.2020.154263.

[186] A. K. Sood, R. K. Ohdar, and S. S. Mahapatra, "Parametric appraisal of mechanical property of fused deposition modelling processed parts," *Mater. Des.*, vol. 31, no. 1, pp. 287–295, 2010, doi: 10.1016/j.matdes.2009.06.016.

[187] S. Guessasma, S. Belhabib, and H. Nouri, "Thermal cycling, microstructure and tensile performance of PLA-PHA polymer printed using fused deposition modelling technique," *Rapid Prototyp. J.*, vol. 26, no. 1, pp. 122–133, 2020, doi: 10.1108/RPJ-06-2019-0151.

[188] R. Anitha, S. Arunachalam, and P. Radhakrishnan, "Critical parameters influencing the quality of prototypes in fused deposition modelling," *J. Mater. Process. Technol.*, vol. 118, no. 1–3, pp. 385–388, 2001, doi: 10.1016/S0924-0136(01)00980-3.

[189] C. Benwood, A. Anstey, J. Andrzejewski, M. Misra, and A. K. Mohanty, "Improving the Impact Strength and Heat Resistance of 3D Printed Models: Structure, Property, and Processing Correlationships during Fused Deposition Modeling (FDM) of Poly(Lactic Acid)," *ACS Omega*, vol. 3, no. 4, pp. 4400–

4411, 2018, doi: 10.1021/acsomega.8b00129.

[190] S. Qi, X. Gao, Y. Su, X. Dong, D. Cavallo, and D. Wang, “Correlation between welding behavior and mechanical anisotropy of long chain polyamide 12 manufactured with fused filament fabrication,” *Polymer (Guildf).*, vol. 213, p. 123318, Jan. 2021, doi: 10.1016/J.POLYMER.2020.123318.

[191] N. Zohdi, R. (Chunhui,) Yang, S. Torres-Giner, and M. Vargas, “Material Anisotropy in Additively Manufactured Polymers and Polymer Composites: A Review,” *Polym. 2021, Vol. 13, Page 3368*, vol. 13, no. 19, p. 3368, Sep. 2021, doi: 10.3390/POLYM13193368.

[192] R. Srinivasan, W. Ruban, A. Deepanraj, R. Bhuvanesh, and T. Bhuvanesh, “Effect on infill density on mechanical properties of PETG part fabricated by fused deposition modelling,” *Mater. Today Proc.*, vol. 27, pp. 1838–1842, Jan. 2020, doi: 10.1016/J.MATPR.2020.03.797.

[193] S. Terekhina, I. Skornyakov, T. Tarasova, and S. Egorov, “Effects of the Infill Density on the Mechanical Properties of Nylon Specimens Made by Filament Fused Fabrication,” *Technol. 2019, Vol. 7, Page 57*, vol. 7, no. 3, p. 57, Aug. 2019, doi: 10.3390/TECHNOLOGIES7030057.

[194] T. J. Suteja and A. Soesanti, “Mechanical Properties of 3D Printed Polylactic Acid Product for Various Infill Design Parameters: A Review,” *J. Phys. Conf. Ser.*, vol. 1569, no. 4, 2020, doi: 10.1088/1742-6596/1569/4/042010.

[195] B. Akhoundi and A. H. Behravesh, “Effect of Filling Pattern on the Tensile and Flexural Mechanical Properties of FDM 3D Printed Products,” *Exp. Mech.*, vol. 59, no. 6, pp. 883–897, 2019, doi: 10.1007/s11340-018-00467-y.

[196] H. K. Dave, N. H. Patadiya, A. R. Prajapati, and S. R. Rajpurohit, “Effect of infill pattern and infill density at varying part orientation on tensile properties of fused deposition modeling-printed poly-lactic acid part,” *Proc. Inst. Mech. Eng. Part C J. Mech. Eng. Sci.*, vol. 235, no. 10, pp. 1811–1827, 2021, doi: 10.1177/0954406219856383.

[197] H. Li, T. Wang, and Z. Yu, “The Quantitative Research of Interaction between Key Parameters and the Effects on Mechanical Property in FDM,” *Adv. Mater. Sci. Eng.*, vol. 2017, 2017, doi: 10.1155/2017/9152954.

[198] P. K. Mishra, P. Senthil, S. Adarsh, and M. S. Anoop, “An investigation to study the combined effect of different infill pattern and infill density on the impact strength of 3D printed polylactic acid parts,” *Compos. Commun.*, vol. 24, p. 100605, Apr. 2021, doi: 10.1016/J.COCO.2020.100605.

[199] C. Lubombo and M. A. Huneault, “Effect of infill patterns on the mechanical performance of lightweight 3D-printed cellular PLA parts,” *Mater. Today Commun.*, vol. 17, pp. 214–228, Dec. 2018, doi: 10.1016/J.MTCOMM.2018.09.017.

[200] M. L. Dezaki and M. K. A. Mohd Ariffin, “The effects of combined infill patterns on mechanical properties in fdm process,” *Polymers (Basel).*, vol. 12, no. 12, pp. 1–20, 2020, doi: 10.3390/polym12122792.

[201] B. Aloyaydi, S. Sivasankaran, and A. Mustafa, "Investigation of infill-patterns on mechanical response of 3D printed poly-lactic-acid," *Polym. Test.*, vol. 87, no. March, p. 106557, 2020, doi: 10.1016/j.polymertesting.2020.106557.

[202] A. Chadha, M. I. Ul Haq, A. Raina, R. R. Singh, N. B. Penumarti, and M. S. Bishnoi, "Effect of fused deposition modelling process parameters on mechanical properties of 3D printed parts," *World J. Eng.*, vol. 16, no. 4, pp. 550–559, 2019, doi: 10.1108/WJE-09-2018-0329.

[203] F. Liang, Y. Shi, Y. Yu, G. Liu, and D. Wang, "Theoretical analysis of FDM printing technology and experimental analysis based on low melting point soft materials," *IOP Conf. Ser. Mater. Sci. Eng.*, vol. 452, no. 2, p. 022111, Dec. 2018, doi: 10.1088/1757-899X/452/2/022111.

[204] J. Xu, K. Liu, Z. Liu, F. Zhang, S. Zhang, and J. Tan, "Electrothermal response optimization of nozzle structure for multi-material rapid prototyping based on fuzzy adaptive control," doi: 10.1108/RPJ-12-2020-0313.

[205] J. Triyono, H. Sukanto, R. M. Saputra, and D. F. Smaradhana, "The effect of nozzle hole diameter of 3D printing on porosity and tensile strength parts using polylactic acid material," *Open Eng.*, vol. 10, no. 1, pp. 762–768, 2020, doi: 10.1515/eng-2020-0083.

[206] V. S. Jatti, S. V. Jatti, A. P. Patel, and V. S. Jatti, "A study on effect of fused deposition modeling process parameters on mechanical properties," *Int. J. Sci. Technol. Res.*, vol. 8, no. 11, pp. 689–693, 2019.

[207] N. Vidakis, M. Petousis, and J. D. Kechagias, "Parameter effects and process modelling of Polyamide 12 3D-printed parts strength and toughness," *Mater. Manuf. Process.*, 2022, doi: 10.1080/10426914.2022.2030871/FORMAT/EPUB.

[208] J. C. Najmon, S. Raeisi, and A. Tovar, *Review of additive manufacturing technologies and applications in the aerospace industry*. Elsevier Inc., 2019.

[209] G. Ćwikła, C. Grabowik, K. Kalinowski, I. Paprocka, and P. Ociepka, "The influence of printing parameters on selected mechanical properties of FDM/FFF 3D-printed parts," *IOP Conf. Ser. Mater. Sci. Eng.*, vol. 227, no. 1, pp. 0–10, 2017, doi: 10.1088/1757-899X/227/1/012033.

[210] J. Nomani, D. Wilson, M. Paulino, and M. I. Mohammed, "Effect of layer thickness and cross-section geometry on the tensile and compression properties of 3D printed ABS," *Mater. Today Commun.*, vol. 22, Mar. 2020, doi: 10.1016/J.MTCOMM.2019.100626.

[211] P. Shubham, A. Sikidar, and T. Chand, "The influence of layer thickness on mechanical properties of the 3D printed ABS polymer by fused deposition modeling," *Key Eng. Mater.*, vol. 706, pp. 63–67, 2016, doi: 10.4028/WWW.SCIENTIFIC.NET/KEM.706.63.

[212] L. M. Galantucci, F. Lavecchia, and G. Percoco, "Quantitative analysis of a chemical treatment to reduce roughness of parts fabricated using fused deposition modeling," *CIRP Ann. - Manuf. Technol.*, vol. 59, no. 1, pp. 247–250, 2010, doi: 10.1016/j.cirp.2010.03.074.

[213] L. Villalpando and J. Urbanic, “Parametric Internal Matrix Structures for Components Built by Fused Deposition Modelling,” *Enabling Manuf. Compet. Econ. Sustain.*, pp. 287–292, 2012, doi: 10.1007/978-3-642-23860-4_47.

[214] I. Durgun and R. Ertan, “Experimental investigation of FDM process for improvement of mechanical properties and production cost,” *Rapid Prototyp. J.*, vol. 20, no. 3, pp. 228–235, 2014, doi: 10.1108/RPJ-10-2012-0091.

[215] J. M. Chacón, M. A. Caminero, E. García-Plaza, and P. J. Núñez, “Additive manufacturing of PLA structures using fused deposition modelling: Effect of process parameters on mechanical properties and their optimal selection,” *Mater. Des.*, vol. 124, pp. 143–157, 2017, doi: 10.1016/j.matdes.2017.03.065.

[216] J. D. Kechagias, S. P. Zaoutsos, D. Chaidas, and N. Vidakis, “Multi-parameter optimization of PLA/Coconut wood compound for Fused Filament Fabrication using Robust Design,” *Int. J. Adv. Manuf. Technol.*, vol. 119, no. 7–8, pp. 4317–4328, 2022, doi: 10.1007/s00170-022-08679-2.

[217] M. Montero, S. Roundy, and D. Odell, “Material characterization of fused deposition modeling (FDM) ABS by designed experiments,” *Proc. Rapid Prototyp. Manuf. Conf.*, pp. 1–21, 2001, [Online]. Available: http://ode11.com/publications/sme_rp_2001.pdf.

[218] M. S. Hossain, J. Ramos, D. Espalin, M. A. Perez, and R. Wicker, “Improving tensile mechanical properties of FDM-manufactured specimens via modifying build parameters,” *undefined*, 2013.

[219] A. Bagsik and V. Schöppner, “Mechanical properties of fused deposition modeling parts manufactured with Ultem*9085,” *Annu. Tech. Conf. - ANTEC, Conf. Proc.*, vol. 2, no. January 2011, pp. 1294–1298, 2011.

[220] D. Popescu, A. Zapciu, C. Amza, F. Baciu, and R. Marinescu, “FDM process parameters influence over the mechanical properties of polymer specimens: A review,” *Polym. Test.*, vol. 69, no. April, pp. 157–166, 2018, doi: 10.1016/j.polymertesting.2018.05.020.

[221] C. Dudescu and L. Racz, “Effects of Raster Orientation, Infill Rate and Infill Pattern on the Mechanical Properties of 3D Printed Materials,” *ACTA Univ. Cibiniensis*, vol. 69, no. 1, pp. 23–30, 2017, doi: 10.1515/aucts-2017-0004.

[222] D. Chaidas and J. D. Kechagias, “An investigation of PLA/W parts quality fabricated by FFF,” *Mater. Manuf. Process.*, vol. 37, no. 5, pp. 582–590, 2021, doi: 10.1080/10426914.2021.1944193.

[223] N. A. Fountas, I. Papantoniou, J. D. Kechagias, D. E. Manolakos, and N. M. Vaxevanidis, “Experimental investigation on flexural properties of FDM-processed PET-G specimen using response surface methodology,” *MATEC Web Conf.*, vol. 349, p. 01008, 2021, doi: 10.1051/matecconf/202134901008.

[224] J. B. Soares, J. Finamor, F. P. Silva, L. Roldo, and L. H. Cândido, “Analysis of the influence of polylactic acid (PLA) colour on FDM 3D printing temperature and part finishing,” *Rapid Prototyp. J.*, vol. 24, no. 8, pp. 1305–1316, Nov. 2018, doi: 10.1108/RPJ-09-2017-0177/FULL/PDF.

[225] P. Vosynek, T. Navrat, A. Krejbychova, and D. Palousek, “Influence of Process Parameters of Printing on Mechanical Properties of Plastic Parts Produced by FDM 3D Printing Technology,” *MATEC Web Conf.*, vol. 237, p. 02014, Nov. 2018, doi: 10.1051/MATECCONF/201823702014.

[226] B. Wittbrodt and J. M. Pearce, “The effects of PLA color on material properties of 3-D printed components,” *Addit. Manuf.*, vol. 8, pp. 110–116, 2015, doi: 10.1016/j.addma.2015.09.006.

[227] A. R. Torrado and D. A. Roberson, “Failure Analysis and Anisotropy Evaluation of 3D-Printed Tensile Test Specimens of Different Geometries and Print Raster Patterns,” *J. Fail. Anal. Prev.*, vol. 16, no. 1, pp. 154–164, 2016, doi: 10.1007/s11668-016-0067-4.

[228] A. Abilgaziyev, T. Kulzhan, N. Raissov, M. H. Ali, W. L. K. O. Match, and N. Mir-Nasiri, “Design and development of multi-nozzle extrusion system for 3D printer,” Nov. 2015, doi: 10.1109/ICIEV.2015.7333982.

[229] P. Kumar Mishra and S. P, “Prediction of in-plane stiffness of multi-material 3D printed laminate parts fabricated by FDM process using CLT and its mechanical behaviour under tensile load,” *Mater. Today Commun.*, vol. 23, p. 100955, Jun. 2020, doi: 10.1016/J.MTCOMM.2020.100955.

[230] H. Song, J. Martinez, P. Bedell, N. Vennin, and S. Lefebvre, “Colored fused filament fabrication,” *ACM Trans. Graph.*, vol. 38, no. 5, Sep. 2017, Accessed: Oct. 15, 2021. [Online]. Available: https://arxiv.org/abs/1709.09689v2.

[231] M. A. H. Khondoker, A. Asad, and D. Sameoto, “Printing with mechanically interlocked extrudates using a custom bi-extruder for fused deposition modelling,” *Rapid Prototyp. J.*, vol. 24, no. 6, pp. 921–934, 2018, doi: 10.1108/RPJ-03-2017-0046.

[232] M. A. H. Khondoker, N. Baheri, and D. Sameoto, “Tendon-Driven Functionally Gradient Soft Robotic Gripper 3D Printed with Intermixed Extrudate of Hard and Soft Thermoplastics,” *3D Print. Addit. Manuf.*, vol. 6, no. 4, pp. 191–203, 2019, doi: 10.1089/3dp.2018.0102.

[233] D. Baca and R. Ahmad, “The impact on the mechanical properties of multi-material polymers fabricated with a single mixing nozzle and multi-nozzle systems via fused deposition modeling,” *Int. J. Adv. Manuf. Technol.*, vol. 106, no. 9–10, pp. 4509–4520, 2020, doi: 10.1007/s00170-020-04937-3.

[234] “Multi Material Upgrade 2.0 is here! - Prusa Printers.” https://blog.prusaprinters.org/multi-material-upgrade-2-0-is-here_8700/ (accessed Oct. 15, 2021).

[235] J. Hergel and S. Lefebvre, “Clean color: Improving multi-filament 3D prints,” *Comput. Graph. Forum*, vol. 33, no. 2, pp. 469–478, 2014, doi: 10.1111/cgf.12318.

[236] Y. Zheng, W. Zhang, D. M. B. Lopez, and R. Ahmad, “Scientometric analysis and systematic review of multi-material additive manufacturing of polymers,” *Polymers (Basel).*, vol. 13, no. 12, 2021, doi: 10.3390/polym13121957.

[237] M. E. Spreeman, H. A. Stretz, and M. D. Dadmun, “Role of compatibilizer in 3D printing of polymer blends,” *Addit. Manuf.*, vol. 27, no. March, pp. 267–277, 2019, doi: 10.1016/j.addma.2019.03.009.

[238] H. Long *et al.*, “Mechanical and thermal properties of bamboo fiber reinforced polypropylene/polylactic acid composites for 3D printing,” *Polym. Eng. Sci.*, vol. 59, no. s2, pp. E247–E260, 2019, doi: 10.1002/pen.25043.

[239] D. Rasselet, A. S. Caro-Bretelle, A. Taguet, and J. M. Lopez-Cuesta, “Reactive compatibilization of PLA/PA11 blends and their application in additive manufacturing,” *Materials (Basel).*, vol. 12, no. 3, 2019, doi: 10.3390/ma12030485.

[240] S. S. Alghamdi, S. John, N. R. Choudhury, and N. K. Dutta, “Additive Manufacturing of Polymer Materials: Progress, Promise and Challenges,” *Polym. 2021, Vol. 13, Page 753*, vol. 13, no. 5, p. 753, Feb. 2021, doi: 10.3390/POLYM13050753.

[241] L. Taito-Matamua, S. Fraser, and J. Ok, “Renewing materials: Implementing 3D printing and distributed recycling in Samoa,” *Unmaking Waste Prod. Consum. Towar. Circ. Econ.*, pp. 191–212, Sep. 2018, doi: 10.1108/978-1-78714-619-820181016/FULL/XML.

[242] B. Wei *et al.*, “Reactive splicing compatibilization of immiscible polymer blends: Compatibilizer synthesis in the melt state and compatibilizer architecture effects,” *Polymer (Guildf).*, vol. 185, p. 121952, Dec. 2019, doi: 10.1016/J.POLYMER.2019.121952.

[243] Z. Y. Tan *et al.*, “Influence of rubber content in ABS in wide range on the mechanical properties and morphology of PC/ABS blends with different composition,” *Polym. Eng. Sci.*, vol. 46, no. 10, pp. 1476–1484, Oct. 2006, doi: 10.1002/pen.20584.

[244] C. Y. Lee, W. T. Wang, C. C. Liu, and L. M. Fu, “Passive mixers in microfluidic systems: A review,” *Chemical Engineering Journal*, vol. 288. Elsevier, pp. 146–160, Mar. 15, 2016, doi: 10.1016/j.cej.2015.10.122.

[245] T. D. Ngo, A. Kashani, G. Imbalzano, K. T. Q. Nguyen, and D. Hui, “Additive manufacturing (3D printing): A review of materials, methods, applications and challenges,” *Composites Part B: Engineering*, vol. 143. Elsevier Ltd, pp. 172–196, Jun. 15, 2018, doi: 10.1016/j.compositesb.2018.02.012.

[246] S. W. Ahmed *et al.*, “On the effects of process parameters and optimization of interlaminate bond strength in 3D printed ABS/CF-PLA composite,” *Polymers (Basel).*, vol. 12, no. 9, Sep. 2020, doi: 10.3390/POLYM12092155.

[247] Y. Fu, A. Downey, L. Yuan, A. Pratt, and Y. Balogun, “In situ monitoring for fused filament fabrication process: A review,” *Additive Manufacturing*, vol. 38. Elsevier B.V., Feb. 01, 2021, doi: 10.1016/j.addma.2020.101749.

[248] H. Valkenaers, F. Vogeler, E. Ferraris, A. Voet, and J.-P. Kruth, “A Novel Approach to Additive Manufacturing: Screw Extrusion 3D-Printing,” no. c, pp. 235–238, 2013, doi: 10.3850/978-981-07-7247-5-359.

[249] A. Bellini and M. Bertoldi, "Liquefier Dynamics in Fused," vol. 126, no. May, 2004, doi: 10.1115/1.1688377.

[250] J. M. J. Netto and Z. D. C. Silveira, "Design of an innovative three-dimensional print head based on twin-screw extrusion," *J. Mech. Des. Trans. ASME*, vol. 140, no. 12, 2018, doi: 10.1115/1.4041175.

[251] S. Whyman, K. M. Arif, and J. Potgieter, "Design and development of an extrusion system for 3D printing biopolymer pellets," *Int. J. Adv. Manuf. Technol. 2018 969*, vol. 96, no. 9, pp. 3417–3428, Mar. 2018, doi: 10.1007/S00170-018-1843-Y.

[252] J. M. Justino Netto, H. T. Idogava, L. E. Frezzatto Santos, Z. de C. Silveira, P. Romio, and J. L. Alves, "Screw-assisted 3D printing with granulated materials: a systematic review," *Int. J. Adv. Manuf. Technol.*, vol. 115, no. 9–10, pp. 2711–2727, 2021, doi: 10.1007/s00170-021-07365-z.

[253] S. M. Alshahrani, J. T. Morott, A. S. Alshetaili, and R. V Tiwari, "Influence of Degassing on Hot-Melt Extrusion Process European Journal of Pharmaceutical Sciences In fl uence of degassing on hot-melt extrusion process," *PHASCI*, vol. 80, no. August, pp. 43–52, 2015, doi: 10.1016/j.ejps.2015.08.008.

[254] J.-F. Agassant, P. Avenas, P. J. Carreau, B. Vergnes, and M. Vincent, "Single-Screw Extrusion and Die Flows," *Polym. Process.*, pp. 301–432, 2017, doi: 10.3139/9781569906064.005.

[255] L. Pan, M. Y. Jia, P. Xue, K. J. Wang, and Z. M. Jin, "Studies on positive conveying in helically channeled single screw extruders," *Express Polym. Lett.*, vol. 6, no. 7, pp. 543–560, 2012, doi: 10.3144/expresspolymlett.2012.58.

[256] M. M. Crowley *et al.*, "Pharmaceutical Applications of Hot-Melt Extrusion : Part I Pharmaceutical Applications of Hot-Melt Extrusion : Part I," vol. 9045, 2008, doi: 10.1080/03639040701498759.

[257] K. Chen, X. Lin, P. Xue, M. Jia, and C. Li, "Experimental Investigation of the Single Screw Extruder With Grooved Melting Zone," *Polym. Eng. Sci.*, vol. 58, no. 9, pp. 1555–1564, Sep. 2018, Accessed: Oct. 24, 2021. [Online]. Available: https://go.gale.com/ps/i.do?p=AONE&sw=w&issn=00323888&v=2.1&it=r&id=GALE%7CA562004646&sid=googleScholar&linkaccess=fulltext.

[258] B. A. Davis, P. J. Gramann, M. Del P. Noriega E., and T. A. Osswald, "Grooved feed single screw extruders - Improving productivity and reducing viscous heating effects," *Polym. Eng. Sci.*, vol. 38, no. 7, pp. 1199–1204, 1998, doi: 10.1002/PEN.10288.

[259] L. P. Tan, A. Lotfi, E. Lai, and J. B. Hull, "Soft computing applications in dynamic model identification of polymer extrusion process," *Appl. Soft Comput. J.*, vol. 4, no. 4, pp. 345–355, 2004, doi: 10.1016/j.asoc.2003.10.004.

[260] H. Patil, R. V Tiwari, and M. A. Repka, "Hot-Melt Extrusion : from Theory to Application in Pharmaceutical Formulation," vol. 17, no. 1, pp. 20–42, 2016, doi: 10.1208/s12249-015-0360-7.

[261] T. Feuerbach and M. Thommes, "Design and characterization of a screw

extrusion hot-end for fused deposition modeling," *Molecules*, vol. 26, no. 3, 2021, doi: 10.3390/molecules26030590.

[262] J. Leng, J. Wu, N. Chen, X. Xu, and J. Zhang, "The development of a conical screw-based extrusion deposition system and its application in fused deposition modeling with thermoplastic polyurethane," *Rapid Prototyp. J.*, vol. 26, no. 2, pp. 409–417, 2020, doi: 10.1108/RPJ-05-2019-0139.

[263] J. W. Tseng *et al.*, "Screw extrusion-based additive manufacturing of PEEK," *Mater. Des.*, vol. 140, pp. 209–221, 2018, doi: 10.1016/j.matdes.2017.11.032.

[264] X. Liu, B. Chi, Z. Jiao, J. Tan, F. Liu, and W. Yang, "A large-scale double-stage-screw 3D printer for fused deposition of plastic pellets," *J. Appl. Polym. Sci.*, vol. 134, no. 31, pp. 1–9, 2017, doi: 10.1002/app.45147.

[265] A. L. Woern, D. J. Byard, R. B. Oakley, M. J. Fiedler, S. L. Snabes, and J. M. Pearce, "Fused particle fabrication 3-D printing: Recycled materials' optimization and mechanical properties," *Materials (Basel).*, vol. 11, no. 8, 2018, doi: 10.3390/ma11081413.

[266] A. Alexandre, F. A. Cruz Sanchez, H. Boudaoud, M. Camargo, and J. M. Pearce, "Mechanical Properties of Direct Waste Printing of Polylactic Acid with Universal Pellets Extruder: Comparison to Fused Filament Fabrication on Open-Source Desktop Three-Dimensional Printers," *3D Print. Addit. Manuf.*, vol. 7, no. 5, pp. 237–247, 2020, doi: 10.1089/3dp.2019.0195.

[267] C. Wong, "A Study of Plastic Recycling Supply Chain 2010 A Study of Plastic Recycling Supply Chain."

[268] H. Shent, R. J. Pugh, and E. Forssberg, "A review of plastics waste recycling and the flotation of plastics," *Resour. Conserv. Recycl.*, vol. 25, no. 2, pp. 85–109, Feb. 1999, doi: 10.1016/S0921-3449(98)00017-2.

[269] M. P. Akash and A. Vasudevan, "Experimental analysis of recycled thermoplastic material," *Mater. Today Proc.*, vol. 45, pp. 6198–6203, 2020, doi: 10.1016/j.matpr.2020.10.516.

[270] J. Hopewell, R. Dvorak, and E. Kosior, "Plastics recycling: challenges and opportunities," *Philos. Trans. R. Soc. B Biol. Sci.*, vol. 364, no. 1526, pp. 2115–2126, Jul. 2009, doi: 10.1098/RSTB.2008.0311.

[271] R. Vasudevan, A. Ramalinga Chandra Sekar, B. Sundarakannan, and R. Velkennedy, "A technique to dispose waste plastics in an ecofriendly way – Application in construction of flexible pavements," *Constr. Build. Mater.*, vol. 28, no. 1, pp. 311–320, Mar. 2012, doi: 10.1016/J.CONBUILDMAT.2011.08.031.

[272] N. Carducci, A. Hoglund, M. Lube, and D. Murdock, "MIXED PLASTIC RECYCLING PLANT Reck 'em Recyclers," 2020.

[273] R. De Angelis, M. Howard, and J. Miemczyk, "Production Planning & Control The Management of Operations Supply chain management and the circular economy: towards the circular supply chain Supply chain management and the circular economy: towards the circular supply chain," *Prod. Plan. Control*, vol.

29, no. 6, pp. 425–437, 2018, doi: 10.1080/09537287.2018.1449244.

[274] P. Morseletto, “Targets for a circular economy,” *Resour. Conserv. Recycl.*, vol. 153, p. 104553, Feb. 2020, doi: 10.1016/J.RESCONREC.2019.104553.

[275] F. A. Cruz Sanchez, H. Boudaoud, M. Camargo, and J. M. Pearce, “Plastic recycling in additive manufacturing: A systematic literature review and opportunities for the circular economy,” *J. Clean. Prod.*, vol. 264, p. 121602, 2020, doi: 10.1016/j.jclepro.2020.121602.

[276] European Commission, “A circular economy for plastics – Insights from research and innovation to inform policy and funding decisions,” *Eur. Comm.*, p. 206, 2019, doi: 10.2777/269031.

[277] P. Zhao, C. Rao, F. Gu, N. Sharmin, and J. Fu, “Close-looped recycling of polylactic acid used in 3D printing: An experimental investigation and life cycle assessment,” *J. Clean. Prod.*, vol. 197, pp. 1046–1055, 2018, doi: 10.1016/j.jclepro.2018.06.275.

[278] I. S. Jawahir and R. Bradley, “Technological Elements of Circular Economy and the Principles of 6R-Based Closed-loop Material Flow in Sustainable Manufacturing,” *Procedia CIRP*, vol. 40, pp. 103–108, Jan. 2016, doi: 10.1016/J.PROCIR.2016.01.067.

[279] A. Cavallo *et al.*, “A biocompatible pressure sensor based on a 3D-printed scaffold functionalized with PEDOT:PSS for biomedical applications,” *Org. Electron.*, vol. 96, p. 106204, Sep. 2021, doi: 10.1016/J.ORGEL.2021.106204.

[280] A. Plymill, R. Minneci, D. A. Greeley, J. Gritton, and D. Greeley, “Graphene and Carbon Nanotube PLA Composite Feedstock Graphene and Carbon Nanotube PLA Composite Feedstock Development for Fused Deposition Modeling Development for Fused Deposition Modeling Graphene and Carbon Nanotube PLA Composite Feedstock Development for Fused Deposition Modeling,” Accessed: Mar. 26, 2022. [Online]. Available: https://trace.tennessee.edu/utk_chanhonoproj/1955.

[281] M. Pollák, M. Kočiško, M. Pollak, M. Kocisko, A. Basistova, and S. Hlavata, “Implementation of innovative information technologies in the education process in the field of mechanical engineering in the Industry 4.0 concept View project Research of generative design tools for additive technology by using a robotic arm View project ,” doi: 10.17973/MMSJ.2021_6_2021031.

[282] N. E. Zander, “Recycled Polymer Feedstocks for Material Extrusion Additive Manufacturing,” *ACS Symp. Ser.*, vol. 1315, pp. 37–51, 2019, doi: 10.1021/BK-2019-1315.CH003.

[283] M. Katschnig, J. Wallner, T. Janics, C. Burgstaller, W. Zemann, and C. Holzer, “Biofunctional Glycol-Modified Polyethylene Terephthalate and Thermoplastic Polyurethane Implants by Extrusion-Based Additive Manufacturing for Medical 3D Maxillofacial Defect Reconstruction,” *Polym. 2020, Vol. 12, Page 1751*, vol. 12, no. 8, p. 1751, Aug. 2020, doi: 10.3390/POLYM12081751.

[284] M. Acevedo, L. Royano, A. I. Parralejo, J. Cabanillas, J. F. González, and J. González, “3D Printing Filaments from Kenaf, Poplar and Agricultural

Residues," *Proc. 1st Int. Conf. Water Energy Food Sustain. (ICoWEFS 2021)*, pp. 489–494, 2021, doi: 10.1007/978-3-030-75315-3_53.

[285] M. Bardot and M. D. Schulz, "Biodegradable Poly(Lactic Acid) Nanocomposites for Fused Deposition Modeling 3D Printing," *Nanomater. 2020, Vol. 10, Page 2567*, vol. 10, no. 12, p. 2567, Dec. 2020, doi: 10.3390/NANO10122567.

[286] A. Manoj and R. C. Panda, "Biodegradable Filament for 3D Printing Process: A Review," *Eng. Sci.*, 2022, doi: 10.30919/ES8D616.

[287] S. Bhagia *et al.*, "Critical review of FDM 3D printing of PLA biocomposites filled with biomass resources, characterization, biodegradability, upcycling and opportunities for biorefineries," *Appl. Mater. Today*, vol. 24, p. 101078, Sep. 2021, doi: 10.1016/J.APMT.2021.101078.

[288] I. J. Solomon, P. Sevvel, and J. Gunasekaran, "A review on the various processing parameters in FDM," *Mater. Today Proc.*, vol. 37, no. Part 2, pp. 509–514, Jan. 2021, doi: 10.1016/J.MATPR.2020.05.484.

[289] T. Kozior and C. Kundera, "Evaluation of the Influence of Parameters of FDM Technology on the Selected Mechanical Properties of Models," *Procedia Eng.*, vol. 192, pp. 463–468, Jan. 2017, doi: 10.1016/J.PROENG.2017.06.080.

[290] A. Rodríguez-Panes, J. Claver, and A. M. Camacho, "The Influence of Manufacturing Parameters on the Mechanical Behaviour of PLA and ABS Pieces Manufactured by FDM: A Comparative Analysis," *Mater. 2018, Vol. 11, Page 1333*, vol. 11, no. 8, p. 1333, Aug. 2018, doi: 10.3390/MA11081333.

[291] D. Syrlybayev, B. Zharylkassyn, A. Seisekulova, M. Akhmetov, A. Perveen, and D. Talamona, "Optimisation of Strength Properties of FDM Printed Parts—A Critical Review," *Polym. 2021, Vol. 13, Page 1587*, vol. 13, no. 10, p. 1587, May 2021, doi: 10.3390/POLYM13101587.

[292] A. Garg, A. Bhattacharya, and A. Batish, "Failure investigation of fused deposition modelling parts fabricated at different raster angles under tensile and flexural loading:," *http://dx.doi.org/10.1177/0954405415617447*, vol. 231, no. 11, pp. 2031–2039, Dec. 2015, doi: 10.1177/0954405415617447.

[293] M. M. Hanon, R. Marczis, and L. Zsidai, "Anisotropy Evaluation of Different Raster Directions, Spatial Orientations, and Fill Percentage of 3D Printed PETG Tensile Test Specimens," *Key Eng. Mater.*, vol. 821, pp. 167–173, 2019, doi: 10.4028/WWW.SCIENTIFIC.NET/KEM.821.167.

[294] S. Ziemian, M. Okwara, and C. W. Ziemian, "Tensile and fatigue behavior of layered acrylonitrile butadiene styrene," *Rapid Prototyp. J.*, vol. 21, no. 3, pp. 270–278, Apr. 2015, doi: 10.1108/RPJ-09-2013-0086/FULL/PDF.

[295] S. F. Khan, H. Zakaria, Y. L. Chong, T. J. Suteja, and A. Soesanti, "Mechanical Properties of 3D Printed Polylactic Acid Product for Various Infill Design Parameters: A Review," *J. Phys. Conf. Ser.*, vol. 1569, no. 4, p. 042010, Jul. 2020, doi: 10.1088/1742-6596/1569/4/042010.

[296] K. S. Kumar, R. Soundararajan, G. Shanthosh, P. Saravanakumar, and M.

Ratteesh, “Augmenting effect of infill density and annealing on mechanical properties of PETG and CFPETG composites fabricated by FDM,” *Mater. Today Proc.*, vol. 45, pp. 2186–2191, Jan. 2021, doi: 10.1016/J.MATPR.2020.10.078.

[297] S. Dev and R. Srivastava, “Experimental investigation and optimization of FDM process parameters for material and mechanical strength,” *Mater. Today Proc.*, vol. 26, pp. 1995–1999, Jan. 2020, doi: 10.1016/J.MATPR.2020.02.435.

[298] R. Chen, Y. Wang, Y. M. Than, S. Suriyarak, and V. Titapiwatanakun, “Rheological Investigation of Hydroxypropyl Cellulose–Based Filaments for Material Extrusion 3D Printing,” *Polym. 2022, Vol. 14, Page 1108*, vol. 14, no. 6, p. 1108, Mar. 2022, doi: 10.3390/POLYM14061108.

[299] B. N. Turner and S. A. Gold, “A review of melt extrusion additive manufacturing processes: II. Materials, dimensional accuracy, and surface roughness,” *Rapid Prototyp. J.*, vol. 21, no. 3, pp. 250–261, Apr. 2015, doi: 10.1108/RPJ-02-2013-0017/FULL/PDF.

[300] M. Kaveh, M. Badrossamay, E. Foroozmehr, and A. Hemasian Etefagh, “Optimization of the printing parameters affecting dimensional accuracy and internal cavity for HIPS material used in fused deposition modeling processes,” *J. Mater. Process. Technol.*, vol. 226, pp. 280–286, Dec. 2015, doi: 10.1016/J.JMATPROTEC.2015.07.012.

[301] T. Beran, T. Mulholland, F. Henning, N. Rudolph, and T. A. Osswald, “Nozzle clogging factors during fused filament fabrication of spherical particle filled polymers,” *Addit. Manuf.*, vol. 23, pp. 206–214, Oct. 2018, doi: 10.1016/J.ADDMA.2018.08.009.

[302] M. A. Attolico, C. Casavola, A. Cazzato, V. Moramarco, and G. Renna, “Effect of extrusion temperature on fused filament fabrication parts orthotropic behaviour,” *Rapid Prototyp. J.*, vol. 26, no. 4, pp. 639–647, May 2020, doi: 10.1108/RPJ-08-2019-0207/FULL/PDF.

[303] B. Wittbrodt and J. M. Pearce, “The effects of PLA color on material properties of 3-D printed components,” *Addit. Manuf.*, vol. 8, pp. 110–116, Oct. 2015, doi: 10.1016/J.ADDMA.2015.09.006.

[304] P. Chancerel and S. Rotter, “Recycling-oriented characterization of small waste electrical and electronic equipment,” *Waste Manag.*, vol. 29, no. 8, pp. 2336–2352, Aug. 2009, doi: 10.1016/J.WASMAN.2009.04.003.

[305] A. Manoj, M. Bhuyan, S. R. Banik, and M. Ravi Sankar, “Review on particle emissions during fused deposition modeling of acrylonitrile butadiene styrene and polylactic acid polymers,” *Mater. Today Proc.*, vol. 44, pp. 1375–1383, Jan. 2021, doi: 10.1016/J.MATPR.2020.11.521.

[306] O. Martin and L. Avérous, “Poly(lactic acid): plasticization and properties of biodegradable multiphase systems,” *Polymer (Guildf).*, vol. 42, no. 14, pp. 6209–6219, Jun. 2001, doi: 10.1016/S0032-3861(01)00086-6.

[307] J. Zheng and S. Suh, “Strategies to reduce the global carbon footprint of plastics,” *Nat. Clim. Chang. 2019 95*, vol. 9, no. 5, pp. 374–378, Apr. 2019,

doi: 10.1038/s41558-019-0459-z.

[308] M. R. Khosravani and T. Reinicke, “On the environmental impacts of 3D printing technology,” *Appl. Mater. Today*, vol. 20, p. 100689, Sep. 2020, doi: 10.1016/J.APMT.2020.100689.

[309] M. Spoerk, J. Gonzalez-Gutierrez, J. Sapkota, S. Schuschnigg, and C. Holzer, “Effect of the printing bed temperature on the adhesion of parts produced by fused filament fabrication,” *https://doi.org/10.1080/14658011.2017.1399531*, vol. 47, no. 1, pp. 17–24, Jan. 2017, doi: 10.1080/14658011.2017.1399531.

[310] Bates-Green and Howie, “Materials for 3D Printing by Fused Deposition,” 2017.

[311] “EasyFil™ ABS - Yellow - 1.75mm - 0.75 KG | Filaments.ca.” https://filaments.ca/collections/3d-filaments/products/easyfil-abs-yellow-1-75mm (accessed Mar. 17, 2022).

[312] R. Pundir, G. H. V. C. Chary, and M. G. Dastidar, “Application of Taguchi method for optimizing the process parameters for the removal of copper and nickel by growing Aspergillus sp.,” *Water Resour. Ind.*, vol. 20, pp. 83–92, Dec. 2018, doi: 10.1016/J.WRI.2016.05.001.

[313] “Taguchi Method Definition.” https://www.isixsigma.com/dictionary/taguchi-method/ (accessed Sep. 06, 2022).

[314] T. Kong, “Introduction Taguchi Methods in Experimental Design.”

[315] “Taguchi Method of Quality Control Definition.” https://www.investopedia.com/terms/t/taguchi-method-of-quality-control.asp (accessed Sep. 14, 2022).

[316] M. J. Cimbala, “Taguchi Orthogonal Arrays,” *Instrumentation, Meas. Stat.*, no. September, pp. 4–6, 2014, [Online]. Available: https://www.mne.psu.edu/me345/Lectures/Taguchi_orthogonal_arrays.pdf.

[317] F. Stephanie, O. Mike, T. Ben, and Z. John, “Design of experiments via taguchi methods: orthogonal arrays - ControlsWiki,” *michigan Chem. Process Dyn. Control. open text B.*, pp. 1–11, 2006, [Online]. Available: https://controls.engin.umich.edu/wiki/index.php/Design_of_experiments_via_taguchi_methods:_orthogonal_arrays.

[318] “Taguchi Orthogonal Array Designs.” https://www.weibull.com/hotwire/issue131/hottopics131.htm (accessed Sep. 06, 2022).

[319] V. Wankhede, D. Jagetiya, A. Joshi, and R. Chaudhari, “Experimental investigation of FDM process parameters using Taguchi analysis,” *Mater. Today Proc.*, vol. 27, pp. 2117–2120, 2019, doi: 10.1016/J.MATPR.2019.09.078.

[320] S. H. Ahn, M. Montero, D. Odell, S. Roundy, and P. K. Wright, “Anisotropic material properties of fused deposition modeling ABS,” *Rapid Prototyp. J.*, vol. 8, no. 4, pp. 248–257, 2002, doi: 10.1108/13552540210441166/FULL/XML.

[321] C. Camposeco-Negrete, "Optimization of FDM parameters for improving part quality, productivity and sustainability of the process using Taguchi methodology and desirability approach," *Prog. Addit. Manuf.*, vol. 5, no. 1, pp. 59–65, Mar. 2020, doi: 10.1007/S40964-020-00115-9/TABLES/3.

[322] M. Srivastava and S. Rathee, "Optimisation of FDM process parameters by Taguchi method for imparting customised properties to components," 2018, doi: 10.1080/17452759.2018.1440722.

[323] M. Heidari-Rarani, N. Ezati, P. Sadeghi, and M. R. Badrossamay, "Optimization of FDM process parameters for tensile properties of polylactic acid specimens using Taguchi design of experiment method," *J. Thermoplast. Compos. Mater.*, Oct. 2020, doi: 10.1177/0892705720964560/ASSET/IMAGES/LARGE/10.1177_0892705720964560-FIG10.JPEG.

[324] M. Kam, A. İpekçi, and Ö. Şengül, "Investigation of the effect of FDM process parameters on mechanical properties of 3D printed PA12 samples using Taguchi method," *J. Thermoplast. Compos. Mater.*, Apr. 2021, doi: 10.1177/08927057211006459/ASSET/IMAGES/LARGE/10.1177_08927057211006459-FIG14.JPEG.

[325] P. Stief, J.-Y. Dantan, A. Etienne, and A. Siadat, "ScienceDirect ScienceDirect A new methodology to analyze the functional and physical architecture of existing products for an assembly oriented product family identification," 2018, doi: 10.1016/j.procir.2019.02.018.

[326] R. Mendricky and D. Fris, "Analysis of the Accuracy and the Surface Roughness of FDM/FFF Technology and Optimisation of Process Parameters," *Tech. Gaz.*, vol. 27, pp. 1166–1173, 2020, doi: 10.17559/TV-20190320142210.

[327] T. C. Yang and C. H. Yeh, "Morphology and Mechanical Properties of 3D Printed Wood Fiber/Polylactic Acid Composite Parts Using Fused Deposition Modeling (FDM): The Effects of Printing Speed," *Polym. 2020, Vol. 12, Page 1334*, vol. 12, no. 6, p. 1334, Jun. 2020, doi: 10.3390/POLYM12061334.

[328] I. Bin Ishak and P. Larochelle, "MotoMaker: a robot FDM platform for multi-plane and 3D lattice structure printing," *https://doi.org/10.1080/15397734.2019.1615943*, vol. 47, no. 6, pp. 703–720, Nov. 2019, doi: 10.1080/15397734.2019.1615943.

[329] D. Garcia, R. Balart, L. Sánchez, and J. López, "Compatibility of recycled PVC/ABS blends. Effect of previous degradation," *Polym. Eng. Sci.*, vol. 47, no. 6, pp. 789–796, Jun. 2007, doi: 10.1002/PEN.20755.

[330] "Effects of Recycling Cycle on Used Thermoplastic Polymer and Thermoplastic Elastomer Polymer."

[331] T. Kuclourya, M. K. Jain, S. Mudliar, and N. B. Thamba, "Statistical analysis and investigation of tensile test data of coir composites reinforced with graphene, epoxy and carbon fibre," *Proc. Inst. Mech. Eng. Part L J. Mater. Des. Appl.*, vol. 234, no. 10, pp. 1343–1354, 2020, doi: 10.1177/1464420720939998.

[332] A. Pandžić, D. Hodzic, A. Milovanović, A. Pandzic, and A. Milovanovic, "EFFECT OF INFILL TYPE AND DENSITY ON TENSILE PROPERTIES OF PLA MATERIAL FOR FDM PROCESS 30TH DAAAM INTERNATIONAL SYMPOSIUM ON INTELLIGENT MANUFACTURING AND AUTOMATION EFFECT OF INFILL TYPE AND DENSITY ON TENSILE PROPERTIES OF PLA MATERIAL FOR FDM PROCESS," 2019, doi: 10.2507/30th.daaam.proceedings.074.

[333] M. R. Ayatollahi, A. Nabavi-Kivi, B. Bahrami, M. Yazid Yahya, and M. R. Khosravani, "The influence of in-plane raster angle on tensile and fracture strengths of 3D-printed PLA specimens," *Eng. Fract. Mech.*, vol. 237, p. 107225, Oct. 2020, doi: 10.1016/J.ENGFRACMECH.2020.107225.

[334] A. W. Fatimatuzahraa, B. Farahaina, and W. A. Y. Yusoff, "The effect of employing different raster orientations on the mechanical properties and microstructure of Fused Deposition Modeling parts," *ISBEIA 2011 - 2011 IEEE Symp. Business, Eng. Ind. Appl.*, pp. 22–27, 2011, doi: 10.1109/ISBEIA.2011.6088811.

[335] "View of THE EFFECT OF LAYER THICKNESS AND RASTER ANGLES ON TENSILE STRENGTH AND FLEXURAL STRENGTH FOR FUSED DEPOSITION MODELING (FDM) PARTS." https://jamt.utem.edu.my/jamt/article/view/4905/3603 (accessed Jul. 21, 2022).

[336] A. van Giezen and B. Wiegmans, "Spoilt - Ocean Cleanup: Alternative logistics chains to accommodate plastic waste recycling: An economic evaluation," *Transp. Res. Interdiscip. Perspect.*, vol. 5, p. 100115, May 2020, doi: 10.1016/J.TRIP.2020.100115.

[337] J. Nikiema and Z. Asiedu, "A review of the cost and effectiveness of solutions to address plastic pollution," *Environ. Sci. Pollut. Res.*, vol. 29, no. 17, pp. 24547–24573, Apr. 2022, doi: 10.1007/S11356-021-18038-5/TABLES/13.

[338] A. B. Stefaniak *et al.*, "Towards sustainable additive manufacturing: The need for awareness of particle and vapor releases during polymer recycling, making filament, and fused filament fabrication 3-D printing," *Resour. Conserv. Recycl.*, vol. 176, p. 105911, Jan. 2022, doi: 10.1016/J.RESCONREC.2021.105911.

[339] N. A. Rosli and I. Ahmad, "Mechanical Properties of Recycled Plastics," pp. 239–258, 2021, doi: 10.1007/978-981-16-3627-1_11.

[340] T. Kuclourya, R. Monroy, E. Cuan-Urquizo, A. Roman-Flores, and R. Ahmad, "Scientometric analysis and critical review of fused deposition modeling in the plastic recycling context," *Clean. Waste Syst.*, vol. 2, p. 100008, Jul. 2022, doi: 10.1016/J.CLWAS.2022.100008.

[341] J. M. Garcia and M. L. Robertson, "The future of plastics recycling," *Science (80-.).*, vol. 358, no. 6365, pp. 870–872, Nov. 2017, doi: 10.1126/SCIENCE.AAQ0324/ASSET/53AC3A00-0BBA-41D7-A05A-BE986DAF5476/ASSETS/GRAPHIC/358_870_F1.JPEG.

[342] M. Attaran, "The rise of 3-D printing: The advantages of additive

manufacturing over traditional manufacturing,” *Bus. Horiz.*, vol. 60, no. 5, pp. 677–688, Sep. 2017, doi: 10.1016/J.BUSHOR.2017.05.011.

[343] X. Tian, T. Liu, C. Yang, Q. Wang, and D. Li, “Interface and performance of 3D printed continuous carbon fiber reinforced PLA composites,” *Compos. Part A Appl. Sci. Manuf.*, vol. 88, pp. 198–205, Sep. 2016, doi: 10.1016/J.COMPOSITESA.2016.05.032.

[344] H. G. Lemu, “Study of capabilities and limitations of 3D printing technology,” *AIP Conf. Proc.*, vol. 1431, no. 1, p. 857, Apr. 2012, doi: 10.1063/1.4707644.

[345] F. Fenollosa, R. Uceda, A. Tejo, L. Calvo, L. Poudelet, and I. Buj, “Research on desktop 3D Printing Multi-Material New Concepts,” *IOP Conf. Ser. Mater. Sci. Eng.*, vol. 1193, no. 1, p. 012043, Oct. 2021, doi: 10.1088/1757-899X/1193/1/012043.

[346] K. S. Johann, A. Reißing, and C. Bonten, “Comparative Analysis of the Solid Conveying of Regrind, Virgin and Powdery Polyolefins in Single-Screw Extrusion,” *J. Manuf. Mater. Process. 2022, Vol. 6, Page 56*, vol. 6, no. 3, p. 56, May 2022, doi: 10.3390/JMMP6030056.

[347] M. A. H. Khondoker and D. Sameoto, “Direct coupling of fixed screw extruders using flexible heated hoses for FDM printing of extremely soft thermoplastic elastomers,” *Prog. Addit. Manuf.*, vol. 4, no. 3, pp. 197–209, Sep. 2019, doi: 10.1007/S40964-019-00088-4/FIGURES/6.

[348] A. Alexandre, F. A. Cruz Sanchez, H. Boudaoud, M. Camargo, and J. M. Pearce, “Mechanical Properties of Direct Waste Printing of Polylactic Acid with Universal Pellets Extruder: Comparison to Fused Filament Fabrication on Open-Source Desktop Three-Dimensional Printers,” *3D Print. Addit. Manuf.*, vol. 7, no. 5, pp. 237–247, Oct. 2020, doi: 10.1089/3DP.2019.0195/ASSET/IMAGES/LARGE/3DP.2019.0195_FIGURE7.JPEG.

[349] N. Kumar, P. K. Jain, P. Tandon, and P. M. Pandey, “Extrusion-based additive manufacturing process for producing flexible parts,” *J. Brazilian Soc. Mech. Sci. Eng.*, vol. 40, no. 3, pp. 1–12, Mar. 2018, doi: 10.1007/S40430-018-1068-X/FIGURES/18.

[350] B. V. Reddy, N. V. Reddy, and A. Ghosh, “Fused deposition modelling using direct extrusion,” *http://dx.doi.org/10.1080/17452750701336486*, vol. 2, no. 1, pp. 51–60, Mar. 2007, doi: 10.1080/17452750701336486.

[351] J. Leng, J. Wu, N. Chen, X. Xu, and J. Zhang, “The development of a conical screw-based extrusion deposition system and its application in fused deposition modeling with thermoplastic polyurethane,” *Rapid Prototyp. J.*, vol. 26, no. 2, pp. 409–417, Feb. 2020, doi: 10.1108/RPJ-05-2019-0139/FULL/XML.

[352] E. Canessa, M. Baruzzo, and C. Fonda, “Study of Moineau-based pumps for the volumetric extrusion of pellets,” *Addit. Manuf.*, vol. 17, pp. 143–150, Oct. 2017, doi: 10.1016/J.ADDMA.2017.08.015.

[353] P. Magnoni, L. Rebaioli, I. Fassi, N. Pedrocchi, and L. M. Tosatti, “Robotic AM System for Plastic Materials: Tuning and On-line Adjustment of Process

Parameters," *Procedia Manuf.*, vol. 11, pp. 346–354, Jan. 2017, doi: 10.1016/J.PROMFG.2017.07.117.

[354] A. L. Woern, D. J. Byard, R. B. Oakley, M. J. Fiedler, S. L. Snabes, and J. M. Pearce, "Fused Particle Fabrication 3-D Printing: Recycled Materials' Optimization and Mechanical Properties," *Mater. 2018, Vol. 11, Page 1413*, vol. 11, no. 8, p. 1413, Aug. 2018, doi: 10.3390/MA11081413.

[355] A. Bellini, S. Güçeri, and M. Bertoldi, "Liquefier Dynamics in Fused Deposition," *J. Manuf. Sci. Eng.*, vol. 126, no. 2, pp. 237–246, May 2004, doi: 10.1115/1.1688377.

[356] R. V. Chiruvella, Y. Jaluria, V. Sernas, and M. Esseghir, "Extrusion of non-newtonian fluids in a single-screw extruder with pressure back flow," *Polym. Eng. Sci.*, vol. 36, no. 3, pp. 358–367, Feb. 1996, doi: 10.1002/PEN.10422.

[357] "Understanding Screw Design for Film Extrusion Process - Macro Engineering and Technology." http://www.macroeng.com/understanding-screw-design-for-film-extrusion-process.php (accessed May 16, 2022).

[358] P. Pitayachaval and P. Watcharamaisakul, "A review of a machine design of chocolate extrusion based co-rotating twin screw extruder," doi: 10.1088/1757-899X/703/1/012012.

[359] J. M. J. Netto and Z. D. C. Silveira, "Design of an innovative three-dimensional print head based on twin-screw extrusion," *J. Mech. Des. Trans. ASME*, vol. 140, no. 12, Dec. 2018, doi: 10.1115/1.4041175/366963.

[360] J. W. Sikora, B. Samujlo, A. Stasiek, and A. Tor-Świątek, "The mechanical properties of plasticized PVC processed in an extruder with a modified feed zone," *Int. Polym. Process.*, vol. 30, no. 3, pp. 359–365, Jul. 2015, doi: 10.3139/217.3040/MACHINEREADABLECITATION/RIS.

[361] Y. Béreaux, J. Y. Charmeau, and M. Moguedet, "A simple model of throughput and pressure development for single screw," *J. Mater. Process. Technol.*, vol. 209, no. 1, pp. 611–618, Jan. 2009, doi: 10.1016/J.JMATPROTEC.2008.02.070.

[362] "Extrusion: How Much L/D Do You Really Need? | Plastics Technology." https://www.ptonline.com/articles/how-much-ld-do-you-really-need (accessed Jul. 04, 2022).

[363] J. F. I. Housz and H. E. H. Meijer, "The melting performance of single screw extruders," *Polym. Eng. Sci.*, vol. 21, no. 6, pp. 352–359, 1981, doi: 10.1002/PEN.760210606.

[364] E. M. Mount, "Extrusion Processes," *Appl. Plast. Eng. Handb. Process. Mater. Appl. Second Ed.*, pp. 217–264, Jan. 2017, doi: 10.1016/B978-0-323-39040-8.00012-2.

[365] T. J. Shankar, S. Sokhansanj, S. Bandyopadhyay, and A. S. Bawa, "A case study on optimization of biomass flow during single-screw extrusion cooking using genetic algorithm (GA) and response surface method (RSM)," *Food Bioprocess Technol.*, vol. 3, no. 4, pp. 498–510, Dec. 2010, doi:

10.1007/S11947-008-0172-9/TABLES/5.

[366] A. S. Sokhey, Y. Ali, and M. A. Hanna, “Effects of die dimensions on extruder performance,” *J. Food Eng.*, vol. 31, no. 2, pp. 251–261, Feb. 1997, doi: 10.1016/S0260-8774(96)00025-8.

[367] J. W. Sikora and E. Sasimowski, “Influence of the length of the plasticating system on selected characteristics of an autothermal extrusion process,” *Adv. Polym. Technol.*, vol. 24, no. 1, pp. 21–28, Mar. 2005, doi: 10.1002/ADV.20021.

[368] N. Chevanan, K. A. Rosentrater, and K. Muthukumarappan, “Effects of processing conditions on single screw extrusion of feed ingredients containing DDGS,” *Food Bioprocess Technol.*, vol. 3, no. 1, pp. 111–120, Jan. 2010, doi: 10.1007/S11947-008-0065-Y/FIGURES/5.

[369] A. R. Vincelette, C. S. Guerrero, P. J. Carreau, and P. G. Lafleur, “A Model for Single-screw Plasticating Extruders,” *Int. Polym. Process.*, vol. 4, no. 4, pp. 232–241, Dec. 1989, doi: 10.3139/217.890232.

[370] M. Engineering and C. Rauwendaal, “Plastics, Rubber and Composites Finite element studies of flow and temperature evolution in single screw extruders Finite element studies of flow and temperature evolution in single screw extruders,” 2013, doi: 10.1179/174328904X24880.

[371] Y. Jaluria, “Numerical simulation of the extrusion process for food materials in a single-screw extruder Related papers Finit e Element Modeling of Fluid Flow, Heat Transfer, and Melt ing of Biomat erials in a Single-s….”

[372] W. Roland, C. Marschik, M. Krieger, B. Löw-Baselli, and J. Miethlinger, “Symbolic regression models for predicting viscous dissipation of three-dimensional non-Newtonian flows in single-screw extruders,” *J. Nonnewton. Fluid Mech.*, vol. 268, pp. 12–29, Jun. 2019, doi: 10.1016/J.JNNFM.2019.04.006.

[373] D. Drotman, M. Diagne, R. Bitmead, and M. Krstic, “CONTROL-ORIENTED ENERGY-BASED MODELING OF A SCREW EXTRUDER USED FOR 3D PRINTING,” 2016, Accessed: Jul. 09, 2022. [Online]. Available: http://asmedigitalcollection.asme.org/DSCC/proceedings-pdf/DSCC2016/50701/V002T21A002/2375621/v002t21a002-dscc2016-9651.pdf?casa_token=EjyqXpZMuVcAAAAA:2esgCwuNGz71zz-AItiIFF9aB7j0X60govEIFvYcnPb88fZAXtFELWKwFCMXrXWhM2O8Vg.

[374] D. Smith, M. A. Spalding, and R. J. Gould, “SELECTING EQUIPMENT TO MINIMIZE PRODUCTION COSTS AND MAXIMIZE PROFITABILITY*,” doi: 10.1177/8756087907087171.

[375] “Get Smarter on Extruder Sizes | Plastics Technology.” https://www.ptonline.com/articles/get-smarter-on-extruder-sizes (accessed Jan. 26, 2022).

[376] J. G. Drobny, “Thermoplastic Polyurethane Elastomers,” *Handb. Thermoplast. Elastomers*, pp. 233–253, 2014, doi: 10.1016/B978-0-323-22136-8.00009-0.

[377] C. Abeykoon, A. McMillan, and B. K. Nguyen, “Energy efficiency in extrusion-related polymer processing: A review of state of the art and potential efficiency improvements,” *Renew. Sustain. Energy Rev.*, vol. 147, p. 111219, Sep. 2021, doi: 10.1016/J.RSER.2021.111219.

[378] D. Berthiaume, “Justification for AC vs. DC drive systems,” *IEEE Conf. Rec. Annu. Pulp Pap. Ind. Tech. Conf.*, pp. 234–238, 1991, doi: 10.1109/PAPCON.1991.239643.

[379] A. Das, E. L. Gilmer, S. Biria, and M. J. Bortner, “Importance of Polymer Rheology on Material Extrusion Additive Manufacturing: Correlating Process Physics to Print Properties,” *ACS Appl. Polym. Mater.*, vol. 3, no. 3, pp. 1218–1249, Mar. 2021, doi: 10.1021/ACSAPM.0C01228/ASSET/IMAGES/LARGE/AP0C01228_0011.JPEG.

[380] S. Whyman, K. M. Arif, and J. Potgieter, “Design and development of an extrusion system for 3D printing biopolymer pellets,” *Int. J. Adv. Manuf. Technol. 2018 969*, vol. 96, no. 9, pp. 3417–3428, Mar. 2018, doi: 10.1007/S00170-018-1843-Y.

[381] S. E. Papadakis and R. E. Bahu, “THE STICKY ISSUES OF DRYING,” *http://dx.doi.org/10.1080/07373939208916484*, vol. 10, no. 4, pp. 817–837, 2007, doi: 10.1080/07373939208916484.

[382] “Fluids and Solids Handling.”

[383] S. Lipár, P. Noga, and G. Hulkó, “Modelling and Control of Extruder Barrel Temperature Field,” *IFAC Proc. Vol.*, vol. 46, no. 26, pp. 191–196, Jan. 2013, doi: 10.3182/20130925-3-FR-4043.00078.

[384] A. La Gala, R. Fiorio, M. Erkoç, L. Cardon, and D. R. D’hooge, “Theoretical Evaluation of the Melting Efficiency for the Single-Screw Micro-Extrusion Process: The Case of 3D Printing of ABS,” *Process. 2020, Vol. 8, Page 1522*, vol. 8, no. 11, p. 1522, Nov. 2020, doi: 10.3390/PR8111522.

[385] U. W. Gedde, M. S. Hedenqvist, M. Hakkarainen, F. Nilsson, and O. Das, “Processing of Polymeric Materials,” *Appl. Polym. Sci.*, pp. 453–487, 2021, doi: 10.1007/978-3-030-68472-3_8.

[386] N. Grizzuti, O. Bifulco, N. Grizzuti, and • O Bifulco, “Effects of coalescence and breakup on the steady-state morphology of an immiscible polymer blend in shear flow,” *Rheol Acta*, vol. 36, pp. 406–415, 1997.

[387] Hopper, “INTRODUCTION TO THE MAIN POLYMER PROCESSES.”

[388] D. V. Rosato, D. V. Rosato, and M. G. Rosato, “Plasticizing,” *Inject. Molding Handb.*, pp. 151–220, 2000, doi: 10.1007/978-1-4615-4597-2_3.

[389] “Understanding Melting in Single-Screw Extruders | Plastics Technology.” https://www.ptonline.com/articles/understanding-melting-in-single-screw-extruders- (accessed Feb. 02, 2022).

[390] C. Abeykoon *et al.*, “Investigation of the process energy demand in polymer

extrusion: A brief review and an experimental study," *Appl. Energy*, vol. 136, pp. 726–737, Dec. 2014, doi: 10.1016/J.APENERGY.2014.09.024.

[391] C. Abeykoon, A. L. Kelly, E. C. Brown, and P. D. Coates, "The effect of materials, process settings and screw geometry on energy consumption and melt temperature in single screw extrusion," *Appl. Energy*, vol. 180, pp. 880–894, Oct. 2016, doi: 10.1016/J.APENERGY.2016.07.014.

[392] J. C. DiNunzio, C. Brough, J. R. Hughey, D. A. Miller, R. O. Williams, and J. W. McGinity, "Fusion production of solid dispersions containing a heat-sensitive active ingredient by hot melt extrusion and Kinetisol® dispersing," *Eur. J. Pharm. Biopharm.*, vol. 74, no. 2, pp. 340–351, Feb. 2010, doi: 10.1016/J.EJPB.2009.09.007.

[393] "T60 Closed Loop Stepper Driver User Manual T60 User Manual-2."

[394] "What is Hoop Stress? - Definition from Trenchlesspedia." https://www.trenchlesspedia.com/definition/2799/hoop-stress (accessed Jun. 30, 2022).

[395] J. Capelle, I. Dmytrakh, J. Gilgert, P. Jodin, and G. Pluvinage, "A COMPARISON OF EXPERIMENTAL RESULTS AND COMPUTATIONS FOR CRACKED TUBES SUBJECTED TO INTERNAL PRESSURE PRIMERJAVA EKSPERIMENTALNIH REZULTATOV IN IZRA^UNA ZA CEVI Z RAZPOKO, KI SO OBREMENJENI Z NOTRANJO RAZPOKO."

[396] A. W. Birley and J. Batchelor, "Single-Screw Extrusion THE EXTRUDER CHARACTERISTIC."

[397] H. M. Yoo, S. Y. Jeong, and S. W. Choi, "Analysis of the rheological property and crystallization behavior of polylactic acid (Ingeo^{TM} Biopolymer 4032D) at different process temperatures," *E-Polymers*, vol. 21, no. 1, pp. 702–709, Jan. 2021, doi: 10.1515/EPOLY-2021-0071/MACHINEREADABLECITATION/RIS.

[398] "Factors of Safety." https://www.engineeringtoolbox.com/factors-safety-fos-d_1624.html (accessed Jun. 21, 2022).

[399] R. B. Song, J. Y. Xiang, and D. P. Hou, "Characteristics of Mechanical Properties and Microstructure for 316L Austenitic Stainless Steel," *J. Iron Steel Res. Int.*, vol. 18, no. 11, pp. 53–59, Nov. 2011, doi: 10.1016/S1006-706X(11)60117-9.

[400] H. Mahfuz, A. Adnan, V. K. Rangari, and S. Jeelani, "MANUFACTURING AND CHARACTERIZATION OF CARBON NANOTUBE/POLYETHYLENE COMPOSITES," *http://dx.doi.org/10.1142/S0219581X05002961*, vol. 4, no. 1, pp. 55–72, Nov. 2011, doi: 10.1142/S0219581X05002961.

[401] "Energy analysis in the extrusion of plastics - Theseus." https://www.theseus.fi/handle/10024/53774 (accessed Jul. 09, 2022).

[402] M. Lay, N. L. N. Thajudin, Z. A. A. Hamid, A. Rusli, M. K. Abdullah, and R. K. Shuib, "Comparison of physical and mechanical properties of PLA, ABS

and nylon 6 fabricated using fused deposition modeling and injection molding," *Compos. Part B Eng.*, vol. 176, p. 107341, Nov. 2019, doi: 10.1016/J.COMPOSITESB.2019.107341.

[403] "How Much Horsepower Do You Need? | Plastics Technology." https://www.ptonline.com/articles/how-much-horsepower-do-you-need (accessed Jan. 26, 2022).

[404] O. Zmeskal, L. Marackova, and T. Lapcikova, "Thermal properties of samples prepared from polylactic acid by 3D printing ARTICLES YOU MAY BE INTERESTED IN," p. 20022, 2020, doi: 10.1063/5.0033857.

[405] J. Z. Liang, "Effects of extrusion conditions on die-swell behavior of polypropylene/diatomite composite melts," *Polym. Test.*, vol. 27, no. 8, pp. 936–940, Dec. 2008, doi: 10.1016/J.POLYMERTESTING.2008.08.001.

[406] S. Salehi, M. Arashpour, J. Kodikara, and R. Guppy, "Sustainable pavement construction: A systematic literature review of environmental and economic analysis of recycled materials," *J. Clean. Prod.*, vol. 313, p. 127936, Sep. 2021, doi: 10.1016/J.JCLEPRO.2021.127936.

[407] L. Milios, L. Holm Christensen, D. McKinnon, C. Christensen, M. K. Rasch, and M. Hallstrøm Eriksen, "Plastic recycling in the Nordics: A value chain market analysis," *Waste Manag.*, vol. 76, pp. 180–189, Jun. 2018, doi: 10.1016/J.WASMAN.2018.03.034.

[408] R. H. J. M. Gradus, P. H. L. Nillesen, E. Dijkgraaf, and R. J. van Koppen, "A Cost-effectiveness Analysis for Incineration or Recycling of Dutch Household Plastic Waste," *Ecol. Econ.*, vol. 135, pp. 22–28, May 2017, doi: 10.1016/J.ECOLECON.2016.12.021.

[409] I. Dubdub and M. Al-Yaari, "Thermal Behavior of Mixed Plastics at Different Heating Rates: I. Pyrolysis Kinetics," *Polym. 2021, Vol. 13, Page 3413*, vol. 13, no. 19, p. 3413, Oct. 2021, doi: 10.3390/POLYM13193413.

[410] R. V. Moharir and S. Kumar, "Challenges associated with plastic waste disposal and allied microbial routes for its effective degradation: A comprehensive review," *J. Clean. Prod.*, vol. 208, pp. 65–76, Jan. 2019, doi: 10.1016/J.JCLEPRO.2018.10.059.

[411] E. Metin, A. Eröztürk, and C. Neyim, "Solid waste management practices and review of recovery and recycling operations in Turkey," *Waste Manag.*, vol. 23, no. 5, pp. 425–432, Jan. 2003, doi: 10.1016/S0956-053X(03)00070-9.

[412] A. Kumar, S. R. Samadder, N. Kumar, and C. Singh, "Estimation of the generation rate of different types of plastic wastes and possible revenue recovery from informal recycling," *Waste Manag.*, vol. 79, pp. 781–790, Sep. 2018, doi: 10.1016/J.WASMAN.2018.08.045.

[413] V. Gaikwad, A. Ghose, S. Cholake, A. Rawal, M. Iwato, and V. Sahajwalla, "Transformation of E-Waste Plastics into Sustainable Filaments for 3D Printing," *ACS Sustain. Chem. Eng.*, vol. 6, no. 11, pp. 14432–14440, Nov. 2018, doi: 10.1021/ACSSUSCHEMENG.8B03105/SUPPL_FILE/SC8B03105_SI_001.P

DF.

[414] J. Manners-bell, “THE IMPLICATIONS OF 3D PRINTING FOR THE GLOBAL LOGISTICS INDUSTRY,” 2012.

[415] K. DePalma, M. R. Walluk, A. Murtaugh, J. Hilton, S. McConky, and B. Hilton, “Assessment of 3D printing using fused deposition modeling and selective laser sintering for a circular economy,” *J. Clean. Prod.*, vol. 264, p. 121567, Aug. 2020, doi: 10.1016/J.JCLEPRO.2020.121567.

[416] B. Maldonado-García, A. K. Pal, M. Misra, S. Gregori, and A. K. Mohanty, “Sustainable 3D printed composites from recycled ocean plastics and pyrolyzed soy-hulls: Optimization of printing parameters, performance studies and prototypes development,” *Compos. Part C Open Access*, vol. 6, p. 100197, Oct. 2021, doi: 10.1016/J.JCOMC.2021.100197.

[417] “ZUV is an electric tricycle that can be 3D-printed from plastic waste.” https://www.dezeen.com/2021/08/04/zuv-eoos-next-tricycle-design/ (accessed Apr. 17, 2022).

[418] “US Army Learning About and Using 3D Printing to Improve Military Readiness - 3DPrint.com | The Voice of 3D Printing / Additive Manufacturing.” https://3dprint.com/233454/army-3d-printing-military-readiness/ (accessed Apr. 17, 2022).

[419] “The New Raw Archives - Perfect 3D Printing Filament.” https://www.morgen-filament.de/category/the-new-raw/ (accessed Apr. 17, 2022).

[420] “Asao Tokolo 3D-prints Tokyo 2020 podiums from donated plastic waste.” https://www.dezeen.com/2021/07/15/podiums-tokyo-2020-olympics-asao-tokolo/amp/ (accessed Apr. 17, 2022).

[421] “Löfbergs, Sculptur pioneer 3D printing of beverage stations from coffee production waste.” https://www.nuffoodsspectrum.in/news/54/7806/lfbergs-sculptur-pioneer-3d-printing-of-beverage-stations-from-coffee-production-waste.html (accessed Apr. 17, 2022).

[422] J. Holmström, M. Walter, and H. Yrjölä, “Rapid manufacturing and its impact on supply chain management Design science research View project FP7-LOGSEC View project Rapid manufacturing and its impact on supply chain management,” Accessed: Jul. 11, 2022. [Online]. Available: https://www.researchgate.net/publication/267819657.

[423] “Idea Reality: Rapid prototyping and the art of failing forward.” https://ultimaker.com/learn/idea-reality-rapid-prototyping-art-of-failing-forward (accessed Jul. 11, 2022).

[424] “3D Printing Companies in Canada - 3D.directory.” https://www.3d.directory/directory/3d-printing-services?country=Canada (accessed Jul. 11, 2022).

[425] “3D Printing From Plastic Waste: 10 Successful Projects | All3DP Pro.” https://all3dp.com/1/3d-printing-from-plastic-waste/ (accessed Jul. 11, 2022).

[426] "Ford and HP are recycling 3D printer waste into truck parts | TechSpot." https://www.techspot.com/news/89074-ford-hp-recycling-3d-printer-waste-truck-parts.html (accessed Jul. 11, 2022).

Appendices

1. Economics of Plastic Recycling

It is essential to have an economic point of view as it is a crucial step for analyzing the importance of plastic recycling [406]. It highlights the feasibility of the entire process [407]. Plastics, if not recycled or incinerated, are often dumped into landfills. There are several federal regulations that bind the economic analyses of the landfills, such as specifications in design, restrictions in location, specific operating standards, and closure requirements [40]. These factors greatly affect the cost of building, using, and closing a landfill [40]. The revenue obtained when compared with the total operating cost of landfilling 1 ton of plastic waste in the US is almost negligible [40]. The landfill owners generally earn revenues by selling landfill gas or electricity to local power suppliers [40].

As discussed in Chapter 1, due to energy generation and potentially less environmental hazards, incineration is a better alternative when compared with landfilling. For an incineration plant, it becomes necessary to analyze a wide range of parameters for economic analyses [408]. However, the type of energy produced and the capacity of the plant play a critical role [40]. The majority of the revenue is generated from the heat produced by these plants and is dependent on the average lower heat factor of the material [40]. Plastics have a high average lower heating factor among the general solid waste [409], and hence incineration method has absolute profitability (profit > $ 0) [40]. However, this is a theoretical approach and is valid only when plastics are incinerated.

Lastly, the last and the most environmentally friendly waste handling technique is the recycling method [410]. As mentioned earlier in the literature, there are seven different resin codes for plastics. Lower resin code plastics such as PET and HDPE have the highest recycling rate, and often economic analyses are done on these plastics [40]. There are generally three factors involved in the economic analyses of plastic recycling- Material recovery cost from the MRFs (Material Recovery Facilities), Plastic reprocessing cost, and Revenue gain from recycled plastics [40]. The PSWs are sorted and prepared for further processing inside the MRFs [411]. The economic analysis of the plastic recycling method depends on these MRFs' investment costs, which are distributed into machine and equipment costs, building, and site location [40]. The revenues for the plastic recycling process are derived from the companies which buy recycled plastic pellets to produce new products for various applications such as automobile parts, food containers, etc. [412]. The profitability of the recycling process is governed by the plastic recycling ratio of the consumers. For more profitability, it is required that more consumers recycle their plastic wastes and more plastic waste reaches MRFs [40]. Hence, plastic recycling should be promoted.

2. Applications of 3D printed recycled plastic products in the real world

The current plastic recycling technologies are not sufficient enough to address the huge amount of plastic waste, and hence 3D printing or DRAM is being looked at as a potential method for recycling purposes [413]. For any technology to become a mass production manufacturing process, it is essential that it meets consumer requirements and market demands [414]. The FDM process, when carried on recycled plastics, is a complex process and still not widely accepted in the market as studies have shown that after repeated recycling, the material could not be 3D printed again using FDM [415]. This is because recycled plastic filaments are not suitable for 3D printing applications demanding specific mechanical properties [135]. For FDM to enter the market in the field of recycled plastics, there is a need to find optimum FDM parameters at different recycling cycles for different materials. As of now, recycled plastics are 3D printed using non-FDM techniques and are widely accepted as DRAM has transformed recycled plastics from various sources into useful products for the real market [416]. Some of these applications have been discussed in this section.

- *Automobile – Transforming plastic wastes into Zero-emission Utility Vehicle (ZUV)*

A collaborative work by Austrian design firm-EOOS and Dutch 3D printing firm-The New Raw has utilized plastic waste and transformed it into an urban mobility vehicle. The frame of the vehicle is completely 3D printed from waste plastics [417].

- *Military- Transforming army base waste to readiness parts*

The US army research laboratory has recently launched an initiative to utilize plastic debris such as plastic bottles, jugs, containers, etc., from the frontline environment and feed them to 3D printers. The lab has created one vehicle bracket per 10 plastic bottles [418].

- *Commercial – Transforming marine wastes to home-based and street furniture*

The New Raw initiative from the Netherlands aims to utilize marine plastic wastes such as fishing nets and shipping wastes and convert them into furniture such as chairs, tables, lamps, sunbeds, etc. The New Raw has its own Zero waste lab, providing consumers with a plastic recycling unit and a robotic arm 3D printer. Consumers can bring their own plastic wastes and transform them into required furniture [419].

- *Sports – Transforming plastic bottles to the podium*

In the recently held Tokyo Olympics in 2020, all the 98 podiums used were made from 3D printing of plastic wastes such as shampoo containers, empty bottles, etc. [420].

- *Food – Transforming food production waste to food stations*

A work under Circular Coffee Community aims to build coffee stations by 3D printing waste plastics such as polypropylene with the help of a robotic 3D printer [421].

3. Nomenclature of Specimens

Nomenclature - M.RA.ET.ID.RP-#T

Where, **M** = Material (**P**- PLA)

RA = Raster angle (**0** - 0°/90°, **3** - 30°/-60°, **4** - 45°/-45°)

ET = Extrusion Temperature (**1** - T1 = 200°C, **2** - T2 = 210°C, **3** - T3 = 220°C)

ID = Infill Density (**3** - 30%, **6** - 60%, **9** - 90%)

RP = Number of reprocessing cycle (**1**- Virgin (1st reprocessing cycle), **2** - 2nd reprocessing cycle, **3** – 3rd reprocessing cycle, **4** - 4th reprocessing cycle)

#T = number of trials (**1** - 1st trial, **2** - 2nd trial, **3** - 3rd trial)

Eg- P.3.2.6.2-2 means a second trial of the PLA sample printed at 30°/-60° raster angle at T2 extrusion temperature having infill density of 60% and processed twice

P.4.3.9.4-3 means the third trial of the PLA sample printed at 45°/-45° raster angle at T3 extrusion temperature having infill density of 90% and processed four times

P.0.1.3.1-1 means the first trial of the PLA sample printed at 0°/90° raster angle at T1 extrusion temperature having infill density of 30% and processed once (virgin specimen)

4. Taguchi Analysis Example

The ultimate tensile strength values of all the experiments of Taguchi Analysis 1 are shown in Table A-1. The average and the variance values are calculated for all the experiments, and the SN values are calculated.

Table A - 1 Tensile test results along with Taguchi Analysis 1

Experiment Number	A	B	C	D	Specimen	Taguchi Analysis 1 Ultimate Tensile Strength (MPa)		
	RA	ID%	ET	RP		Average (y_i)	Variance (s_i^2)	Signal-to-noise ratio (SN_i)
1	1	1	1	1	P.0.1.3.1	20.720	1.748	23.900
2	1	2	2	2	P.0.2.6.3	13.813	8.101	13.720
3	1	3	3	3	P.0.3.9.4	9.298	0.016	37.290
4	2	1	2	3	P.3.2.3.4	7.223	0.576	19.569
5	2	2	3	1	P.3.3.6.1	23.980	1.573	25.629
6	2	3	1	2	P.3.1.9.3	15.294	14.551	12.062
7	3	1	3	2	P.4.3.3.3	10.969	2.126	17.527
8	3	2	1	3	P.4.1.6.4	8.587	0.033	33.469
9	3	3	2	1	P.4.2.9.1	25.038	0.044	41.535

After calculating the SN values for all the experiments, the SN values and the range are calculated sequentially for each parameter at each level from Tables A – 2 to A –8.

Table A - 2 SN values for all experiments – Calculations for the three levels of Parameter A

Experiment Number	A	B	C	D	Taguchi Analysis 1
	RA	ID%	ET	RP	Signal-to-noise ratio (SN_i)
1	1[a]	1	1	1	23.900[a]
2	1[a]	2	2	2	13.720a[a]
3	1[a]	3	3	3	37.290[a]
4	2[b]	1	2	3	19.569[b]
5	2[b]	2	3	1	25.629[b]
6	2[b]	3	1	2	12.062[b]
7	3[c]	1	3	2	17.527[c]
8	3[c]	2	1	3	33.469[c]
9	3[c]	3	2	1	41.535[c]

Table A - 3 SN values for all experiments – Calculations for the three levels of Parameter A

Experiment Number	A (RA)	B (ID%)	C (ET)	D (RP)
1	24.970	-	-	-
2	19.087	-	-	-
3	30.843	-	-	-
Δ	11.757	-	-	-
Rank	-	-	-	-

For finding SN values of parameter A at the first, second and third level, the SN values with superscript 'a', 'b' and 'c' are averaged, respectively.

Table A - 4 SN values for all experiments – Calculations for the three levels of Parameter B

Experiment Number	A	B	C	D	Taguchi Analysis 1
	RA	ID%	ET	RP	Signal-to-noise ratio (SN_i)
1	1	1[a]	1	1	23.900[a]
2	1	2[b]	2	2	13.720[b]
3	1	3[c]	3	3	37.290[c]
4	2	1[a]	2	3	19.569[a]
5	2	2[b]	3	1	25.629[b]
6	2	3[c]	1	2	12.062[c]
7	3	1[a]	3	2	17.526[a]
8	3	2[b]	1	3	33.469[b]
9	3	3[c]	2	1	41.535[c]

Table A - 5 SN values for all experiments – Calculations for the three levels of Parameter B

Experiment Number	A (RA)	B (ID%)	C (ET)	D (RP)
1	24.970	20.332	-	-
2	19.087	24.273	-	-
3	30.843	30.295	-	-
Δ	11.757	9.963	-	-
Rank	-	-	-	-

For finding SN values of parameter B at the first, second and third level, the SN values with superscript 'a', 'b' and 'c' are averaged, respectively.

Table A - 6 SN values for all experiments – Calculations for the three levels of Parameter C

Experiment Number	A	B	C	D	Taguchi Analysis 1
	RA	ID%	ET	RP	Signal-to-noise ratio (SN_i)
1	1	1	1[a]	1	23.900[a]
2	1	2	2[b]	2	13.720[b]
3	1	3	3[c]	3	37.290[c]
4	2	1	2[b]	3	19.569[b]
5	2	2	3[c]	1	25.629[c]
6	2	3	1[a]	2	12.062[a]
7	3	1	3[c]	2	17.526[c]
8	3	2	1[a]	3	33.469[a]
9	3	3	2[b]	1	41.535[b]

Table A - 7 SN values for all experiments – Calculations for the three levels of Parameter C

Experiment Number	A (RA)	B (ID%)	C (ET)	D (RP)
1	24.970	20.332	24.143	-
2	19.087	24.273	24.941	-
3	30.843	30.295	26.815	-
Δ	11.757	9.963	3.672	-
Rank	-	-	-	-

For finding SN values of parameter C at the first, second and third level, the SN values with superscript ‘a’, ‘b’ and ‘c’ are averaged, respectively.

Table A - 8 SN values for all experiments – Calculations for the three levels of Parameter D

Experiment Number	A	B	C	D	Taguchi Analysis 1
	RA	ID%	ET	RP	Signal-to-noise ratio (SN_i)
1	1	1	1	1[a]	23.900[a]
2	1	2	2	2[b]	13.720[b]
3	1	3	3	3[c]	37.290[c]
4	2	1	2	3[c]	19.569[c]
5	2	2	3	1[a]	25.629[a]
6	2	3	1	2[b]	12.062[b]
7	3	1	3	2[b]	17.526[b]
8	3	2	1	3[c]	33.469[c]
9	3	3	2	1[a]	41.535[a]

Table A - 9 SN values for all experiments – Calculations for the three levels of Parameter D

Experiment Number	A (RA)	B (ID%)	C (ET)	D (RP)
1	24.970	20.332	24.143	30.355
2	19.087	24.273	24.941	14.436
3	30.843	30.295	26.815	30.109
Δ	11.757	9.963	3.672	15.919
Rank	2	3	4	1

For finding SN values of parameter D at the first, second and third level, the SN values with superscript ‘a’, ‘b’ and ‘c’ are averaged, respectively.

Higher the range value, more is the significance of the factor [316]. This is because a small change in signal will cause a larger effect on the output variable being measured [316]. From Table A – 9, it can be observed that for 4P-L3 analysis or Taguchi Analysis 1, RP is the most significant factor because of highest range value.

5. Mass efficiency calculations for shredder and filament maker

- **Shredder efficiency (ɳ)**

ɳ = [(Weight of shredded plastic (Wa)) / (Weight of specimen (Wb))] * 100

Based on experimental trials, specimens of a batch were weighed before shredding (Wb) and then weighed after four cycles of shredding (Wa). The analysis were –

For P.0.3.9.2 specimens (12 specimens) – Wb = 110.89 g, Wa = 100.05 g - ɳ = 90.22%

For P.4.3.3.1 specimens (11 specimens) – Wb = 80.19 g, Wa = 72.09 g - ɳ = 89.89%

For P.0.2.6.2 specimens (6 specimens) – Wb = 50.88 g, Wa = 44.97 g - ɳ = 88.39%

Average of efficiencies – 89.5 %

Approximate efficiency – **89%**

- **Filament maker efficiency (ε)**

ε = [(Weight of filament (Wf))/(Weight of shredded plastic before filament extrusion process (Wa))]

Based on experimental trials, shredded specimens of a batch were weighed before filament extrusion process (Wa) and then weighed in their filament form (Wf). The analysis were –

For P.4.3.3.1 specimens– Wa = 72.09 g, Wf = 51.45 g - η = 71.38% - Approximate Efficiency = **70%**

For P.0.2.6.2 specimens – Wa = 44.97 g, Wf = 29.89 g - η = **66.47%**

For P.0.3.9.2 specimens–Wa = 100.05 g, Wf = 65.14 g - η = **65.11%**

6. Applications of the proposed hybrid system

The market application for this system is plastic, eco-friendly 3D printing products, and the main customers' target for these systems can be categorized into two segments. The first is related to On-Demand Manufacturing Companies (ODM), specifically 3D Printing Farms, and the second is Prototyping Services Companies. Typically, these enterprises produce low-batch customized components or prototypes from commercial chains such as retail, automotive, aeronautic, aerospace, and medical [422]. Up to date, it is documented that a typical 3D printing system can produce a maximum of 30% waste from production, and prototype iterations can take up to 5000 trials before the final product launch [423]. Therefore, the proposed system aims to open a business opportunity to reuse the plastic waste generated and increase cash flow by creating cheaper and more rapid second-life products and increasing profit by reducing waste disposal costs. In Canada, there are already 80 companies that provide this production services, accounting for 3% of the global market, while the USA is the largest by region with an approximately 40% of the entire market [424].

In terms of remarkable product applications using recycled plastic within additive manufacturing, there are several examples, such as the case of the German automaker Audi [425], which now has a 3D printing factory assembly aids from its used packaging materials, as shown in Figure A-1. Other companies such as Coca-Cola are printing urban furniture from plastic bottle waste, and the US carmaker Ford is producing interior car components from leftover polymer powder from its 3D printing processes and combining it with 3D printed plastic dental molds from the SmileDirect company to create plastic parts for its Super Duty F-250 truck [426]. Other cases can also be found in the furniture and decorative home applications, such as beach furniture in Greece [425] and public benches in Amsterdam that were 3D printed from local waste plastic [425].

Figure A - 1 A technician at Audi holds up a manufacturing tool and the plastic packing waste it was 3D printed from [425]